ENVIRONMENTAL RESEARCH

RESEARCH AND TECHNOLOGY BRANCH

Environment
Ontario

Jim Bradley, Minister

ISBN 0-7729-6435-1

CLAY/LEACHATE COMPATIBILITY STUDY HYDRAULIC CONDUCTIVITY OF OTTAWA/CARLETON "LEDA" CLAY BARRIER SOILS PERMEATED WITH DOMESTIC WASTE LEACHATE

R. A. C. PROJECT NO. 299 PL

Report prepared for Environment Ontario by:

Robert M. Quigley, Federico Fernandez
and Christy Ohikere

Geotechnical Research Centre
Faculty of Engineering Science
The University of Western Ontario
London, Ontario
N6A 5B9

DECEMBER 1989

RECYCLABLE

Copyright: Queen's Printer for Ontario, 1989
This publication may be reproduced for non-commercial purposes with appropriate attribution.

90-03012/

DISCLAIMER

This report has been reviewed by the Research Advisory Committee of Environment Ontario and approved for publication. Approval does not necessarily signify that the contents reflect the views and policies of the Ministry of the Environment, nor does mention of trade names or commercial products constitute endorsement or recommendation for use.

TABLE OF CONTENTS

		Page
PREFACE		1
1.0	INTRODUCTION	2
2.0	REGIONAL SOIL CONDITIONS	3
3.0	MATERIALS	4
3.1	Descriptions of Test Soils	5
3.1.1	Physical Properties	5
3.1.2	Mineralogical Characteristics	6
3.1.3	Chemical Characteristics	8
3.1.4	Discussion	9
3.2	Description of Test Leachate	10
4.0	METHODS	11
4.1	Hydraulic Conductivity	11
4.2	Influent and Effluent Chemistry	13
4.3	Post-Testing Sample Assessment	14
5.0	RESULTS	15
5.1	Hydraulic Conductivity	15
5.1.1	Reference k Testing with Water	15
5.1.2	Compatibility k Testing with Leachate	17
5.2	Influent and Effluent Chemistry	21
5.3	Post-Testing Sample Assessment	27
5.3.1	Visual Assessment	27

Page

5.3.2 X-Ray Assessment of K^+ Fixation 28

5.3.3 Cation Exchange Capacity Changes and Discussion 29

6.0 DISCUSSION 30

7.0 CONCLUSIONS 32

8.0 REFERENCES 33

TABLES 1 TO 5 34

FIGURES 1 TO 28 39

APPENDIX I - Testing Program to Select the Four Typical Leda Clay Samples 67

APPENDIX II - Leachate Stability 110

APPENDIX III - Preliminary Chemical Assessment of Site #10 Samples 118

PREFACE

Leachate solutions generated by rainwater infiltration into and through various types of waste must be compatible with the liner (synthetic or natural) used to retain the waste. Should chemical interaction destroy the liner, leachate would escape into the local groundwater possibly destroying a vital local resource.

The purpose of this particular project has been to assess the compatibility of Leda clay from the Ottawa/Carleton region of Ontario with typical domestic waste leachate. Measurement of hydraulic conductivity has been the assessment tool.

The project has been sponsored as a contract by the Ontario Ministry of the Environment (Project #299 PL, Purchase Order A97937, Requisition No. 110532 dated April 8, 1987). A contract format was selected since the work is, in part, site specific and will probably be used in a future environmental hearing.

Our liaison officer has been Mr. Robert A. Dunn, P.Eng., District Officer, Ontario MOE, Ottawa. We thank Mr. Dunn for his understanding extensions to our contract deadlines caused by problems in selecting both the Leda clay samples and suitable domestic leachate, and the first author's extensive sabbatical travels in 1989.

We also acknowledge the assistance of Geocon Inc. and MacLaren Engineers Ltd. who did the soil sampling at Sites #10 and #19 and Dr. K.T. Law at the Institute for Building Research at NRC who generously supplied us with a weathered near surface Leda clay sample. This latter sample yielded some of our most interesting results. A useful review carried out by Dr. B. Iyer on behalf of MacLaren Engineers Ltd. is also acknowledged.

1.0 INTRODUCTION

The purpose of this Research Contract has been to establish the compatibility of Leda clay with domestic waste leachate using hydraulic conductivity as the assessment tool. The terms of the contract required testing of four typical Leda clay samples considered representative of potential waste disposal sites in the Ottawa/Carleton region.

The four samples selected consisted of two soft, clay samples from Candidate Site #10, one stiff sample from Site #19 and one weathered and fissured surface sample from the grounds of the National Research Council designated Site #E.

Domestic waste leachate from the Westminster Landfill site near London, Ontario was used as the influent permeant for the hydraulic conductivity tests. All four tests were run until the effluent chemistry reached influent concentration levels. Potassium was the most significantly retarded species measured and was used as the chemical control on testing time.

Extensive chemical analyses were carried out during and after permeation. This was followed by post-testing sample assessment which included x-ray diffraction and cation exchange capacity measurements to study any K^+ fixation effects.

Reporting on the project has included four progress reports dated June 22, 1987, January 22, 1988, May 3, 1988 and June 15, 1988. A draft of the final report was submitted on July 29, 1988 for Ministry review. Answers to the review comments are included in the text of this final report.

2.0 REGIONAL SOIL CONDITIONS

A map of the Ottawa region taken from Crawford and Eden (1965) is presented on Figure 1. The location of the three sites from which clay samples have been obtained are shown by the solid triangles. Site #10 is a candidate landfill site, Site #19 was a possible energy-from-waste site and Site #E is located on the grounds of the National Research Council of Canada laboratories. The letters A to K on the map refer to study locations discussed by Crawford and Eden.

The small scale cross-section below the regional map illustrates the amount of erosion that has probably taken place in the area. In areas of extensive erosion, the clays are heavily preconsolidated compared to nearly normally consolidated clays in uneroded areas.

Reference to the map suggests that Site #10, which is probably similar to Crawford and Eden's Site I, is in a high elevation area of thick clay which should have experienced little erosion and will thus consist of soft clay. This was confirmed by geotechnical investigations and the consolidation tests reported later in this report. Site #19, which is near K, appears to be a high elevation site with less clay but some erosion. The NRC site is an even higher elevation site but the clays are thin and highly desiccated.

Figure 2, also adapted from Crawford and Eden (1965) shows the regional relationships between elevation and preconsolidation pressure. Although the zones are broad, the trends are clear; the higher the elevation the less consolidated and softer the clay deposit.

Consolidation data for study Sites #10, #19 and #E are plotted on Figure 2 as large solid squares. The value of σ_p' for Site #19 overlies a data point for neighbouring Site K documented by Crawford and Eden. The value of σ_p' for Site #E lies more or less on the extrapolation of the line for Crawford and Eden's Site #E even though the test soil was unsaturated and from the desiccated surface zone clays at NRC. Finally, the σ_p' line for the surface clays at Site #10 lies fairly close to the line for Crawford and Eden's Site I, although the Site #10 soils appear less preconsolidated and possibly represent a nearly uneroded, undesiccated geologic section.

An additional σ_p' data point for elevation 58.6 m at Site #10 is also plotted on Figure 2. This point is off the trend line established by the other three points and is believed to represent a siltier stratum at depth.

3.0 MATERIALS

The four test soils selected for hydraulic conductivity testing and the influent test leachate are described here. The results of extensive mineralogical work carried out to make the sample selections are presented in Appendix I.

The four test soils were selected on the basis of a combination of technical and non-technical factors. For example, two samples were selected from Site #10 since consultations with MacLaren Engineers Inc. indicated it was a preferred or candidate site and therefore in need of

most attention.

The leachate used came from the Westminster Landfill south of London, Ontario. This leachate was used since it was possible to obtain fresh leachate directly from the collection system without long distance shipping. Also, London and Ottawa are similar sized municipalities so the leachates should be similar in composition although it is acknowledged that the licensed mix of wastes could ultimately be different at Ottawa.

3.1 Description of Test Soils

3.1.1 Physical Properties

The two Site #10 samples consisted of soft, grey sensitive silty clay from depths of 3.8 and 11.5 m. A thin sand cover at the site appears to have prevented extensive dessication resulting in soft clays with high water contents of 55 and 67% which exceed their corresponding liquid limits of 51 and 65% (Table 1). Consolidation curves for these two samples are presented on Figure 3. The curves are S-shaped indicating sensitive soils prone to large settlements if the preconsolidation pressure is exceeded. σ_p' values of ~ 55 and ~ 80 kPa are indicated by the curves. The shallow sample displays a maximum C_c value of 0.76 compared to 0.62 for that from 11.5 m.

The Site #19 sample was also a silty clay having a water content of 48% which is almost the same as its liquid limit value of 49%. Although the clay came from only 3.3 m depth, the consolidation curve shown on Figure 4 indicates a σ_p' value of ~ 214 kPa. This indicates that this sample is overconsolidated probably by erosion of overlying sediments as

discussed in Section 2.0. The σ_p' value plots very close to Point K of Crawford and Eden (Figure 2). This clay is also very compressible if consolidated beyond σ_p' as indicated by a maximum C_c value of 0.69.

The Site #E sample from the grounds of the National Research Council was a highly fissured, blocky weathered greyish clay from 1.14 m depth, having a water content of only 35%. The corresponding liquid limit for this sample was 70%, a high value suggesting the presence of swelling clays. The consolidation curve presented on Figure 4b, for a specimen from 1.26 m depth, is a very broad flat curve characteristic of overconsolidated clay which in this case was probably caused primarily by near surface desiccation. This clay is not particularly compressible having a C_c of 0.36 which is about half that of the other three samples.

3.1.2 Mineralogical Characteristics

As shown by the powder patterns on Figure 5 (and summarized in Table 2), all four samples contain abundant quartz, moderate to abundant feldspar and moderate amounts of illite. Carbonate comprises 3 to 7.5% of the Site #10 and Site #19 samples but appears to have been leached out of the Site #E sample. Chlorite seems present in moderate amounts in the Site #10 samples, in trace amounts in the Site #19 sample and completely absent from the Site #E sample. Swelling clays are usually present in small amounts in Leda clay as confirmed by minor to trace amounts in the samples from Sites #10 and #19. The Site #E sample, however, contained abundant swelling clay, probably produced in part by oxidation weathering of original chlorite normally found in Leda clay.

The above four sets of powder traces were obtained on specimens taken

from Shelby tubes close to the actual test specimens (Appendix I). Because of soil stratification and lamination, which are indicated by the large variations in water content (Figure I-10), silty layers and very high water content clay layers are found in close vertical proximity. Therefore, additional test specimens were taken very close to the k-test samples and oriented by high pressure squeezing to study their mineralogy. Pressure orientation enhances the clay peaks by orienting the plate-shaped clay particles perpendicular to the direction of stress application. The x-ray traces obtained on the water-wet specimens are shown on Figure 6.

The four traces on Figure 6 indicate very different types of Leda clay. The upper trace for Sa #10-3-WOF represents a silty specimen with abundant amphibole and rather poorly defined clay peaks. The second trace is typical of the two clayey test soils from Sa #10-3-WOF and #10-2-WOE actually subjected to leachate permeation. The trace shows strong chlorite and illite peaks which are typical of Leda clay. The third trace for Sa #19-1-3 (also clayey) shows the presence of illite and chlorite plus a significant amount of smectite identified by the 1.58, 1.88 and 2.26 nm peaks. Finally, the bottom trace for the Site #E clayey weathered surface soil shows the presence of abundant smectite (1.52 nm), abundant interlayered illite/smectite (I/S peak at 1.24 nm), abundant illite and very little chlorite.

From a clay/leachate compatibility point of view, the smectite and interlayered illite/smectite are the most important since they are subject to c-axis contraction due to K^+ fixation if their charge deficiency is close to that of vermiculite (i.e. approximately -0.6/unit cell of 10 oxygens). This aspect of the project is discussed further in the

section on post-testing sample assessment.

Detailed mineralogical analyses including numerous x-ray traces are presented in Appendix I which was prepared as part of the sample selection process and submitted as Progress Report #2.

3.1.3 Chemical Characteristics

Selected chemical analyses performed on the four test samples are presented in Table 2. The chemical analyses were performed on pore water squeezed from the clays at 10 MPa.

The results show Sa #10-2-WOE to have a moderately high salt content of 6,500 mg/L compared to Sa #19-1-3 which has a very low value of 300 mg/L. The other two samples have values of 1,400 and 1,500 mg/L. The four test soils, therefore, exhibit a fairly wide range of porewater salt contents, another reason for their selection.

Cation analyses performed on the pore fluids were used to calculate the percentage of adsorbed Na^+ on the clays as expressed by the sodium adsorption ratio (SAR) values. The data indicate that the most saline clay (Sa #10-2-WOE) should have ~ 23% of its exchange sites occupied by Na^+ compared to much lower values of 1 to 7 for the other clays.

Three of the soils are slightly alkaline (pH = 8.1 to 8.2). The weathered, carbonate-free soil (Site #E) yielded neutral pore water (pH = 7.0).

The results of combined KCℓ/silver thiourea exchange of the four clays are presented on Table 5. The sum of the adsorbed cations (total cations less porewater cations) yields an approximate value of the cation exchange capacity (CEC) provided unmeasured species are not present on the clays.

Based on these analyses, the four natural test soils have CEC values ranging from 14 to 31.8 meq/100 g. The highest value for Sa #E-NRC seems compatible with the presence of smectite previously described. The relative size of these CEC values is discussed further in the section on post-testing assessment (Section 5.3.3).

The distribution of adsorbed cations (Table 5) was used to calculate the exchangeable sodium percentage (ESP) values. The results suggest that Sa #10-2-WOE has Na^+ adsorbed on 43% of its exchange sites compared to lower values of 6 to 20% for the other clays. This makes sense since this clay was the most saline as indicated in Table 2.

Normally the SAR and ESP values are very similar to one another. In this set of tests, however, the ESP values are considerably higher than the corresponding SAR values. We have not attempted to resolve this chemical problem although we have noted on other projects that some soil illites tend to lose sodium during washing with KCℓ and silver thiourea solutions.

3.1.4 Discussion

Based on the above discussion, it is clear that the four test soils not only emphasize candidate Site #10 (two samples) but also represent a wide variety of soil conditions under which Leda clay exists. The range of properties and characteristics of the four test soils are summarized as follows:

1. Preconsolidation from ~ 55 kPa to > 200 kPa.
2. Weathered and unweathered.
3. Abundant swelling clay to minor swelling clay.

4. High water content (67%) to low water content (35%).
5. Low to high liquid limits (49 to 70%).
6. Moderately saline (6.5 g/L) to leached (0.3 g/L).
7. SAR from ~ 1 to ~ 23 $(meq/L)^{\frac{1}{2}}$.
8. CEC from 14 to 31.8 meq/100 g.

The requirement that four "typical" Leda clays be studied has been satisfied.

3.2 Description of Test Leachate

The test leachate was collected from the Westminster Landfill site on April 5, 1988 and divided into two portions; one for laboratory storage at room temperature and use in the hydraulic conductivity testing program and the other for storage and study at 10°C.

The composition of the leachate immediately prior to the first permeation run is presented in the second column in Table 3. Sodium and its chloride pair are the most abundant measured species (647 and 1323 mg/L) along with significant amounts of potassium, calcium and magnesium (372, 247 and 280 mg/L). Potassium is a very important constituent since the mineralogical studies indicated that a vermiculitic component in the Leda clays is subject to c-axis contraction caused by K^+ fixation.

Another important species is ammonium (NH_4^+) which was not measured. Very recent diffusion studies using leachate indicated that NH_4^+ also fixes on vermiculite and is present in the Westminster leachate at levels somewhat higher than the K^+ (Barone, Yanful, Quigley and Rowe, 1989).

Fresh leachate is normally slightly acidic due to the presence of

organic acids early in the life of the landfill. The test leachate had a pH of 6.9.

The chemical stability of leachate is believed to be controlled by bacterial activity which causes Ca^{++} to precipitate as $CaCO_3$ and Fe^{++} to precipitate as FeS_2 forming black slimy flocs (Yanful, Fernandez and Quigley, 1987). This created some interesting chemical measurement problems for both the influent leachate and the effluent, especially with respect to Ca^{++} which demonstrated a lot of scatter until it was discovered that $CaCO_3$ was also precipitating in the effluent collection bottles. These factors are described more fully in the Results section and in Appendix II.

At the end of Test Run #3 and the final run (either #4 or #5) the composition of the leachate in the permeameter cells above the soil samples was checked for comparison to the initial bottle value and these data are also presented in Table 3. Generally speaking, the final reservoir leachate was fairly similar to the initial "bottle" leachate, except for the significant and expected decreases in calcium and iron.

4.0 METHODS

4.1 Hydraulic Conductivity

Computer-controlled hydraulic conductivity equipment described briefly by Fernandez and Quigley (1985) was used for the testing. The influent liquids are forced at constant rate, q, through ~ 2 cm thick undisturbed soil samples inserted into fixed ring permeameters, 5.4 cm in diameter. The pressure head at the inlet side of the sample is measured by pressure

transducer and k is calculated using Darcy's Law [q = Q/t = kiA].

The permeameters were assembled with an internal spring loading system which applied a steady state effective stress of 40 kPa to the four samples. This low stress was necessary to avoid consolidation of the very soft samples from Site #10 which had preconsolidation pressures of only 55 and 80 kPa.

The flow rate selected for permeation was normally 15 to 20 x 10^{-5} mL/s. This low rate created small maximum drag forces (J_{max}) at the base of the 2 cm thick samples to minimize seepage-induced consolidation. Most of the settlement which did occur can, therefore, be explained by chemical modifications to the strength of the soil.

A thin steel rod sitting on the top stone above the test specimen extends through the cell cap to a dial gauge which monitors settlement. Settlement first occurs as a result of static loading (40 kPa), then as a result of drag forces during seepage. Both were monitored and presented as part of the k test results.

The influent reservoirs (actually steel cylinders with motor-driven pistons) hold about 70 cc of permeant representing about 2 to 3 pore volumes, depending on the void ratio of the test specimen. Once the reservoir cylinders become empty, q is stopped and the cylinders are refilled with leachate. At the end of run #3, the fluid above the porous stone in the permeameter cell was also syphoned out without removal of the spring-induced effective stresses and more influent was added from the source bottle of stock leachate. This "permeameter leachate" was chemically analyzed as discussed in Section 3.2.

Three of the cells were filled with Leda clay from Shelby tubes by

trimming the extruded samples to a diameter 2 mm greater than that of the cell (56 compared to 54 mm), then pushing them into the cells through a cutting shoe slightly larger than the cell. A T-shaped cutting edge was used to trim the top of the samples to a thickness of 20 mm before a disk of filter paper and the top stainless steel porous stone were placed on the sample. The three undisturbed Leda clay samples are considered to have been almost saturated at the start of testing.

The very stiff Leda clay from near surface at Site #E (NRC) contained so many open fissures that fracture flow caused very high k values. This sample was very thoroughly remolded (slurried) and compacted into the permeameter using a 12.5 cm diameter rod (Harvard miniature compaction rod). This sample was considered very important because of its high smectite content, apparently produced by oxidation weathering.

In addition to permeation by leachate, one run was made on the four samples using 0.01 N $CaSO_4$ as the permeant (Standard ASTM water) to establish reference permeability values for comparison to those calculated from the consolidation tests and those measured with leachate.

4.2 Influent and Effluent Chemistry

The cation chemistry of the effluent liquids was established by atomic absorption spectrometry about every 0.5 to 1.0 pore volumes on samples of 3 to 6 mL which were normally diluted by a factor of 2 for iron and up to 500 for sodium. Chloride and pH were measured by specific ion electrodes.

The chemistry of the influent liquid was checked twice during the test period. In addition, the chemical stability of the leachate stock was

assessed by continous monitoring of pH, Ca and Fe in 23 bottles stored at room temperature for about 60 days. This was done to help explain some of the scatter in the chemical test results.

4.3 Post-Testing Sample Assessment

Upon completion of leachate permeation, each sample was extruded and visually inspected. Photographs were taken if important visual evidence of alteration was observed.

X-ray diffraction analyses were carried out on pressed pellets of wet soil extracted from the top, middle and bottom of each 20 mm thick sample. Pressure orientation of the plate-shaped clay particles by consolidation at 140 MPa resulted in strong x-ray peaks. By comparing the traces for the leachate-permeated soil with natural soil, it was possible to observe any K^+ fixation and c-axis contraction of vermiculite that might have occurred.

The effects of K^+ fixation on the x-ray traces looked so important that special tests were run on the soils before and after permeation to measure both the adsorbed cations and the cation exchange capacity. The method employed was a combination of $KC\ell$ exchange and silver thiourea exchange, the latter being the method of Chabbra (1975).

5.0 RESULTS

5.1 Hydraulic Conductivity

The hydraulic conductivity testing was conducted in two phases: 1) reference k testing using influent water; and 2) leachate compatibility k testing using influent leachate. The two phases of testing are described separately.

5.1.1 Reference k Testing with Water

The results of the reference k testing, using 0.01 N $CaSO_4$ in distilled water as the permeant, are presented on Figures 7 to 11, inclusive. Each figure includes separate plots of hydraulic conductivity and settlement vs pore volumes of influent passed through the sample. [1.0 pore volume represents the water-filled void space within a test specimen.] This kind of reference water is generally accepted as fairly representative of fresh or non-saline ground water and is commonly used for research testing. Tap water, distilled water and 0.005 N $CaSO_4$ are also occasionally used.

Sa #10-3-WOF: For this sample, a reference final k (k_f) of 1.95 x 10^{-7} cm/s was obtained for the faster flow rate of 44.5 x 10^{-5} mL/s and final gradient of ~ 100 (Figure 7). The maximum stress at the base of the samples was 60 kPa corresponding to the sum of σ_v' = 40 kPa and J_{max} = 20 kPa.

The initial settlement due to static loading was 0.396 mm (2.0% of the original thickness, Th_o) followed by another 0.248 mm of seepage settlement (1.2% of Th_o). A somewhat higher k of 3.5 x 10^{-7} cm/s was obtained at the

slower flow rate (8.9×10^{-5} mL/s) which produced $i \approx 10$ and very small J_{max} of 2 kPa. This sample was tested at stresses very close to or slightly above the measured σ_p' of 55 kPa, hence the large settlement.

Sa #10-2-WOE: This sample yielded a $k_f = 6.4 \times 10^{-8}$ cm/s at $i_f \approx 300$ and maximum static plus seepage stresses of 100 kPa (Figure 8). The higher J_{max} value (60 kPa) relates to the lower k of this soil (compared to #10-3-WOF) which causes greater seepage stresses at constant q.

The total static and seepage settlement amounted to about 1.306 mm which represents about 6% of Th_o. This soft clay specimen was also tested close to or slightly above its measured σ_p' value of 80 kPa, hence the large percentage settlement.

Sa #19-1-3: The reference k_f for this sample was 1.8×10^{-7} cm/s at $i_f = 110$ and maximum static plus seepage stresses of 61 kPa (Figure 9). The low J_{max} for this sample (21 kPa) relates to its relatively high k.

Total static plus seepage settlements amounted to 0.199 mm which corresponds to only 1.0% of Th_o. This clay was tested at maximum stresses much less than its measured σ_p' value of 214 kPa, hence the very small settlement.

Sa #E-NRC: The initial k test run on an undisturbed sample of this highly fissured clay yielded k values $> 10^{-5}$ cm/s at heads and gradients too low to be measured accurately. Application of $\sigma_v' = 320$ kPa was insufficient to close the fractures and significantly reduce the values of k. Two additional samples were therefore prepared, one sample (Figure 10) by compaction of the soil chunks in the permeability cell using a Harvard Miniature 12.5 mm diameter rod, and the other by compaction after slurrying it in a mortar and pestle. In both cases the water content was

initially close to 35%.

The partially remoulded specimen (Figure 10) yielded a k_f value of 4.8×10^{-7} cm/s which is quite high considering its high smectite content and relatively low water content of 34.7%. This high k is believed to reflect residual fractures still present in the compacted soil. The presence of fractures also explains the low i_f of 15 and J_{max} of only 3 kPa. After seating the static σ_v' of 40 kPa on the sample it actually swelled 0.067 mm by drawing moisture from the upper porous stone. Subsequent seepage with reference water caused an additional swelling of 0.027 mm.

Complete remoulding of the soil prior to compaction (Figure 11) eliminated the residual fractures as evidenced by the low values of k (6.05×10^{-9} cm/s), a much higher gradient (435) and a higher J_{max} of 85 kPa. The sample compressed 0.304 mm due to the 40 kPa of static loading applied. During seepage an additional settlement of 0.211 mm took place, the total settlement corresponding to 2.58% of the original thickness.

Discussion: The maximum effective stresses acting at the base of the two Site #10 samples (60 and 100 kPa) were above the preconsolidation pressures of the samples. Considerable settlement therefore occurred during seepage at flow rates of 44×10^{-5} mL/s. On the basis of these tests it was decided to use influent flow rates below 20×10^{-5} mL/s for the compatibility k tests with leachate.

5.1.2 Compatibility k Testing with Leachate

The results of the leachate compatibility k testing are presented on

Figures 12 to 15 inclusive. Three of the tests (Figures 12, 13 and 14) were run in two steps with a 10-day no-flow period between them. The purpose was to allow the test on smectitic Sa #E-NRC to catch up and to assess any creep effects in the Site #10 samples which would be loaded up to or beyond σ_p' if a landfill is built. All tests were terminated after the samples had reached equilibrium with the influent K^+ which was the most significant species retarded by the clays.

It should be noted that reference k values using water were not obtained on these samples since in some cases this would have dramatically altered the porewater chemistry before leachate permeation. This would then not be representative of the field conditions on exposure to leachate.

Sa #10-3-WOF: The first permeation interval in this test yielded a $k_f = 1.05 \times 10^{-7}$ cm/s at $i_f \approx 80$ and $J_{max} \approx 15$ kPa (Figure 12). At this point ~ 6.7 P.V. had passed through over a time interval of 15 days. During the latter half of this period of permeation there was no further consolidation of the sample even though k was decreasing very slightly with time. The seepage settlement was only 0.13 mm or 0.7% of Th_o.

The effective stresses at the base of the test specimen amounted to ~ 55 kPa which is the estimated σ_p' for this sample (see Figure 3a). During the 10-day resting period, the bonded structure of this sensitive clay appears to have been weakened and re-establishing the flow caused a substantial amount of additional settlement (0.589 mm = 2.9% of Th_o). This decrease in void ratio caused a substantial decrease in k to a final value of 2.5×10^{-8} cm/s at $i_f \approx 260$ and $J_{max} \approx 50$ kPa.

Sa #10-2-WOE: This test was run at a maximum basal effective stress

of 70 kPa which was sufficiently low compared to σ_p' = 80 kPa that consolidation did not significantly influence the hydraulic conductivity. A k_f value of 4.3 x 10^{-8} cm/s was measured at $i_f \approx 150$ and $J_{max} \approx 30$ kPa (Figure 13).

The fairly large static settlement (0.933 mm) appears to have resulted from sample disturbance and is unavoidable to a certain extent in tests on sensitive clays. The subsequent seepage settlement was 0.342 mm and was continuing at a very small rate when the test was terminated.

Sa #19-1-3: This test was run with maximum basal stresses of ~ 75 kPa which was well below the σ_p' of 214 kPa. Stress-induced settlement should therefore not have been a problem at this site. The very small static settlement of 0.033 mm (0.17% of Th_o) seems to confirm this (Figure 14). Permeation by the leachate caused a steady long-term settlement which had reached 0.073 mm (0.37% of Th_o) when the test was terminated. It appears that the leachate must be responsible for this creep consolidation because the reference k test with water did not creep at approximately the same stress level.

The end of testing k_f was 3.9 x 10^{-8} cm/s at $i_f \approx 165$ and $J_{max} \approx$ 35 kPa. The hydraulic conductivity was still slowly decreasing in response to the creep consolidation even though the sample appeared to be in chemical equilibrium with the leachate.

Sa #E-NRC: This sample yielded a nearly constant k throughout the testing time of 45 days or 9 P.V. (Figure 15). The final k_f was 3.6 x 10^{-9} cm/s at $i_f \approx 730$ and $J_{max} \approx 140$.

Although the static settlement of this compacted sample was a modest 0.138 mm, considerable seepage settlement occurred (0.339 mm) and was

continuing when the test was terminated. In the three other tests, k was decreasing slightly in response to the continuous decrease in void ratio. In this smectitic clay, k_f was essentially constant in spite of the slowly decreasing void ratio.

Discussion: A comparison of the k_f values obtained with water and leachate is presented in the following tabulation and on Figure 16.

Sample No.	Water		Leachate	
	k_f	e_f	k_f	e_f
10-3-WOF	19.5×10^{-8}	1.484	2.5×10^{-8}	1.187
10-2-WOE	6.4×10^{-8}	1.723	4.3×10^{-8}	1.544
19-1-3	18.0×10^{-8}	1.369	3.9×10^{-8}	1.397
E-NRC	0.61×10^{-8}	0.978	0.36×10^{-8}	0.966

On Figure 16 it seems clear that there are two distinct trend lines for high void ratio Leda clays; a lower k trend line for leachate and a higher k trend line for water. Bearing in mind that all data points on Figure 16 started at somewhat different initial void ratios, the arrows still strongly suggest that leachate permeation induces creep consolidation and a reduction in void ratio if the tests are run at effective stresses close to σ_p' or on remoulded clay. The single test run at stresses well below σ_p' (Sa #19-1-3) demonstrated only slight creep consolidation but still terminated with a lower k_f on the leachate trend line.

The explanation for the two trend lines and the tendency for creep seems related to chemical changes discussed next.

5.2 Influent and Effluent Chemistry

Curves showing the variation in effluent pH, chloride, iron, sodium, potassium, calcium and magnesium with pore volumes passed through are presented on Figures 17 to 24, inclusive. On all plots, the initial soil porewater concentration of the species under consideration is presented as a horizontal dashed line. The "bottle" value, marked with a single asterisk, represents the composition of the "new" permeant at recharge. The reservoir value, marked with a double asterisk, represents the last of the influent leachate directly above the sample in the permeameter at the end of run #3 and the final run.

Sa #10-3-WOF (Figures 17 and 18): The effluent pH values quickly dropped from 8.1 for the pore water to about 7.4 for the first 6 P.V. of leachate flow, the leachate having a pH of ~ 6.9. After this, the effluent pH was about 8.1 despite leachate values of 7.1 to 7.3.

Since the leachate chloride concentration of 1323 mg/L is much higher than that of the resident pore water (634 mg/L) the effluent values quickly rose to ~ 1250 mg/L terminating at a value of 1145 mg/L, identical to the influent leachate in the permeameter. Arrival of almost full concentration occurred within 0.5 P.V. followed by a slow increase in concentration (tailing).

Iron concentrations in the effluent are very low (< 2 mg/L) in comparison to the initial "bottle" values of 66 and 25 mg/L. The decrease

in the "bottle" value reflects the formation of iron-rich carbonate precipitate described in Section 3.2 and Appendix II. The drop to 5 or 6 mg/L in the reservoir which is in contact with the porous stone above the clay probably reflects the alkalinity of the clay.

The effluent Na^+ concentration values shown on Figure 18 reflect rapid arrival of Na^+ to influent values of ~ 600 mg/L within 0.5 P.V. The soil itself has Na^+ values of only 285 mg/L so considerable Na^+ was added to the soil pore water.

Potassium which is present at only 15 mg/L in the soil pore water is strongly retarded by the clay as shown on Figure 18. Effluent K^+ values reach reservoir values (~ 270 mg/L) after about 6 or 7 P.V.

Calcium values for the effluent show an initial increase from a porewater value of 34 mg/L to an influent value of 240 mg/L at only 1.1 P.V. of flow. Following this, the effluent values drop rapidly to a steady concentration of about 100 mg/L which corresponds to the reservoir value. The drop in effluent concentration reflects the time dependent drop in Ca^{++} in the influent reservoir and bottle samples due to "biological" precipitation.

The effluent magnesium curve is interesting since the effluent values exceed the influent values between 0.6 and 2.6 P.V. This is probably Mg^{++} adsorbed on the clay being displaced by Na^+, K^+ and Ca^{++} from the leachate (see Table 5). Influent and effluent concentrations are in equilibrium at the end of testing at 285 mg/L which is far above the porewater value of 61 mg/L.

In summary, all species in the influent are more abundant than in the original pore water. All species appear to have reached equilibrium

within 3 or 4 P.V. except K^+ which is retarded for about 6 P.V. Mg^{++} is the only species which appears to display a halo effect due to cation exchange.

Sa #10-2-WOE (Figures 19 and 20): This saline sample is quite different from the previous sample, having $C\ell^-$ and Na^+ porewater concentrations in excess of the leachate values.

The pH trends are the same as for Sa #10-3-WOF although the final effluent values seem to be having difficulty reaching the porewater value of 8.1.

The effluent $C\ell^-$ dropped rapidly from initial porewater values of 3555 mg/L to values of ~ 1200 mg/L within 2 P.V. at which level they were comparable to the reservoir leachate.

The effluent iron behaved exactly as in the previous sample, with little evidence of any passing through the sample.

The Na^+ curve (Figure 20) looks similar to the $C\ell^-$ curve (Figure 19) except that Na^+ appears to have taken up to 4 P.V. to reach equilibrium rather than the 2 P.V. for $C\ell^-$.

K^+ is again retarded for about 6 or 7 P.V. before reaching equilibrium with the influent at ~ 275 mg/L.

The Ca^{++} data points display much scatter and are difficult to interpret. All effluent values are below the corresponding influent values. It is suggested that this is a reflection of $CaCO_3$ precipitation in the effluent bottles near the end of permeation and not a reflection of non-equilibrium with the influent.

The effluent Mg^{++} again displays a slight halo effect since the concentrations from 2 to 3 P.V. (~ 320 mg/L) exceed the influent values

of ~ 290 mg/L.

In summary, Na^+ and Cl^- values in the leachate are less than the porewater values for this clay resulting in flushing from the samples. K^+, Ca^{++} and Mg^{++}, on the other hand, were added to the bulk samples. The resulting cation exchange should be reflected in the post-testing assessment.

Sa #19-1-3 (Figures 21 and 22): This low salinity sample had porewater concentrations of all species far below the influent leachate values. In all cases, except iron, these species were added to the test sample.

The pH and total Fe curves were as previously described.

The Cl^- effluent seemed to reach final influent reservoir concentration (1145 mg/L) after 3 P.V. but never did reach the "bottle" values. The corresponding effluent Na^+ values reached a final reservoir value of ~ 600 mg/L after about 6 P.V. indicating some retardation relative to Cl^-.

The K^+ curve suggests retardation for ~ 9.5 P.V. at which point K^+ reaches the final influent reservoir value of ~ 330 mg/L. This is significantly more retardation than that displayed by Sa #10-3-WOF and #10-2-WOE which required 6 to 7 P.V. of leachate flow.

The Ca^{++} effluent reaches concentrations above the influent value in less than 0.5 P.V. This indicates rapid Ca^{++} desorption from this clay (i.e. a Ca^{++} halo).

The Mg^{++} effluent reaches influent values of ~ 300 mg/L within 1.0 P.V. and for this clay displays no halo effect. Early arrival of Mg^{++} (C/C_o = 0.5 at ~ 0.2 P.V.) may indicate desorbed Mg^{++} rather than

macropore flow since $C/C_o = 0.5$ for Cl^- seems to have arrived at 0.4 P.V. or so.

In summary, this low salt soil displays a clear Ca^{++} halo and early arrival of Mg^{++} apparently due to cation exchange by K^+ and Na^+ both of which are retarded. Iron did not pass through the sample in significant amounts.

Sa #E-NRC (Figures 23 and 24): This weathered, low salt clay contains abundant K^+ collapsible vermiculite and should display the most retardation and most pronounced halo effects of the four samples.

The effluent pH values fall within the range of influent reservoir and "bottle" values, which would be expected due to the similar pH values of leachate and soil (6.9 to 7.2).

As before, iron did not pass through the sample in measurable amounts.

The effluent chloride values reached influent values within 1.0 P.V. at 1323 mg/L which is not far below the chlorinity of the natural pore water.

Na^+ appears to have reached influent reservoir values within a couple of P.V. due to a drop in reservoir concentration from 647 mg/L (bottle) to 530 mg/L (reservoir). This drop may be measurement error or diffusion related.

K^+ is highly retarded and for 2 P.V. was measured in the effluent at very low porewater values of 15 mg/L. At 9.5 P.V. the effluent concentration of ~ 270 mg/L had almost reached the reservoir value of 292 mg/L.

Mg^{++} also displays retardation to 9.5 P.V. before the effluent reached the reservoir value of ~ 300 mg/L. This is a large amount of retardation and probably reflects the affinity of soil vermiculite for Mg^{++} over the

Ca^{++} adsorbed on the clays.

The Ca^{++} effluent curve (Figure 24) displays a large halo caused by the adsorption of K^{+} and Mg^{++} noted above. Because of the normally unstable and decreasing Ca^{++} in the influent, the size of the halo is difficult to define. Nevertheless, an area representing an approximate amount of displaced Ca^{++} is shown hatched on this particular figure.

In summary, this clay significantly retarded and adsorbed both Mg^{++} and K^{+} which displaced Ca^{++} producing a large calcium halo. Na^{+} seems not to have been retarded but was added to the pore water by permeation. The regime of adsorbed cations before and after permeation (Table 5) confirms that a large amount of Ca^{++} was displaced as discussed later.

Discussion: The effluent concentration curves discussed for each soil all indicate final concentrations close to reservoir influent concentrations and hence equilibrium of the soil with the leachate flowing through it.

Potassium was the most strongly retarded species requiring about 6 P.V. of flow for the two Site #10 samples and about 9.5 to 10 P.V. for the Site #19 and #E samples.

Several very low Ca^{++} values are shown on some of the effluent curves. Acidification of some of the excess effluent at the end of the k test program resulted in much higher values which plotted back onto trend lines near the influent reservoir concentrations. This indicates that precipitation of Ca^{++} in the form of $CaCO_3$ was probably the problem, resulting in erroneously low values. The activity of bacteria within the effluent bottles is a probable explanation.

Adsorption of K^{+} by all samples and adsorption of Mg^{++} by Sa #E-NRC

results in desorption of other species. This desorption, if intense enough, creates a hump on the effluent curves which is the equivalent of a halo. Sa #10-3-WOF showed a Mg^{++} halo; Sa #10-2-WOE showed a slight Mg^{++} halo and a prolonged Na^{+} removal; Sa #19-1-3 showed a strong Ca^{++} halo; and Sa #E-NRC showed a very strong Ca^{++} halo.

Some of these trends are clearly reflected in the post-testing assessment chemistry.

5.3 Post-Testing Sample Assessment

5.3.1 Visual Assessment

When leachate permeation was complete, the four cells were dismantled and the samples observed for evidence of chemical or physical change.

All four clays were observed to be uniformly grey with no evidence of discoloration or cracking. One feature that was very obvious, however, was an accumulation of black slime (precipitate) in the permeameter cells above the samples. A colour photograph for Sa #19-1-3, which is typical of what was seen above all four samples, is shown on Figure 25.

From left to right in the photo, the reader may observe: 1) the black, slime coated, two-spring loading system; 2) the top stone; 3) the top of the clay sample, and 4) the clean bottom stone. The slime obviously passed through the top stone onto the filter paper but did not cross the soil interface according to the visual observations.

Previous studies have confirmed that this black material is amorphous ferrous sulphide which precipitates along with calcite as a result of

bacterial reduction of both iron and sulphate.

5.3.2 X-ray Assessment of K^+ Fixation

Leachate saturated samples were prepared for x-ray diffraction by high pressure squeezing as described in the Methods section. Specimens were taken from near the top, middle and bottom of the samples once permeation was completed and the leachate-wet surface subjected to x-ray diffraction.

Two sets of x-rays are shown on Figures 26 and 27 comparing the natural water-wet clay specimens with leachate permeated and equilibrated clay specimens from Samples #10-3-WOF and #E-NRC. Reference to Figure 26 indicates that leachate has collapsed a portion of the 1.47 nm vermiculite/smectite peak of the natural clay. This results from K^+ fixation and c-axis contraction by the vermiculite to produce illite. The result is a decrease in the height of the 1.47 nm peak and an increase in the height of the 1.0 nm peak. Samples #10-2-WOE and #19-1-3 also showed this phenomenon, in each case with a residual 1.45 nm chlorite/smectite peak.

Weathered Sa #E-NRC showed a more spectacular collapse than the other three samples as shown by the traces on Figure 27. Both the 1.52 and 1.24 nm peaks are almost completely collapsed by leachate permeation creating a very strong 1.0 nm illite peak. Negligible 0.7 nm chlorite peaks are present so the residual 1.52 nm peaks are probably real smectite.

Arrows next to the 1.4/1.5 and 1.0 nm peaks indicate the relative height of these peaks. The ratio of the 1.45 nm to 1.0 nm peaks in any one trace gives an indication of the relative amount of vermiculite and

illite present before and after leachate permeation. Table 4 contains a summary of the 16 peak height ratios and Figure 28 illustrates in summary form the collapse characteristics of the four soils when permeated with leachate.

Three of the samples contain modest amounts of vermiculite relative to illite (10-3-WOF, 10-2-WOE and 19-1-3) as indicated by "natural" 1.5 nm:1.0 nm peak height ratios of 0.3 to 0.4 (Figure 28). All three show some collapse to ratios of 0.13 to 0.20. The weathered vermiculitic sample from Site #E-NRC shows a spectacular collapse from a "natural" ratio of 1.1 to very low values of 0.05 to 0.10 after leachate permeation. This indicates very significant K^+ fixation and possibly major changes in CEC.

5.3.3 Cation Exchange Capacity Changes and Discussion

The amount of collapse observed on the x-ray traces was so significant for the wet samples that special tests were run to see if K^+ fixation had actually reduced the CEC values. The results in Table 5 show that this has indeed occurred especially for Samples #10-2-WOE (-22%) and #E-NRC (-45%). Sa #10-3-WOF and #19-1-3 were less affected although the former registered an apparent 11% increase and the latter a 13% decrease.

Reference to the data for #E-NRC indicates that the CEC has decreased by 14.3 meq/100 g. Most of this decrease is reflected in the large decrease in Ca^{++} from 20.7 to 4.0 meq/100 g. It is this Ca^{++} which formed the large hump or halo on the Ca^{++} effluent curve (Figure 24). Fixation of adsorbed K^+ is the cause of the drop in CEC, since it is caught between the collapsed silicate sheets. The slight increase in adsorbed K^+ (4.1 to

5.5 meq/100 g) probably reflects release from residual smectite.

Sa #10-2-WOE was the saline sample which originally contained 12.0 meq/100 g of adsorbed Na^+ in the natural state. This dropped to 4.1 meq/100 g as a result of leachate permeation with corresponding increases in both adsorbed K^+ and Ca^{++}. This explains the extra time (~ 4 P.V.) for Na^+ to reach equilibrium as observed for the Na^+ effluent curve on Figure 20.

The two small Mg^{++} halos for Sa #10-3-WOF and #10-2-WOE are also confirmed by the adsorption data. Both show less Mg^{++} after leachate permeation than before it. Sa #19-1-3 also shows less Mg^{++} after permeation but no halo effects are visible. Early arrival of Mg^{++} shown by this effluent curve (Figure 22) may signal exchange.

6.0 DISCUSSION

Most of the southern Ontario clayey soils studied to date have exhibited only modest c-axis contraction and K^+ fixation as a result of permeation with normal domestic leachate, at least in the wet state (Quigley et al, 1988). The charge deficiency of the swelling clay component seems to be borderline between smectite and vermiculite (-0.5 to -0.6/unit cell of 10 oxygens). As a result, the swelling clay collapses extensively in the presence of dilute KCl <u>if air dried</u> but not if kept water-wet or leachate-wet as is the case for an operating liner or natural barrier.

The significant contraction of the swelling clays found in the four Ottawa/Carleton Leda clay samples seems to be something new, especially

the phenomenal collapse of the Site #E-NRC sample. This collapse, clearly visible on the x-ray traces, was confirmed by special chemical analyses which showed a decrease in CEC from 32 to 17½ meq/100 g for the weathered, vermiculitic Site #E sample.

The above discussed K^+ fixation and collapse phenomena occurred at a K^+ concentration of only 331 mg/L (0.01 N) in the Westminster leachate. This seems to be a fairly normal value for southern Ontario leachate. Ammonium (NH_4^+) is also common in leachates at concentrations up to 1000 mg/L. It is about the same size as K^+ and also serves to collapse vermiculite.

K^+ and NH_4^+ fixation and c-axis contraction seem, therefore, to be phenomena which must be considered for Leda clays in the Ottawa-Carleton region. For most very stiff to hard compacted clays, a trend towards an increased **k** should result if the soils remain at constant void ratio. For the Ottawa/Carleton Leda clays, the net result of leachate permeation seems to have been a decrease in bond strength between the particles which caused creep consolidation in excess of that observed for permeation of water. The gradually decreasing void ratio caused a corresponding decrease in **k**, compensating for any physico-chemical factors that might normally cause an increase in **k**.

The influence of leachate saturation on other engineering properties of Leda clay such as shear strength and compressibility are beyond the scope of this report.

7.0 CONCLUSIONS

Four Leda clay samples of widely varying composition and physical properties have been permeated with domestic waste leachate to assess their mutual compatibility, using hydraulic conductivity, k, as the assessment tool. The major conclusions of the study are as follows:

1. The hydraulic conductivity of all samples decreased as a result of leachate permeation. This decrease in k was in spite of K^+ fixation and c-axis contraction of soil vermiculite to illite.

2. An inferred effect of leachate permeation was an apparent weakening of the structure of the Leda clay resulting in continuing creep consolidation during seepage not observed for water permeation. This creep had not terminated at the end testing as it had for water. The effects of saturation of Leda clay by domestic waste leachate on shear strength and compressibility remain to be defined.

3. All samples are believed to have been close to chemical equilibrium with the influent leachate since effluent concentrations had reached influent values when the tests were terminated.

4. The decreases in k seem most significant at high void ratios (1.2 to 1.6).

5. The weathered vermiculitic Leda clay from Site #E (NRC) also demonstrated creep consolidation during leachate permeation, even at a relatively low void ratio of 0.98. K^+ fixation and c-axis contraction resulting in a decrease in volume of the solids phase probably caused most of this creep during which k remained remarkably constant.

8.0 REFERENCES

Barone, F.S., Yanful, E.K., Quigley, R.M. and Rowe, R.K., 1989. Effect of multiple contaminant migration on diffusion and adsorption of some domestic waste contaminants in a natural clayey soil. Canadian Geotechnical Journal, Vol. 26, No. 2, pp. 189-198. Also Research Report GEOT-5-88, Faculty of Engineering Science, University of Western Ontario, 35 p.

Chabbra, R., 1975. The measurement of the cation exchange capacity and exchangeable cations in soils: A new method. Proceedings of the International Clay Conference, pp. 439-449.

Crawford, C.B. and Eden, W.J., 1965. A comparison of laboratory results with in-situ properties of Leda clay. Proc. 6th Int'l. Conf. on Soil Mechanics and Foundation Engineering, Vol. 1, pp. 31-35.

Quigley, R.M., Fernandez, F. and Rowe, R.K., 1988. Clayey barrier assessment for impoundment of domestic waste leachate (southern Ontario) including clay/leachate compatibility by hydraulic conductivity testing. Canadian Geotechnical Journal, Vol. 25, No. 3, pp. 574-581.

Yanful, E.K., Fernandez, F. and Quigley, R.M., 1987. The chemical instability of domestic waste leachate and its geotechnical implications. Research Report GEOT-15-87, Faculty of Engineering Science, University of Western Ontario, 14 p.

Table 1. Physical Characteristics of Test Soils

Sample	Site #10		Site #19	Site #E
Item	3.82 m	11.51 m	3.29 m	1.14 m
Borehole No.	10-3	10-2	19.1	N/A
Sample No.	WOF	WOE	3	N/A
Elevation (m)	72.05	64.76	66.38	93.41
Water content, w_n (%)	55	67	48	35
Liquid limit, w_L (%)	51	65	49	70
Plastic limit, w_p (%)	23	29	22	35
Plasticity index, Ip	28	36	27	35
Preconsolidation Pressure, σ'_p (kPa)	- 55	- 80	- 214	100-300
Max. Comp. Index, C_c(max)	0.76	0.62	0.69	0.36
Permeability at σ'_v = 40 kPa (cm/s)	20×10^{-8}	6.4×10^{-8}	18×10^{-8}	(1) 48×10^{-8} (2) 0.6×10^{-8}

Notes: 1) Compacted fissured sample
2) Compacted slurried sample.

Table 2. Mineralogical and Chemical Characteristics of Test Soils

Sample	Site #10		Site #19	Site #E
Item	3.82 m	11.51 m	3.29 m	1.14 m
Sample Number	10-3-WOF	10-2-WOE	19-1-3	E-NRC
Mineralogy:				
Quartz	Abund	Abund	Abund	Abund
Feldspar	Mod	Mod	Mod-Minor	Abund
Carbonate (%)	6.1	3.0	7.5	0.2
Illite	Mod	Mod	Mod	Mod
Chlorite	Mod	Mod	Tr	Nil
Smectite/Vermiculite	Tr	Tr	Minor	Abund
Pore Water:				
pH	8.1	8.1	8.2	7.0
Salinity, mg/L	1,500	6,500	300	1,400
Na^+ "	285	1,500	32	335
K^+ "	15	57	11	15
Ca^{++} "	34	43	45	350
Mg^{++} "	61	185	33	38
Chloride "	634	3,555	14	1,859 ?
SAR $(meq/L)^{\frac{1}{2}}$	- 7	- 23	- 1	- 5

Table 3. Chemical Composition of Influent Leachate

Chemical Species	Initial Bottle Value (mg/L)	End of Run Reservoir Value (mg/L)				
		Run #1	Run #2	Run #3	Run #4	Run #5
10-3-WOF						
# P.V.(1)	-	2.33	2.30	2.07	2.85	2.28
pH	6.9	NM	NM	7.4	NM	7.3
Cl	1323	NM	NM	1221	NM	1145
Na	647	NM	NM	560	NM	600
K	372	NM	NM	240	NM	270
Ca	247	NM	NM	135	NM	105
Mg	280	NM	NM	270	NM	285
Fe	66	NM	NM	5	NM	6
10-2-WOE						
# P.V.	-	1.97	2.06	1.85	2.41	1.04
pH	6.9	NM	NM	7.7	NM	7.1
Cl	1323	NM	NM	1381	NM	1230
Na	647	NM	NM	600	NM	660
K	372	NM	NM	224	NM	278
Ca	247	NM	NM	130	NM	108
Mg	280	NM	NM	245	NM	300
Fe	66	NM	NM	15	NM	12
19-1-3						
# P.V.	-	2.14	2.22	2.00	2.77	2.20
pH	6.9	NM	NM	7.4	NM	7.8
Cl	1323	NM	NM	1345	NM	1145
Na	647	NM	NM	520	NM	600
K	372	NM	NM	212	NM	330
Ca	247	NM	NM	160	NM	65
Mg	280	NM	NM	260	NM	290
Fe	66	NM	NM	6	NM	2
E-NRC						
# P.V.	-	2.23	2.48	2.44	1.81	-
pH	6.9	NM	7.2	NM	7.1	-
Cl	1323	NM	1274	NM	995	-
Na	647	NM	530	NM	635	-
K	372	NM	200	NM	292	-
Ca	247	NM	270	NM	160	-
Mg	280	NM	240	NM	300	-
Fe	66	NM	2	NM	8	-

Note: (1) Number of pore volumes of leachate for run indicated.
(2) NM = Not measured.

Table 4. Peak Height Ratios[1] of Natural and Leachate Permeated Samples

Sa #	Natural	Top[2]	Middle	Bottom
10-3-WOF	0.39	0.16	0.16	0.13
10-2-WOE	0.27	0.19	0.15	0.20
19-1-3	0.35	0.20	0.14	0.18
E-NRC	1.10	0.10	0.05	0.05

Notes: 1) Ratio of 1.5 nm to 1.0 nm peak heights on pressure oriented, wet, whole soil samples.

2) Top, middle and bottom refer to location of specimen in the 20 mm thick permeameter sample.

Table 5. Total and Porewater Cations; Cation Exchange Capacity

Item	Sample	#10-3-WOF		#10-2-WOE		#19-1-3		#E-NRC	
		Natural[1]	Leachate[2]	Natural	Leachate	Natural[1]	Leachate[2]	Natural	Leachate
Total Cations:									
Na	(meq/100 g)	3.41	3.94	16.13	5.59	1.45	4.49	3.60	4.01
K	"	1.03	2.91	2.48	4.52	1.48	4.37	4.15	5.76
Ca	"	6.32	7.64	6.79	8.27	13.19	8.13	21.25	4.24
Mg	"	4.14	3.57	8.00	6.87	6.92	5.83	3.91	5.65
Porewater Cations:									
Na	(meq/100 g)	0.56	1.10	4.08	1.52	0.07	1.34	0.38	0.96
K	"	0.02	0.25	0.10	0.35	0.01	0.36	0.01	0.24
Ca	"	0.08	0.15	0.13	0.18	0.11	0.16	0.60	0.21
Mg	"	0.23	0.94	0.93	1.33	0.13	1.20	0.11	0.78
Adsorbed Cations:									
Na	(meq/100 g)	2.85	2.84	12.05	4.07	1.38	3.15	3.22	3.05
K	"	1.01	2.66	2.38	4.17	1.47	4.01	4.14	5.52
Ca	"	6.24	7.49	6.66	8.09	13.08	7.97	20.65	4.03
Mg	"	3.91	2.63	7.07	5.54	6.79	4.63	3.80	4.87
CEC	(meq/100 g)	14.0	15.6	28.2	21.9	22.7	19.8	31.8	17.5
ESP[3]	(%)	- 20	- 18	- 43	- 19	- 6	- 16	- 10	- 17

Notes: (1) Natural cation regime before testing.

(2) Cation regime after completion of leachate permeation.

(3) ESP = exchangeable sodium percentage (% Na adsorbed).

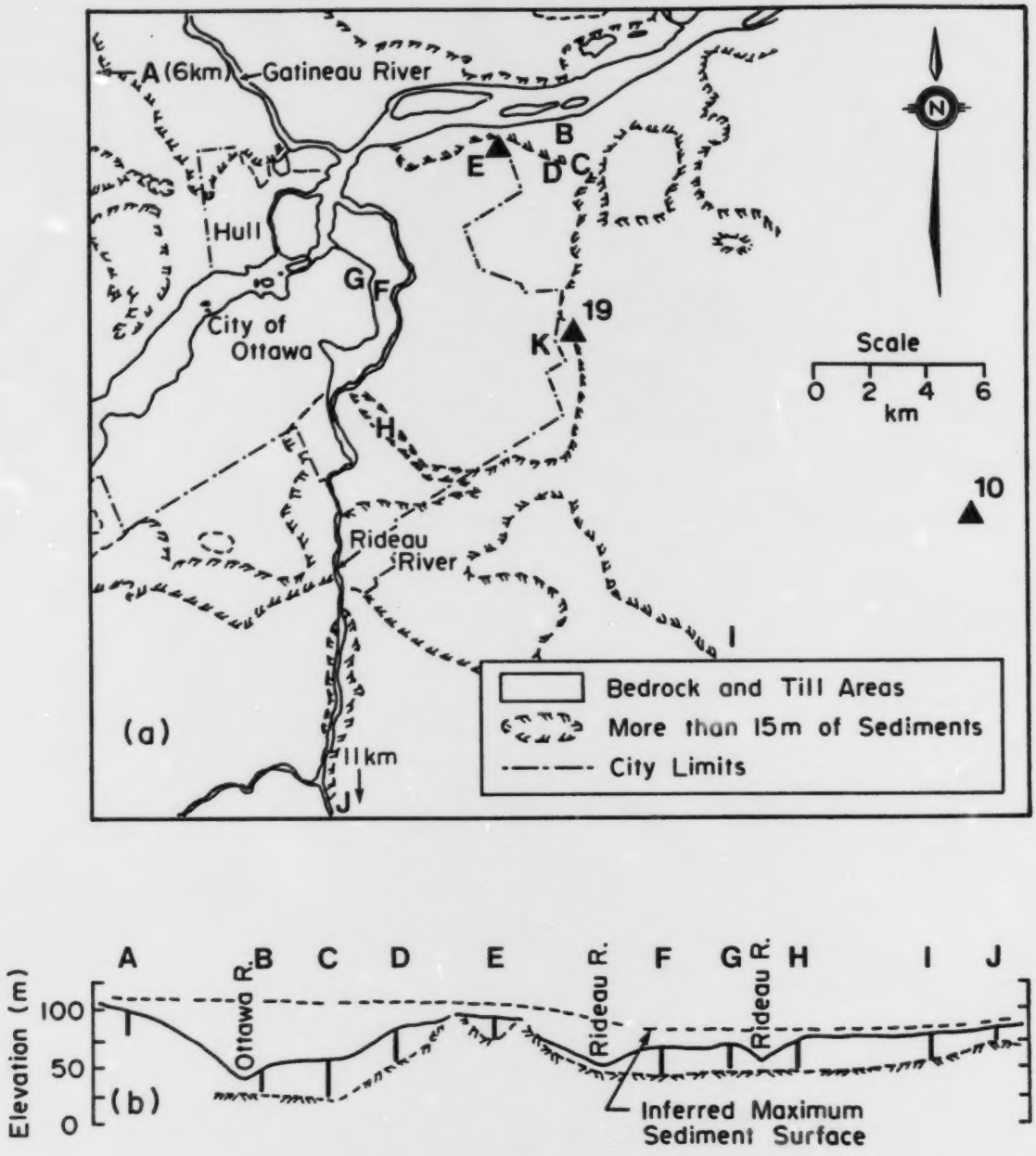

FIGURE 1. (a) OTTAWA-CARLETON REGION MAP SHOWING LOCATIONS OF NRC STUDY BORINGS (A TO K) AND THE UWO STUDY SITES (▲); (b) GENERALIZED CROSS-SECTION

[Adapted from Crawford and Eden, 1965]

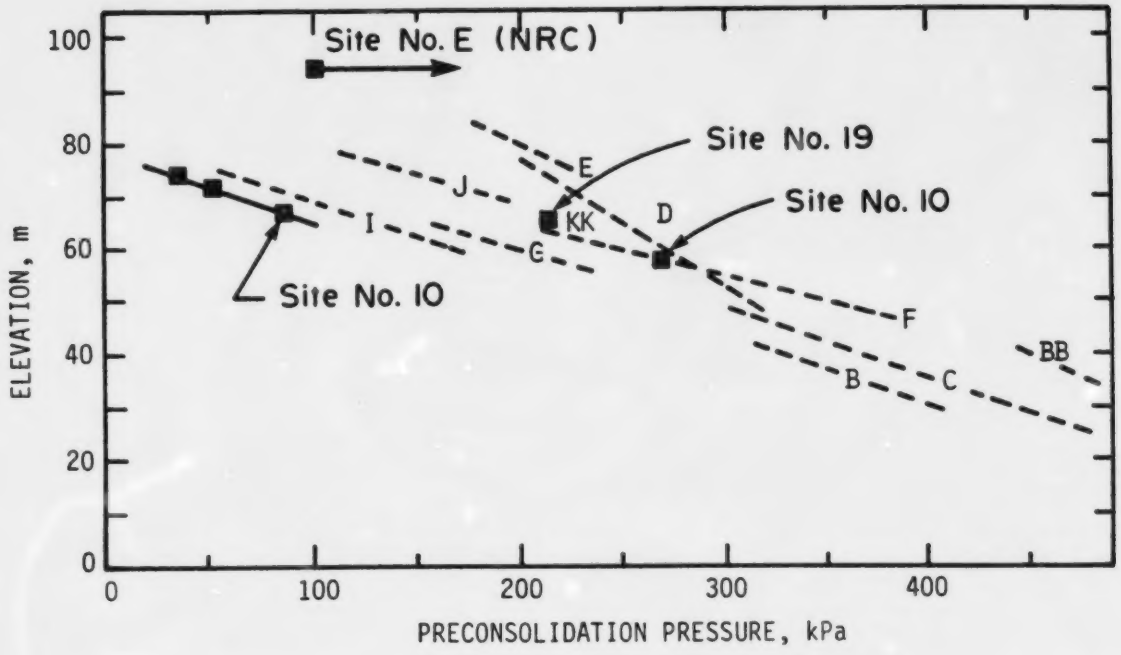

FIGURE 2. REGIONAL RELATIONSHIPS BETWEEN ELEVATION AND PRECONSOLIDATION PRESSURE, σ'_p

[Adapted directly from Crawford and Eden, 1965]

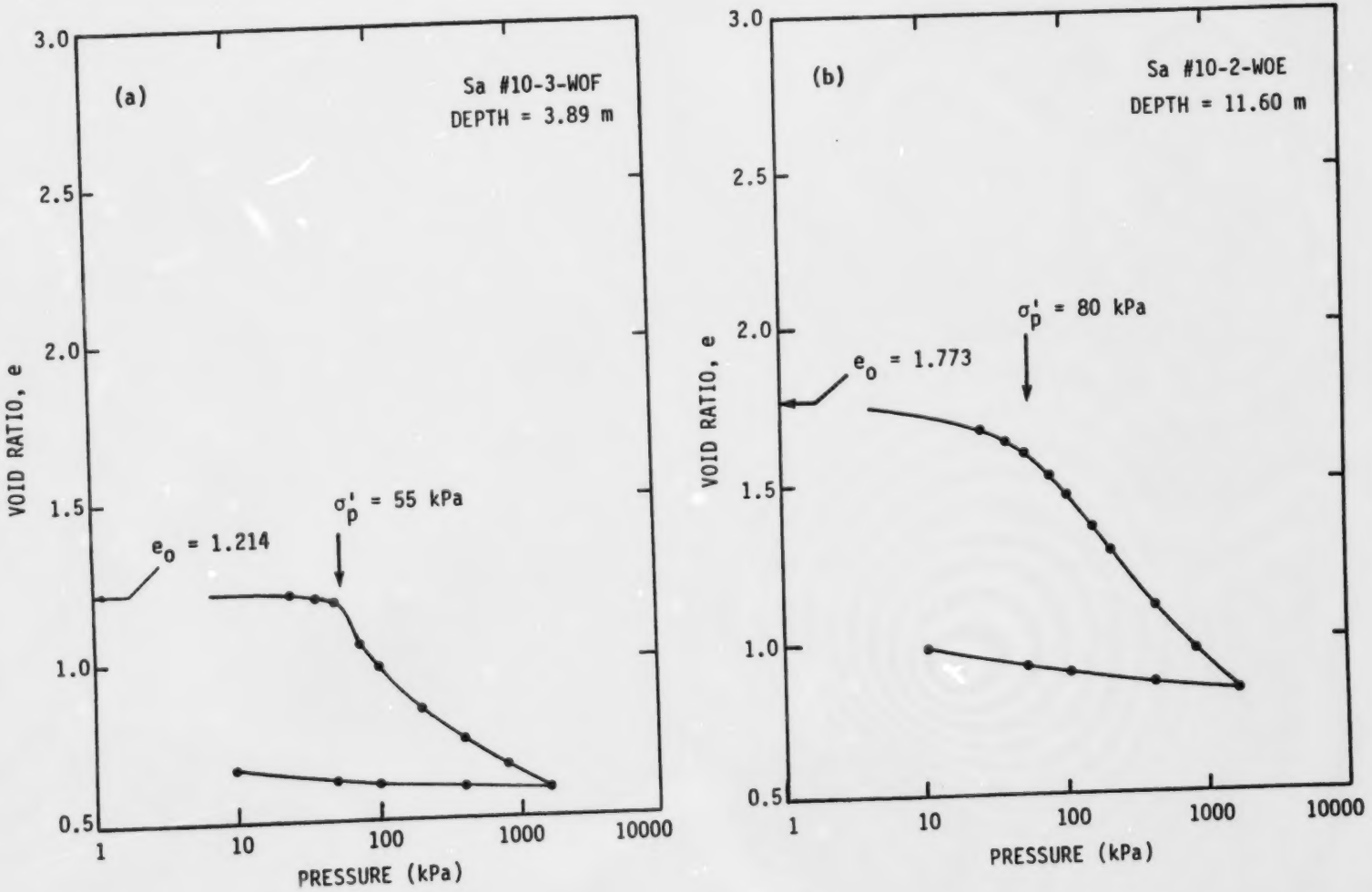

FIGURE 3. CONSOLIDATION CURVES OBTAINED ON TWO TEST SPECIMENS FROM SITE #10: (a) Sa #10-3-WOF AT 3.89 m; (b) Sa #10-2-WOE AT 11.60 m

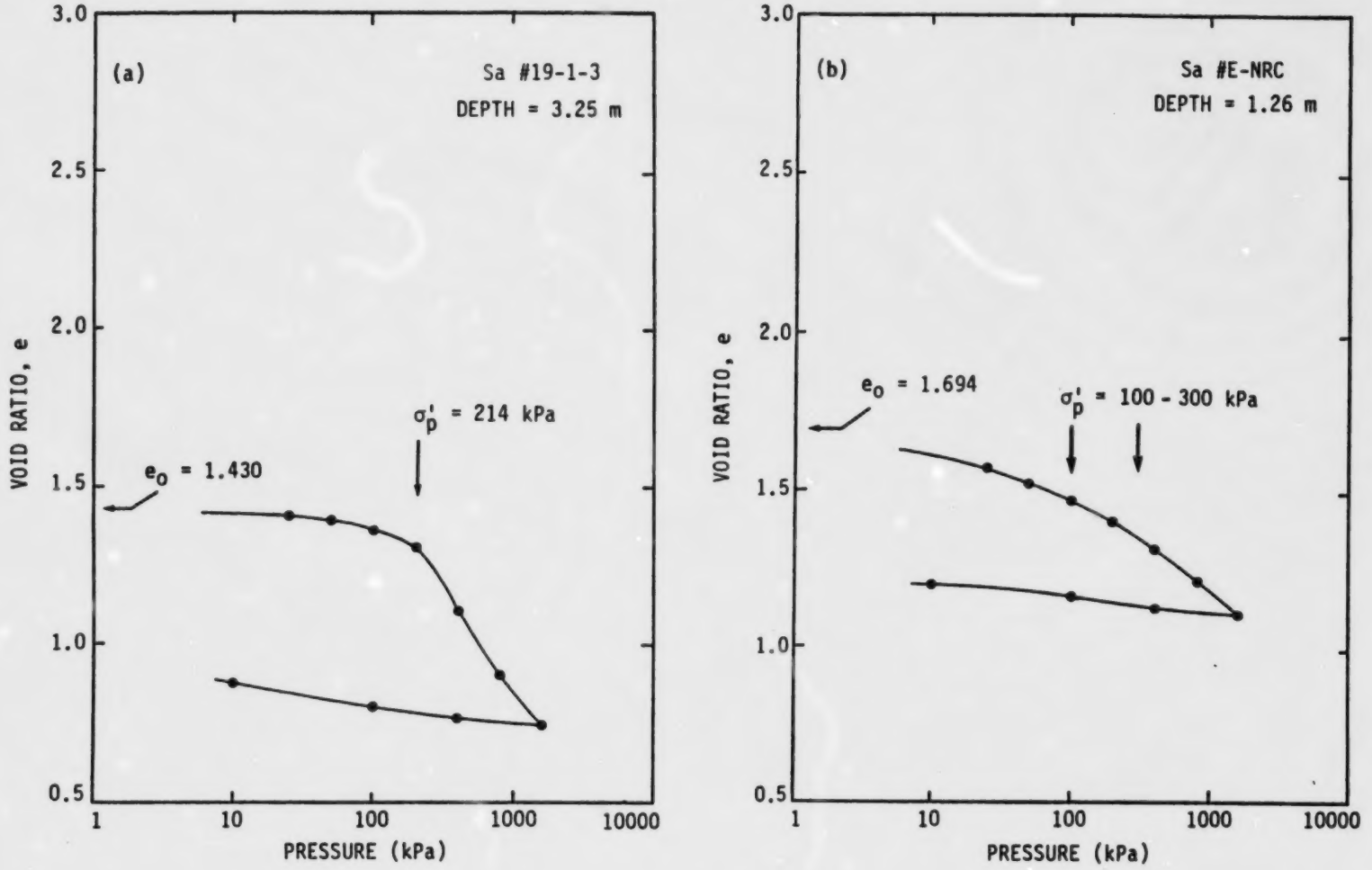

FIGURE 4. CONSOLIDATION CURVES OBTAINED ON TEST SPECIMENS: (a) SITE #19, SAMPLE #19-1-3 AT 3.25 m; (b) SITE #E, SAMPLE FROM 1.26 m

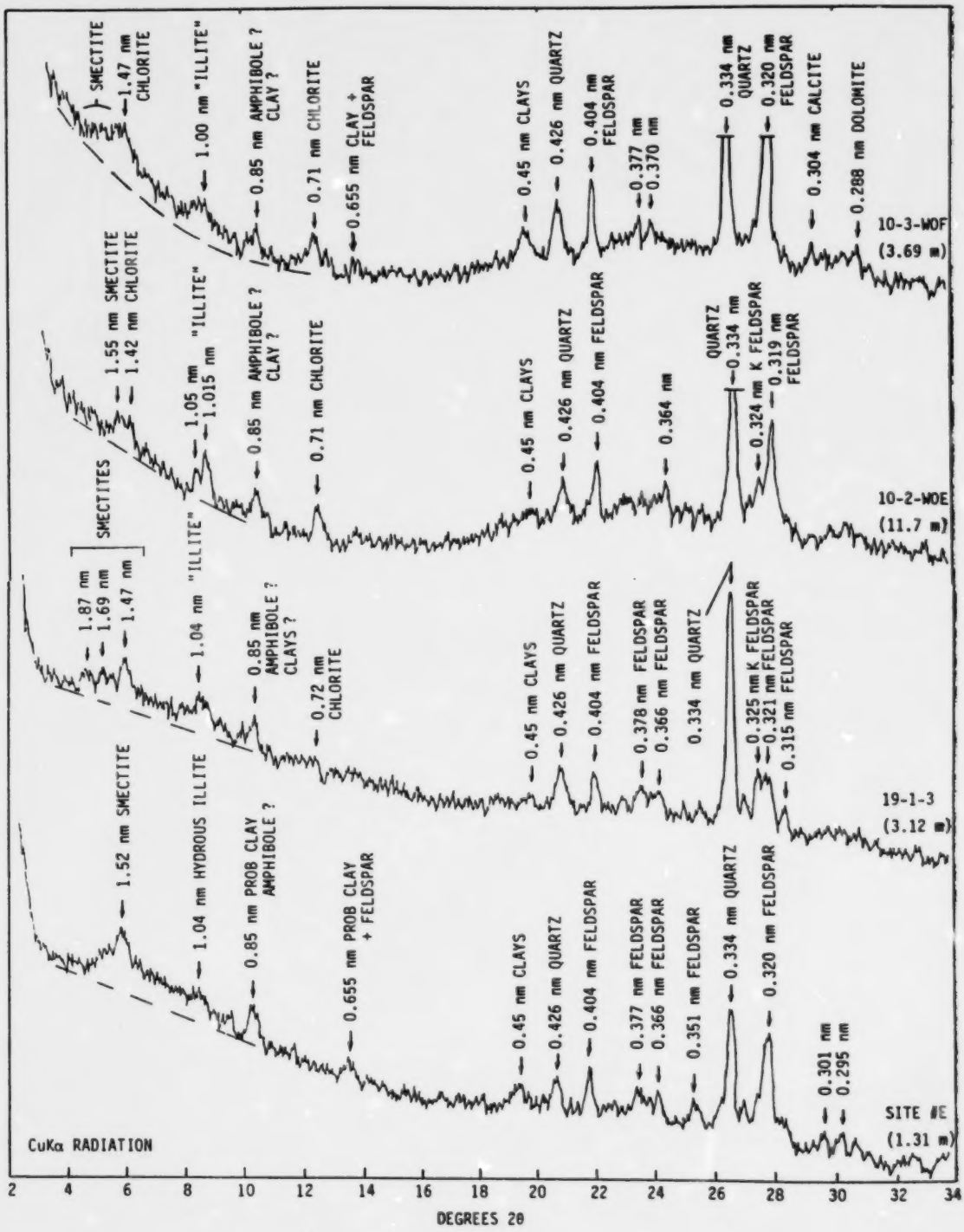

FIGURE 5. X-RAY POWDER PATTERNS OF THE FOUR LEDA CLAY TEST SOILS

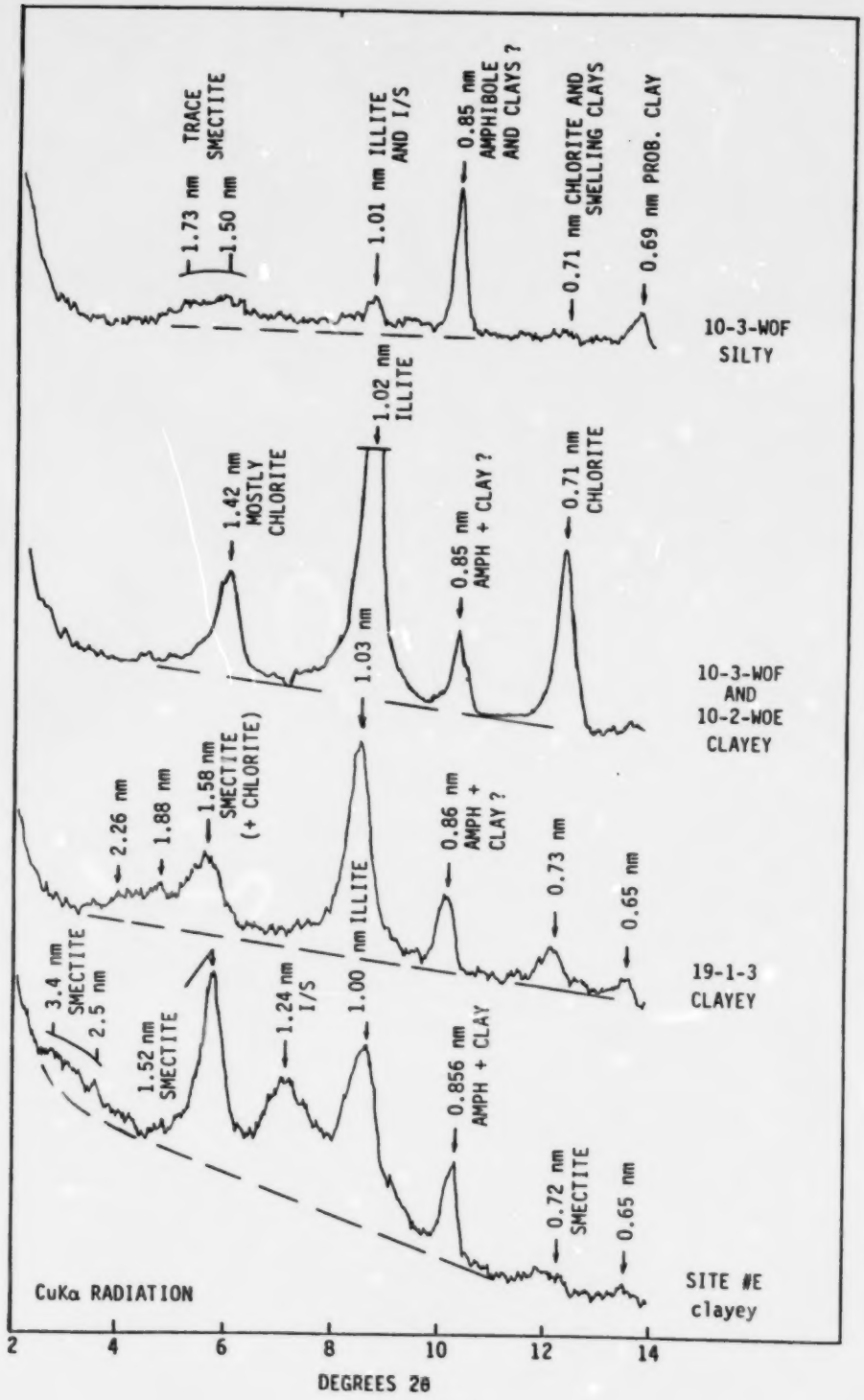

FIGURE 6. X-RAY TRACES OF WATER-WET, WHOLE SOIL TEST SAMPLES, PRESSURE ORIENTED AT 120 kPa

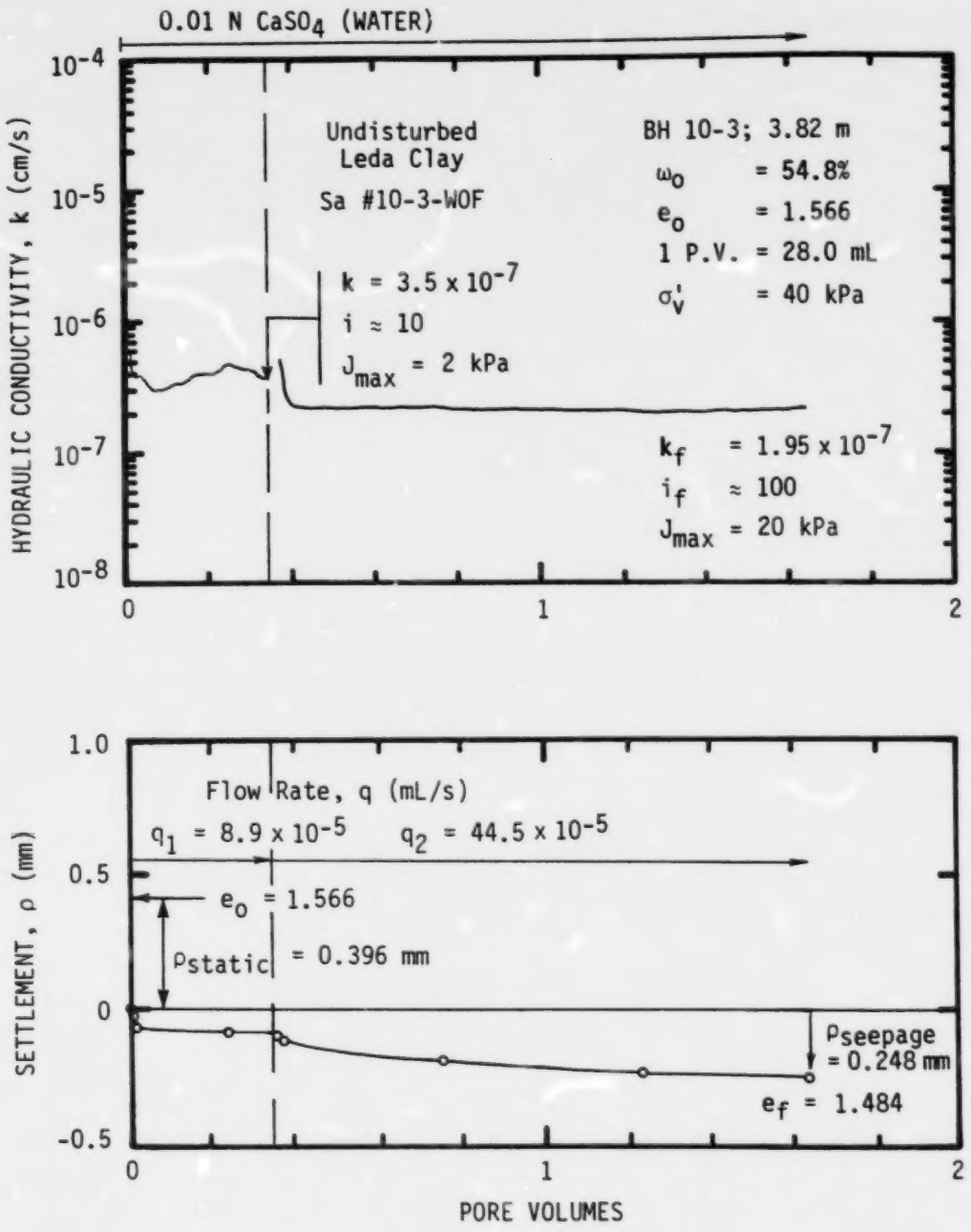

FIGURE 7. HYDRAULIC CONDUCTIVITY AND SETTLEMENT VS PORE VOLUMES; SITE 10, BH #10-3, 3.82 m DEPTH. REFERENCE PERMEANT: 0.01 N $CaSO_4$ SOLUTION IN WATER

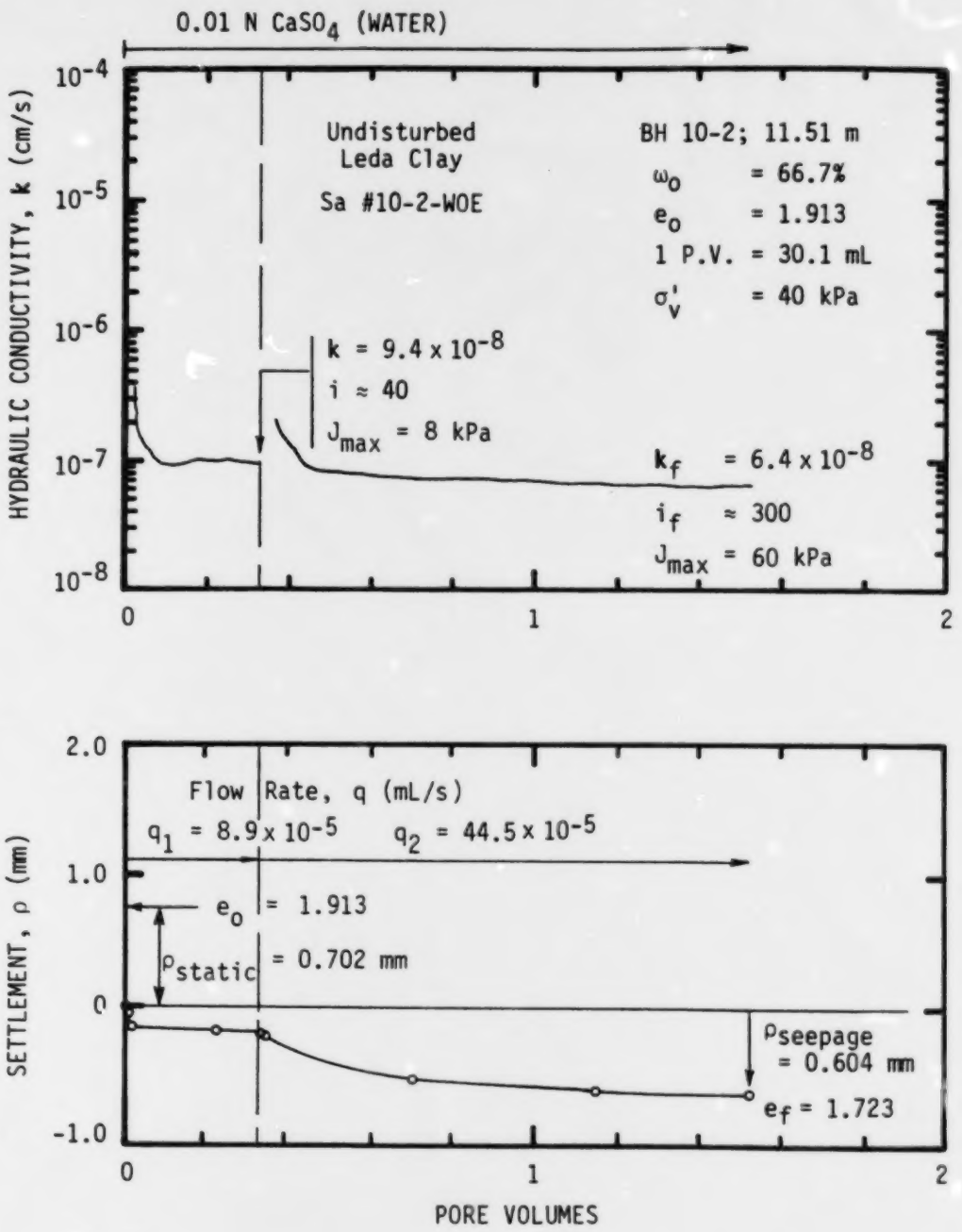

FIGURE 8. HYDRAULIC CONDUCTIVITY AND SETTLEMENT VS PORE VOLUMES; SITE 10, BH #10-2, 11.51 m DEPTH. REFERENCE PERMEANT: 0.01 N $CaSO_4$ SOLUTION IN WATER

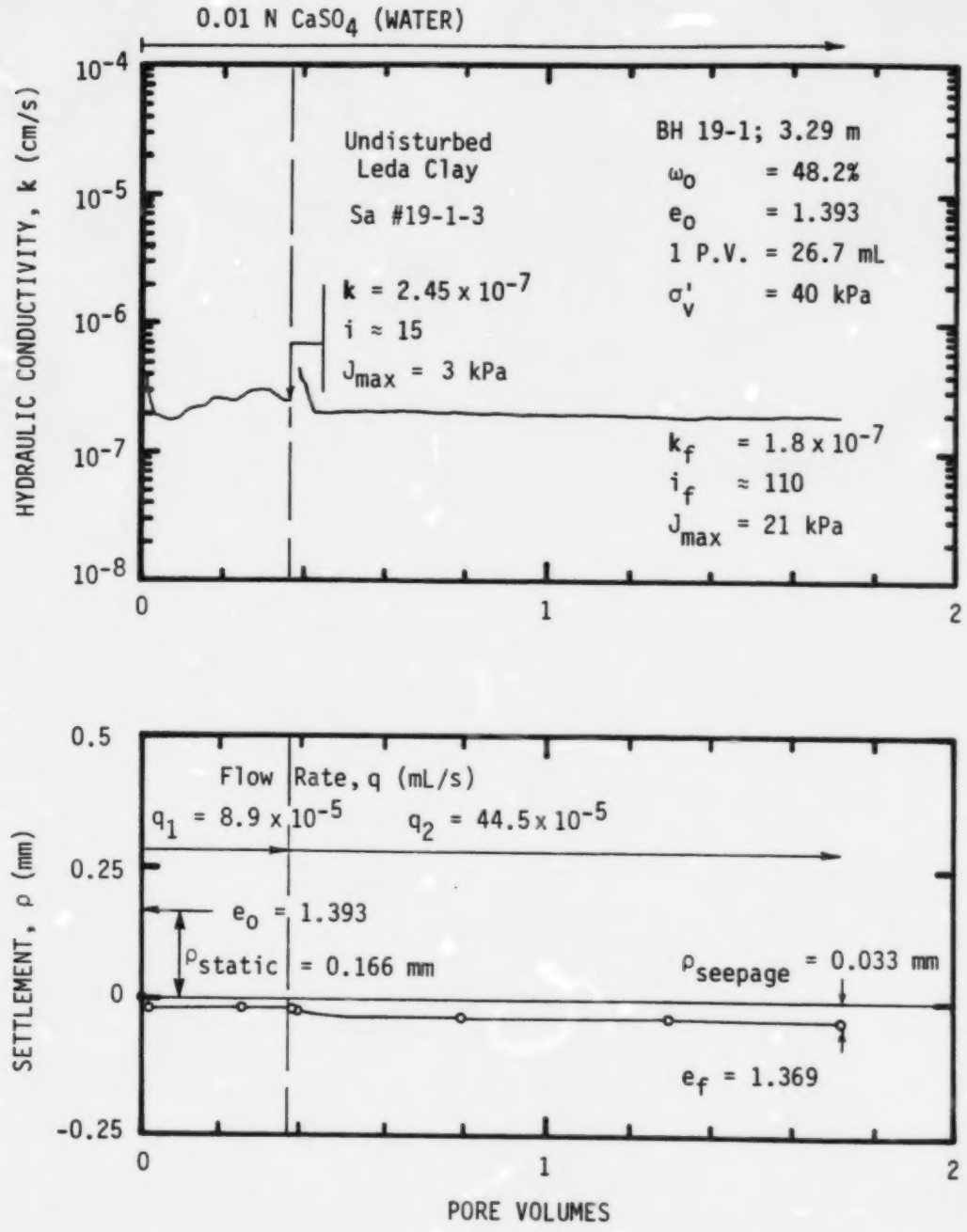

FIGURE 9. HYDRAULIC CONDUCTIVITY AND SETTLEMENT VS PORE VOLUMES; SITE 19, BH #19-1, 3.29 m DEPTH. REFERENCE PERMEANT: 0.01 N $CaSO_4$ SOLUTION IN WATER

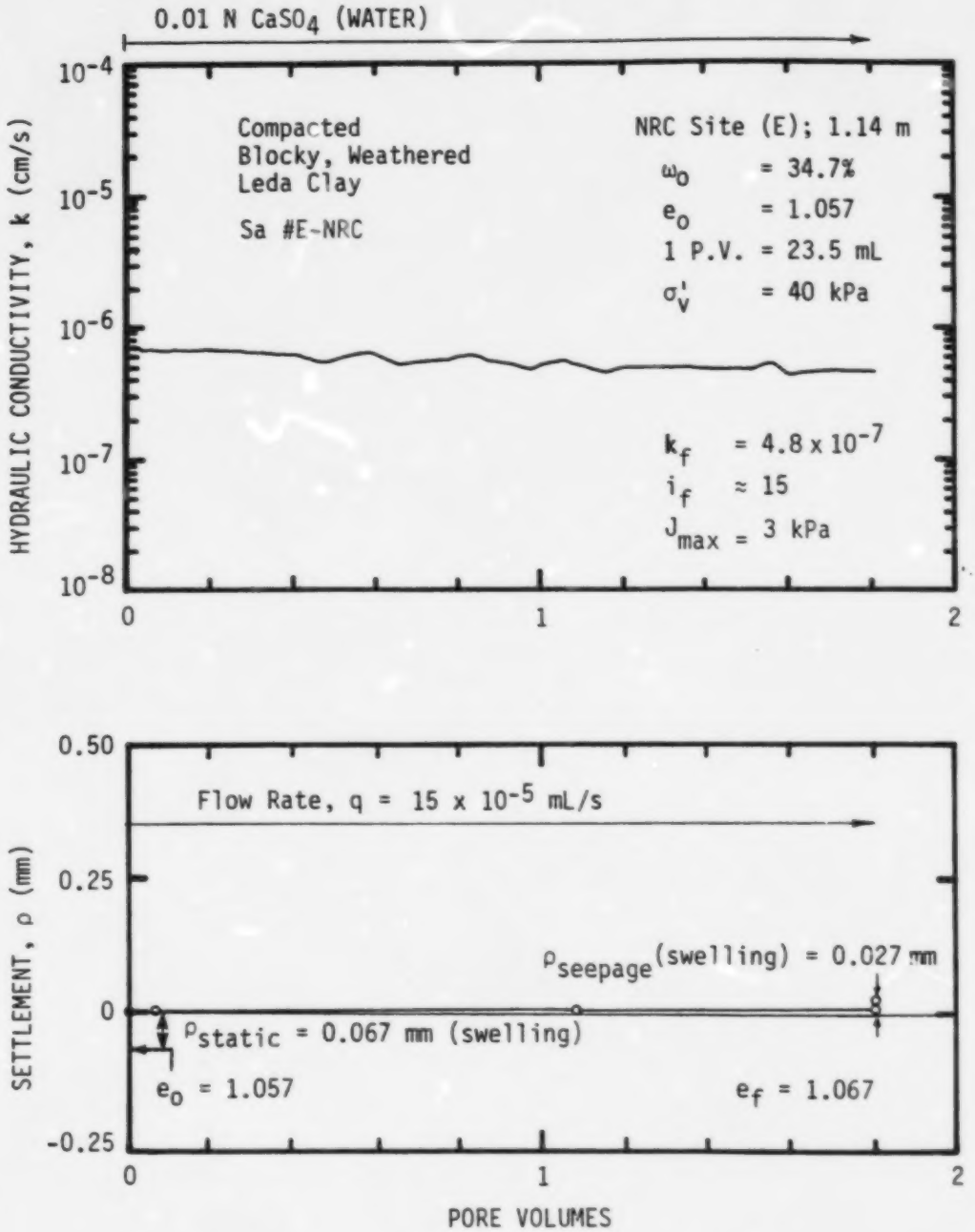

FIGURE 10. HYDRAULIC CONDUCTIVITY AND SETTLEMENT VS PORE VOLUMES, NRC SITE (E), 1.14 m DEPTH, COMPACTED. REFERENCE PERMEANT: 0.01 N $CaSO_4$ SOLUTION IN WATER

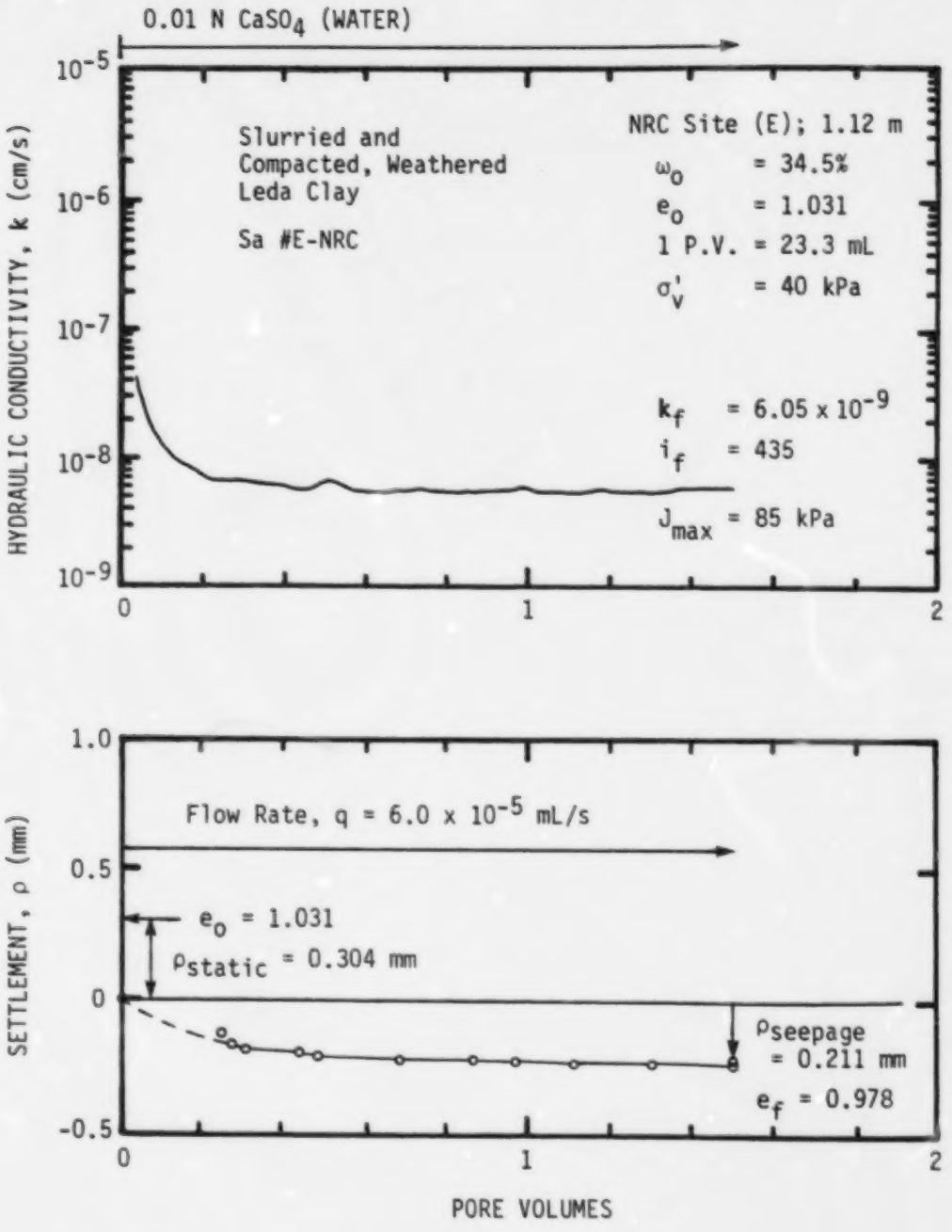

FIGURE 11. HYDRAULIC CONDUCTIVITY AND SETTLEMENT VS PORE VOLUMES, NRC SITE (E), 1.12 m DEPTH, SLURRIED AND COMPACTED. REFERENCE PERMEANT: 0.01 N $CaSO_4$ SOLUTION IN WATER

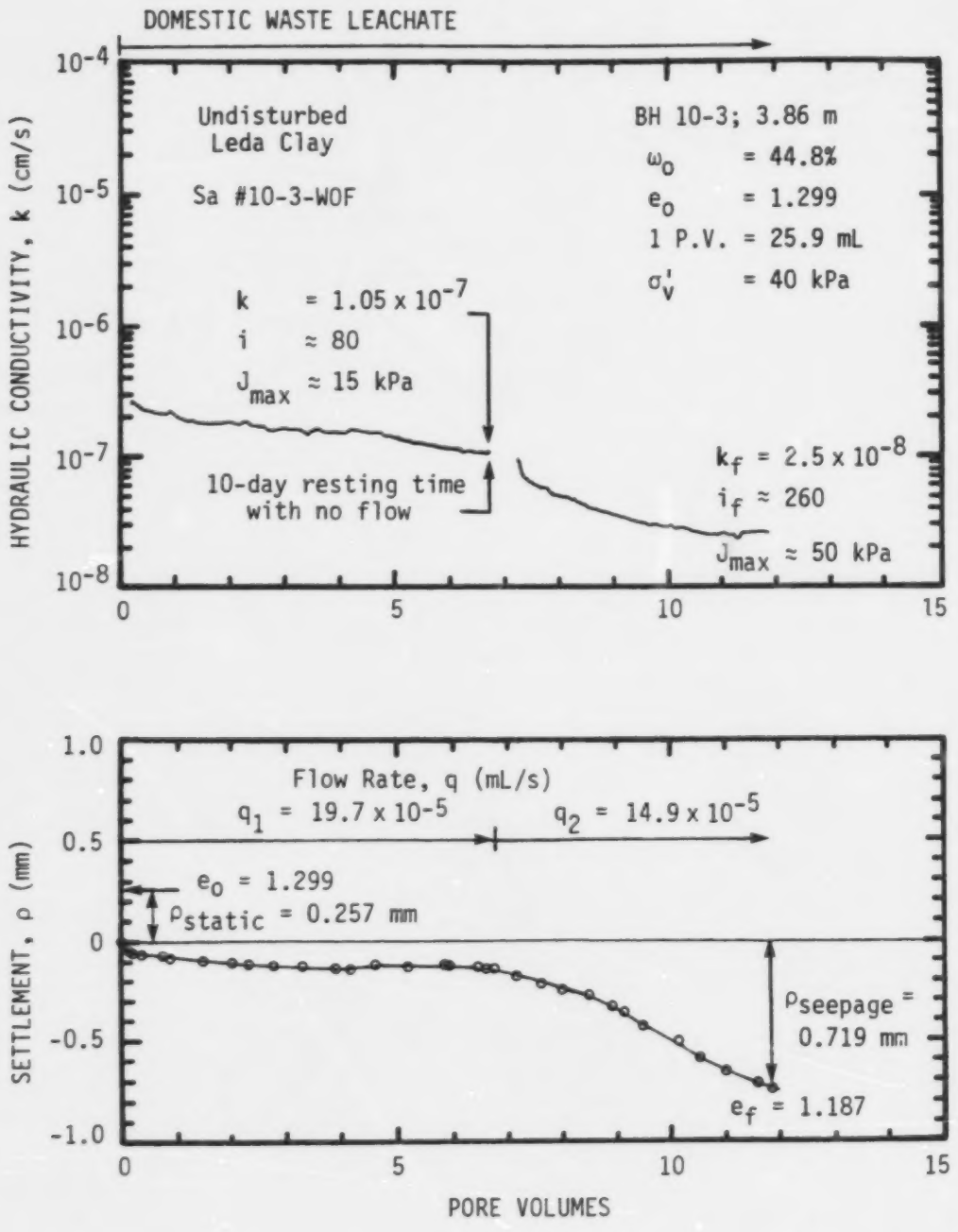

FIGURE 12. HYDRAULIC CONDUCTIVITY AND SETTLEMENT VS PORE VOLUMES; SITE 10, BH #10-3, 3.86 m DEPTH. PERMEANT: DOMESTIC WASTE LEACHATE

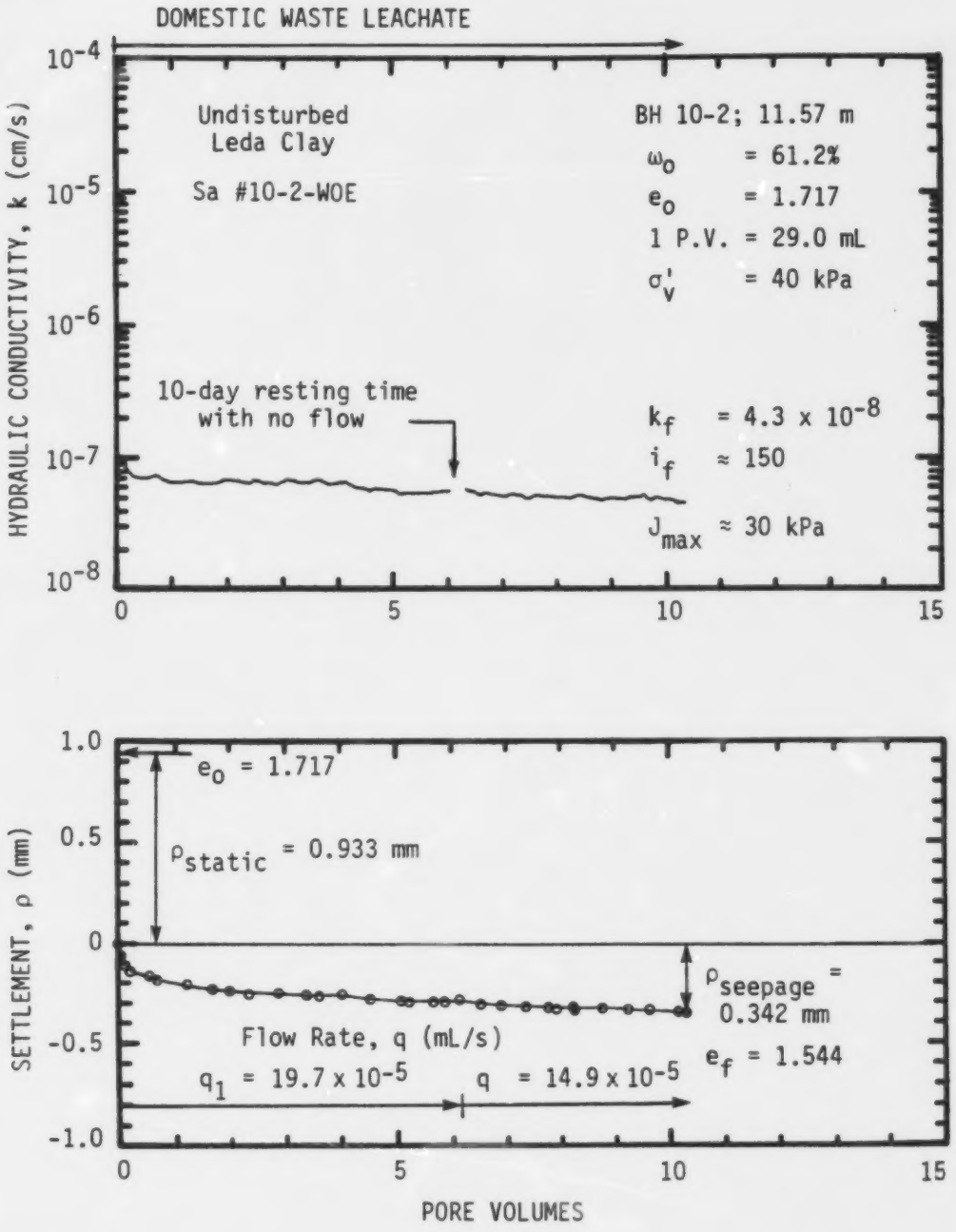

FIGURE 13. HYDRAULIC CONDUCTIVITY AND SETTLEMENT VS PORE VOLUMES; SITE 10, BH #10-2, 11.57 m DEPTH. PERMEANT: DOMESTIC WASTE LEACHATE

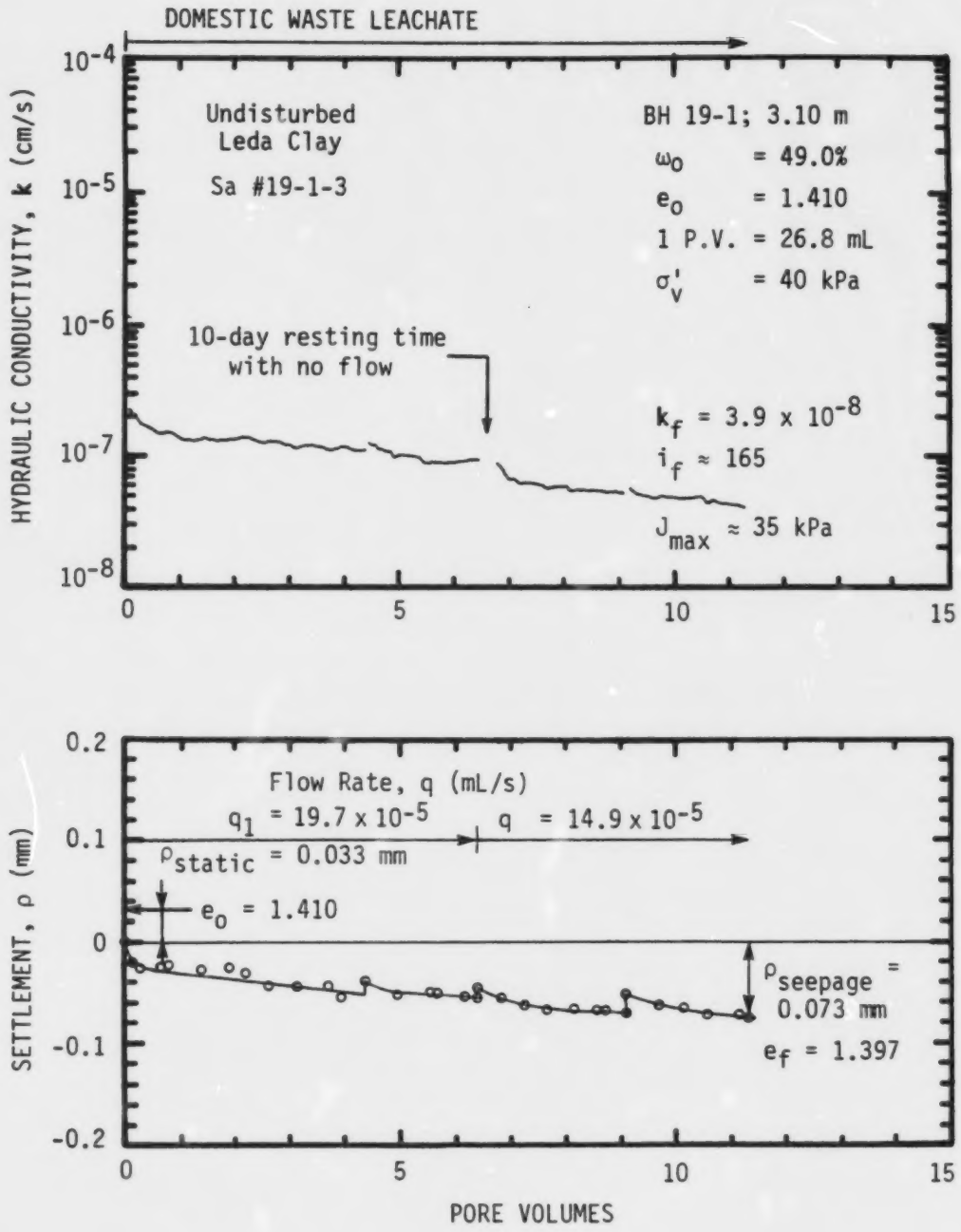

FIGURE 14. HYDRAULIC CONDUCTIVITY AND SETTLEMENT VS PORE VOLUMES; SITE 19, BH #19-1, 3.10 m DEPTH. PERMEANT: DOMESTIC WASTE LEACHATE

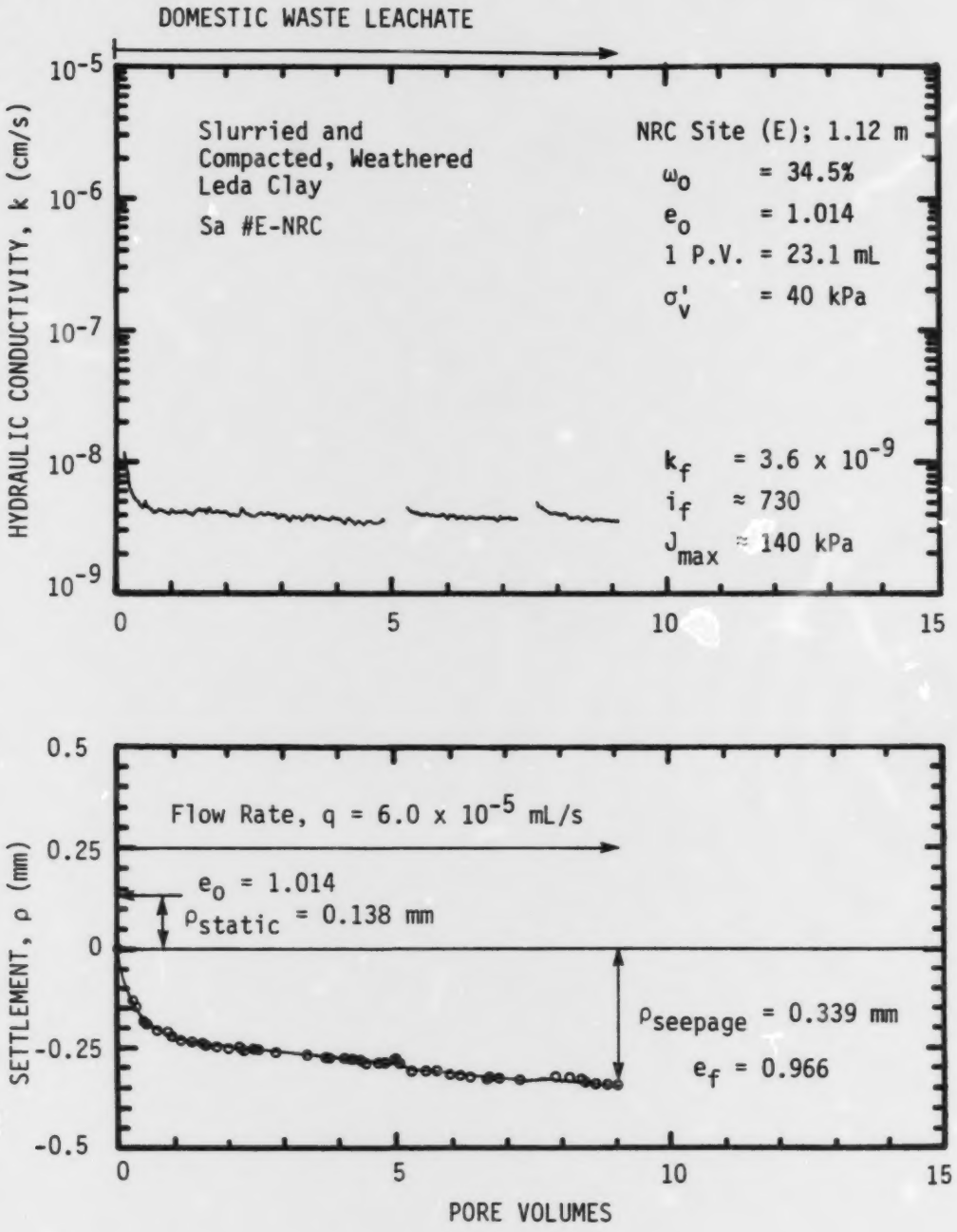

FIGURE 15. HYDRAULIC CONDUCTIVITY AND SETTLEMENT VS PORE VOLUMES; NRC SITE (E); 1.12 m DEPTH, SLURRIED AND COMPACTED. PERMEANT: DOMESTIC WASTE LEACHATE

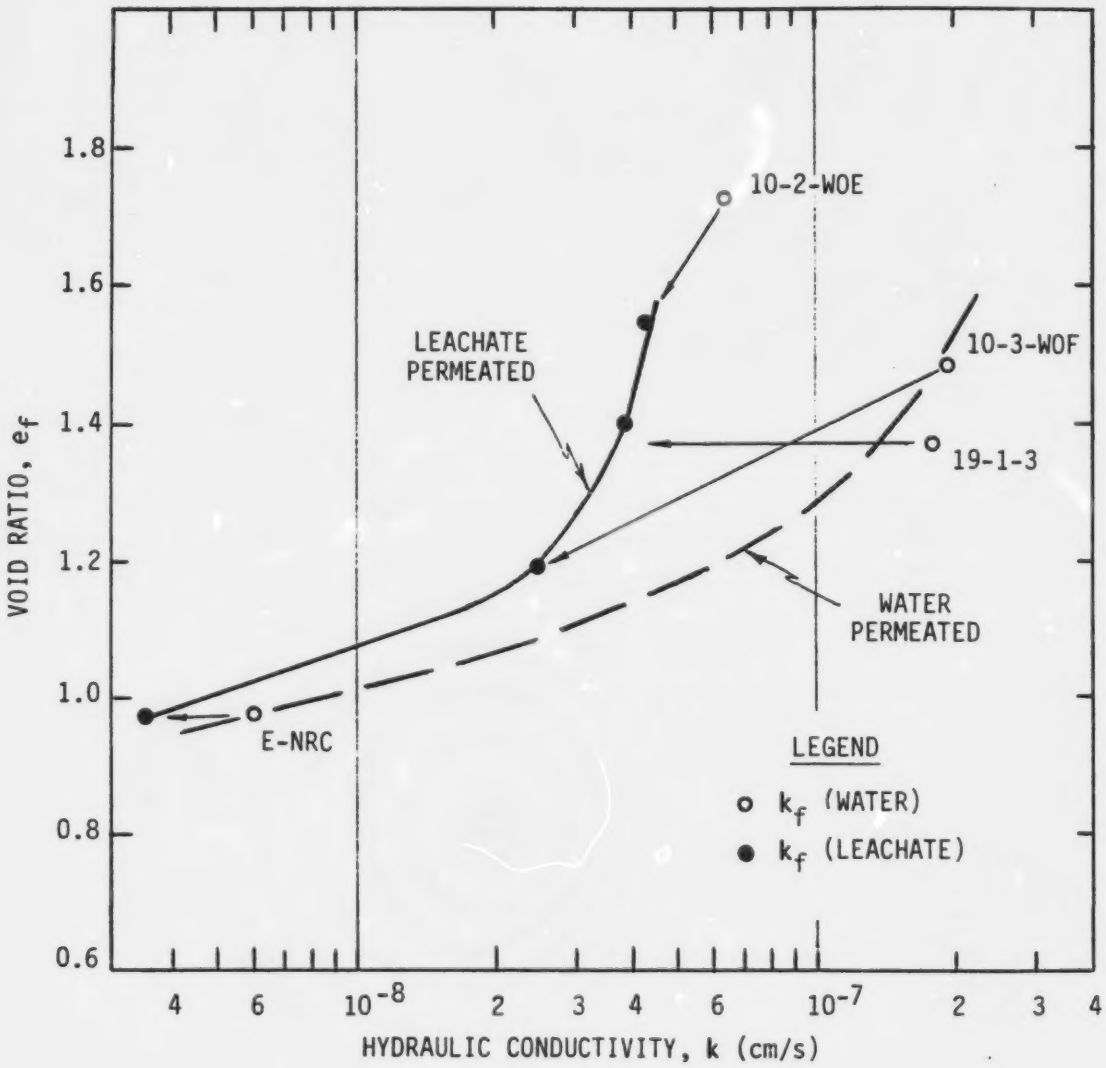

FIGURE 16. SUMMARY PLOT SHOWING EFFECT OF LEACHATE PERMEATION ON THE HYDRAULIC CONDUCTIVITY OF THE FOUR LEDA TEST CLAYS

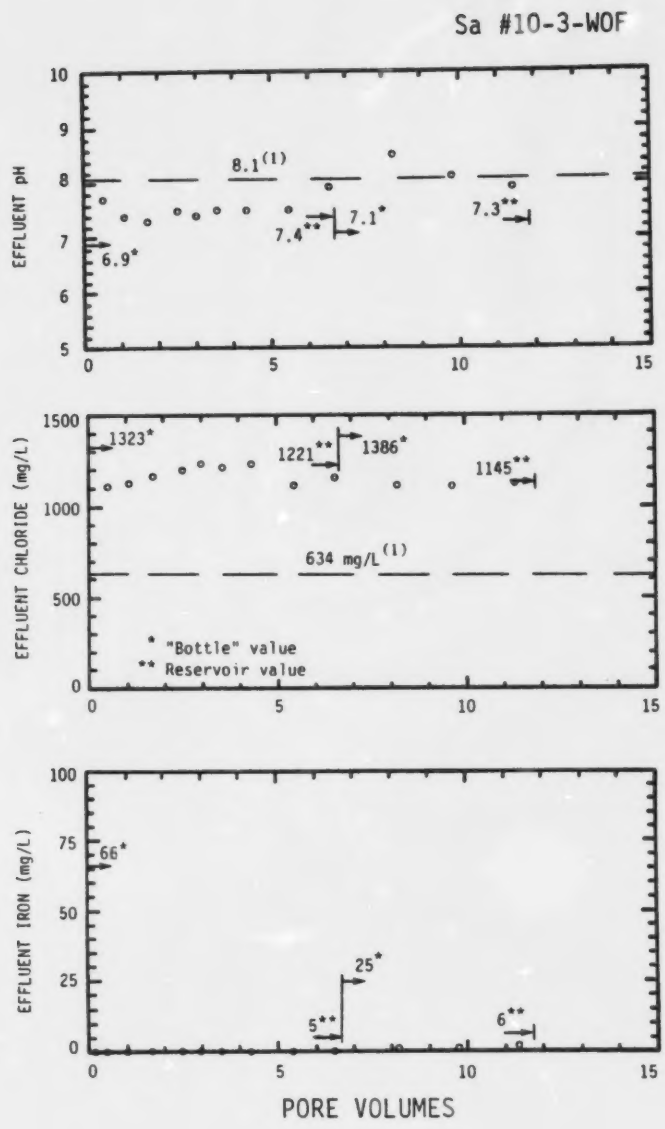

FIGURE 17. EFFLUENT pH, CHLORIDE AND IRON VS PORE VOLUMES; SITE 10, BH #10-3, 3.86 m DEPTH
PERMEANT: DOMESTIC WASTE LEACHATE

Note: (1) "Initial Pore Water" Value indicated by dashed line

Sa #10-3-WOF

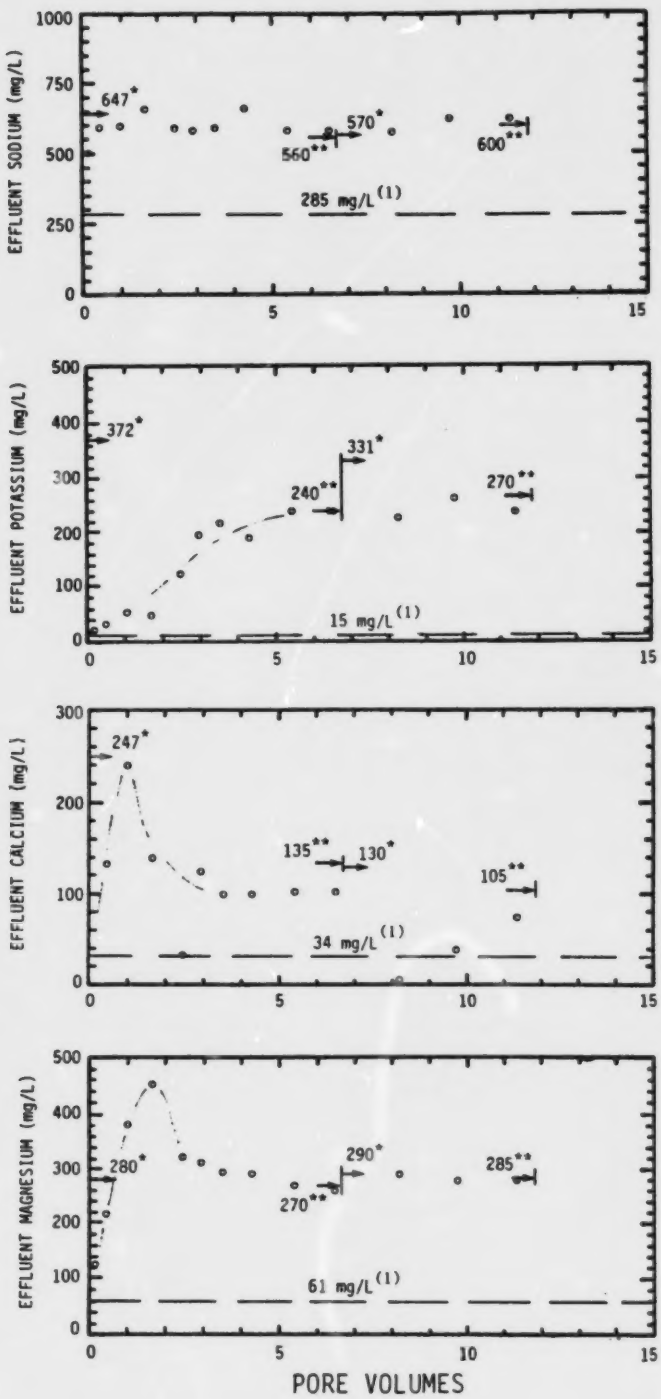

FIGURE 18. EFFLUENT SODIUM, POTASSIUM, CALCIUM AND MAGNESIUM VS PORE VOLUMES; SITE 10, BH #10-3, 3.86 m DEPTH
PERMEANT: DOMESTIC WASTE LEACHATE
Note: (1) "Initial Pore Water" Value indicated by dashed line

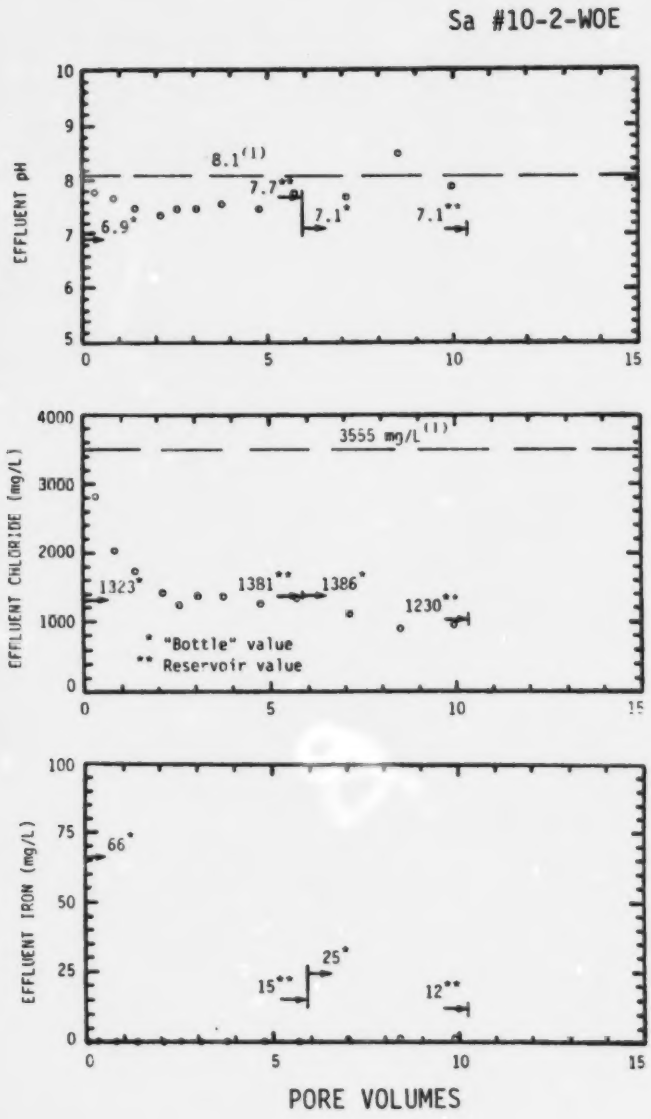

FIGURE 19. EFFLUENT pH, CHLORIDE AND IRON VS PORE VOLUMES; SITE 10, BH #10-2, 11.57 m DEPTH
PERMEANT: DOMESTIC WASTE LEACHATE
Note: (1) "Initial Pore Water" Value indicated by dashed line

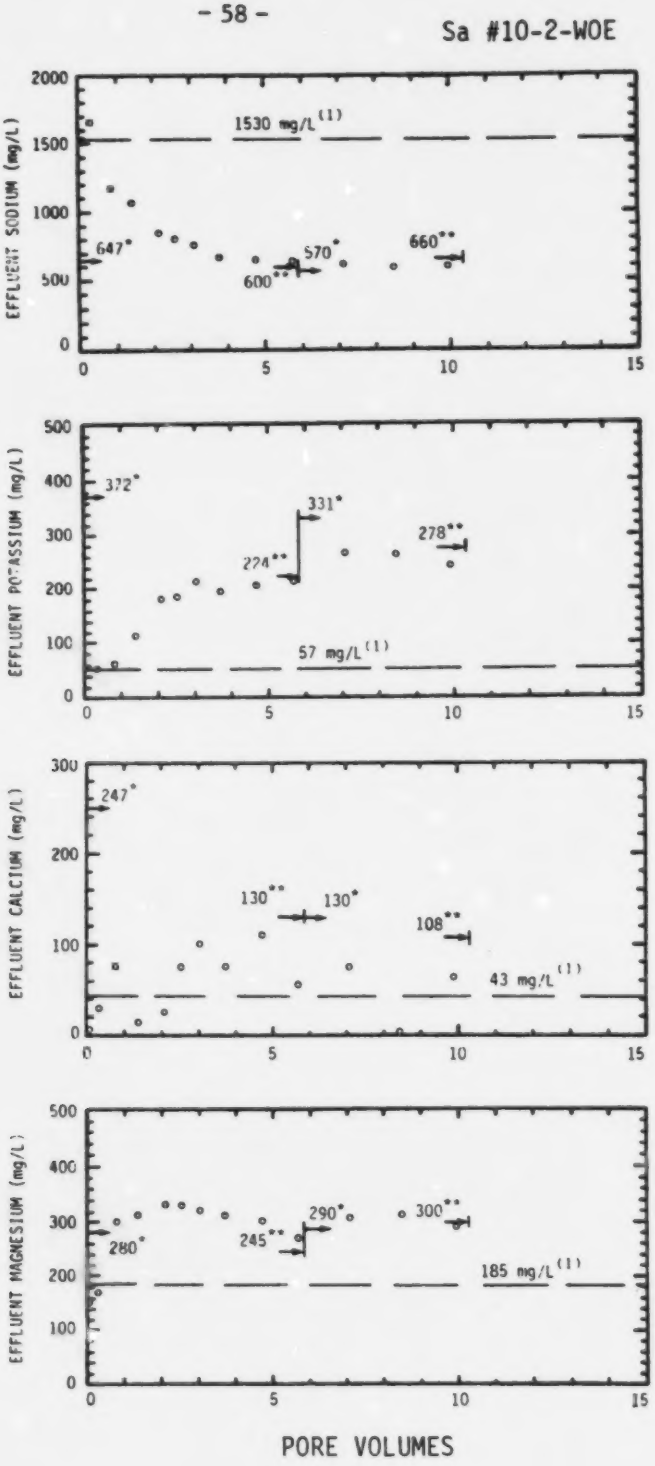

FIGURE 20. EFFLUENT SODIUM, POTASSIUM, CALCIUM AND MAGNESIUM VS PORE VOLUMES; SITE 10, BH #10-2, 11.57 m DEPTH
PERMEANT: DOMESTIC WASTE LEACHATE
Note: (1) "Initial Pore Water" Value indicated by dashed line

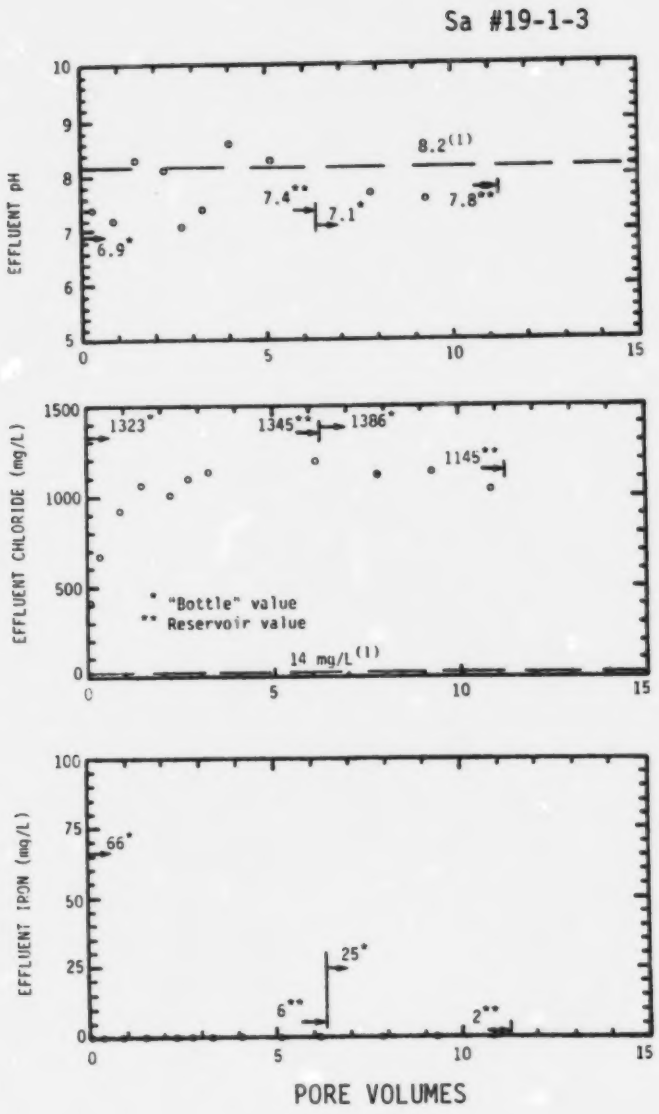

FIGURE 21. EFFLUENT pH, CHLORIDE AND IRON VS PORE VOLUMES; SITE 19, BH #19-1, 3.10 m DEPTH
PERMEANT: DOMESTIC WASTE LEACHATE

Note: (1) "Initial Pore Water" Value indicated by dashed line

Sa #19-1-3

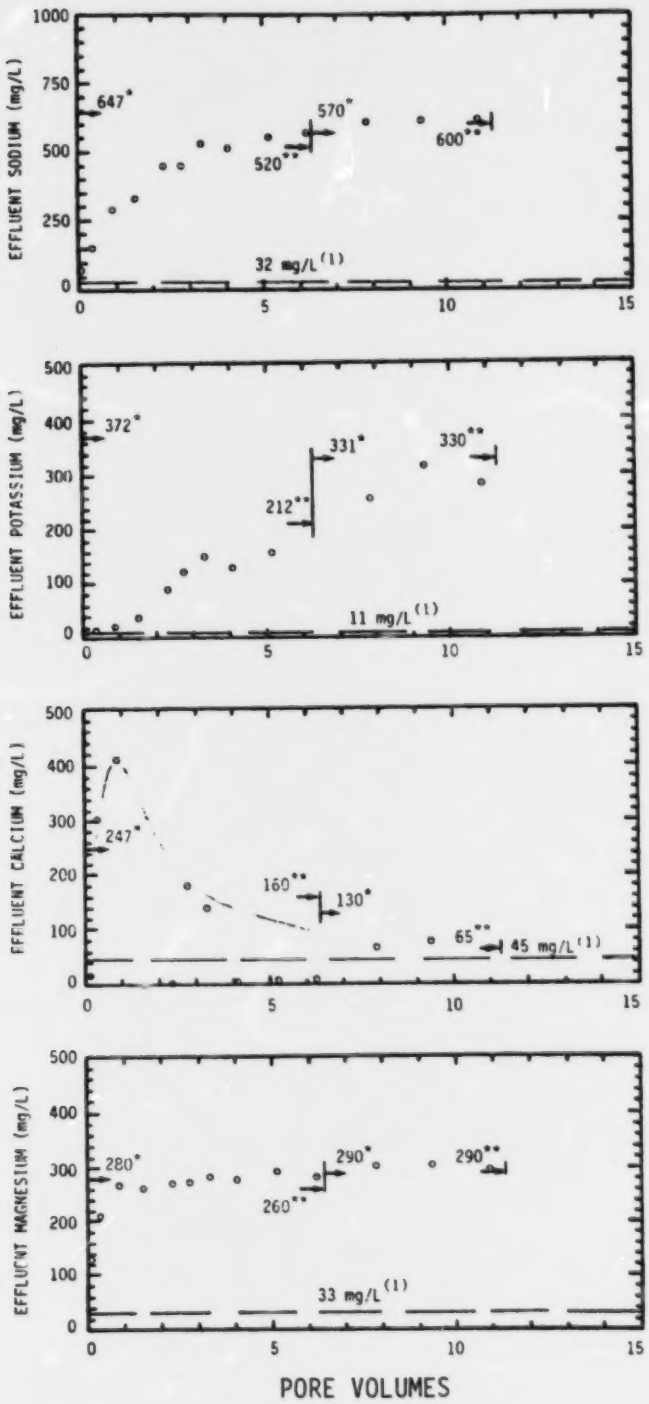

FIGURE 22. EFFLUENT SODIUM, POTASSIUM, CALCIUM AND MAGNESIUM VS PORE VOLUMES; SITE 19, BH #19-1, 3.10 m DEPTH
PERMEANT: DOMESTIC WASTE LEACHATE
Note: (1) "Initial Pore Water" Value indicated by dashed line

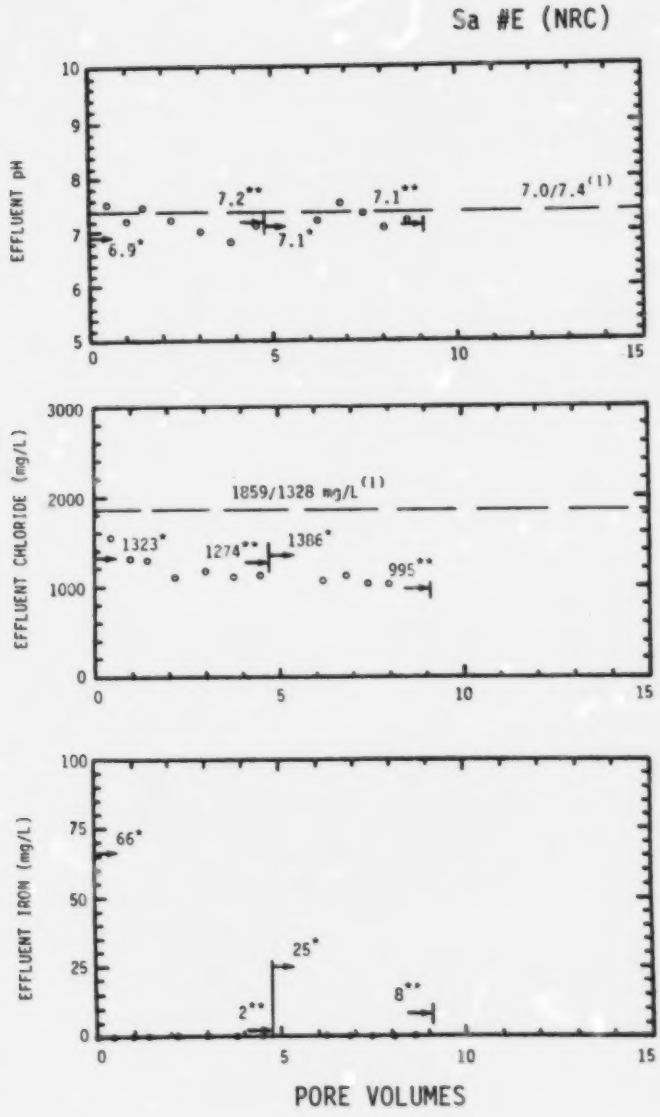

FIGURE 23. EFFLUENT pH, CHLORIDE AND IRON VS PORE VOLUMES; NRC SITE (E), 1.12 m DEPTH
PERMEANT: DOMESTIC WASTE LEACHATE

Note: (1) "Initial Pore Water" Value indicated by dashed line

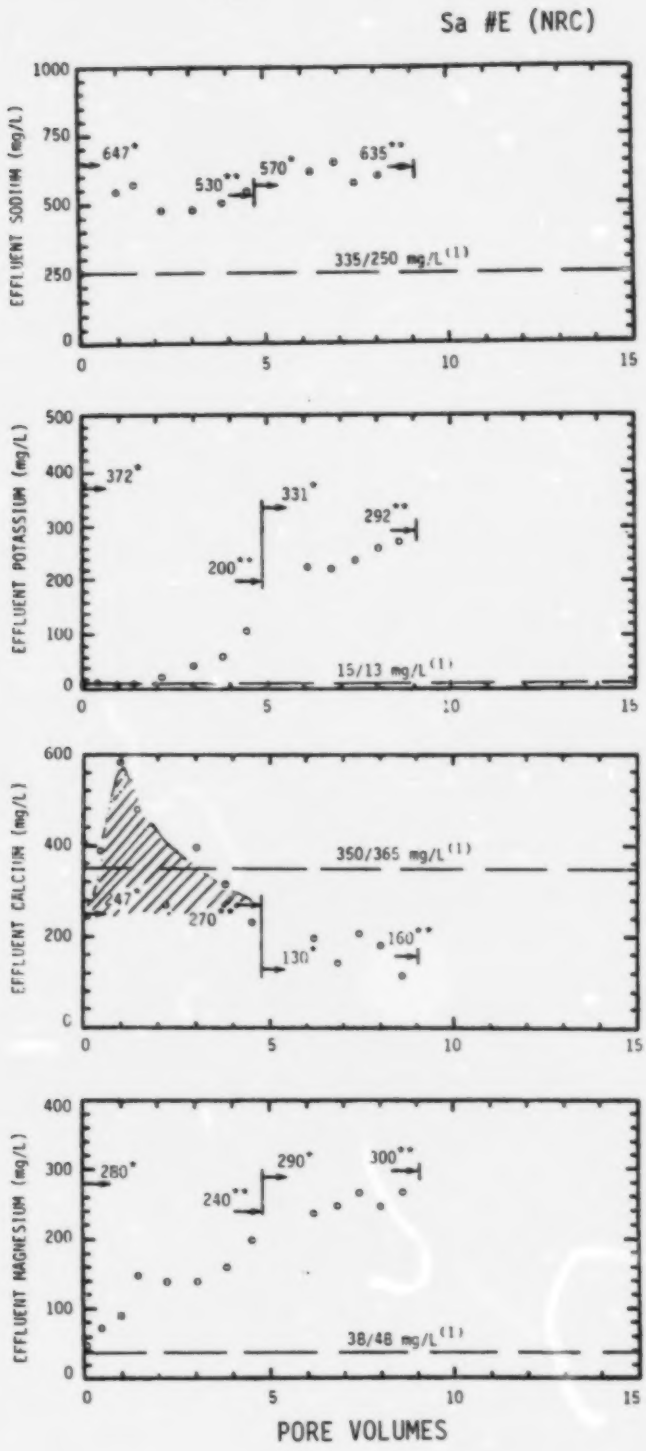

FIGURE 24. EFFLUENT SODIUM, POTASSIUM CALCIUM AND MAGNESIUM VS PORE VOLUMES; NRC SITE (E), 1.12 m DEPTH
PERMEANT: DOMESTIC WASTE LEACHATE
Note: (1) "Initial Pore Water" Value indicated by dashed line

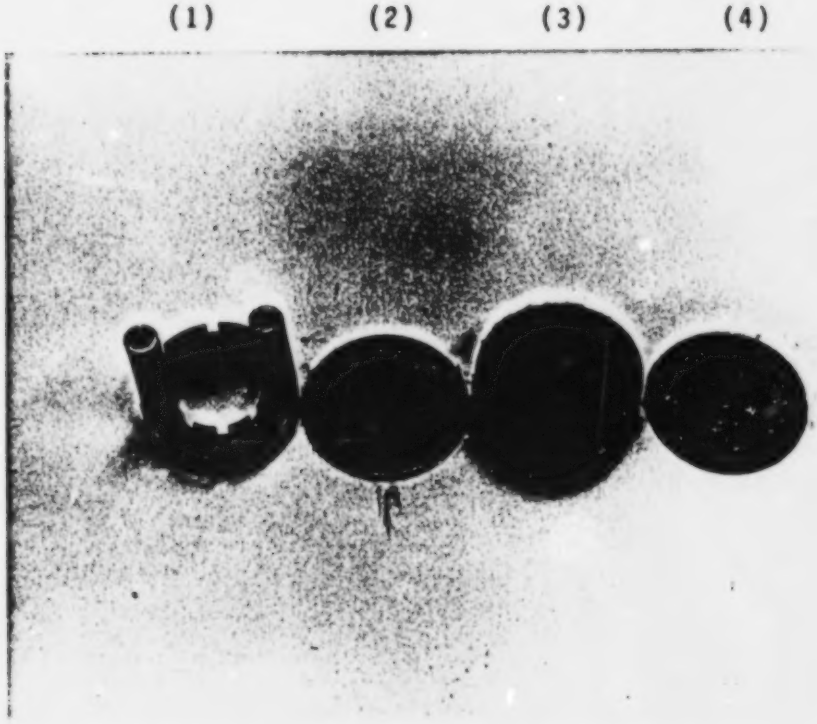

FIGURE 25. DISMANTLED PERMEAMETER CELL USED FOR Sa #19-1-3 SHOWING BLACK SLIME ACCUMULATION: (1) TWO SPRING LOADING SYSTEM; (2) TOP POROUS STONE; (3) SOIL SAMPLE WITH FILTER PAPER ON TOP; (4) CLEAN BOTTOM STONE

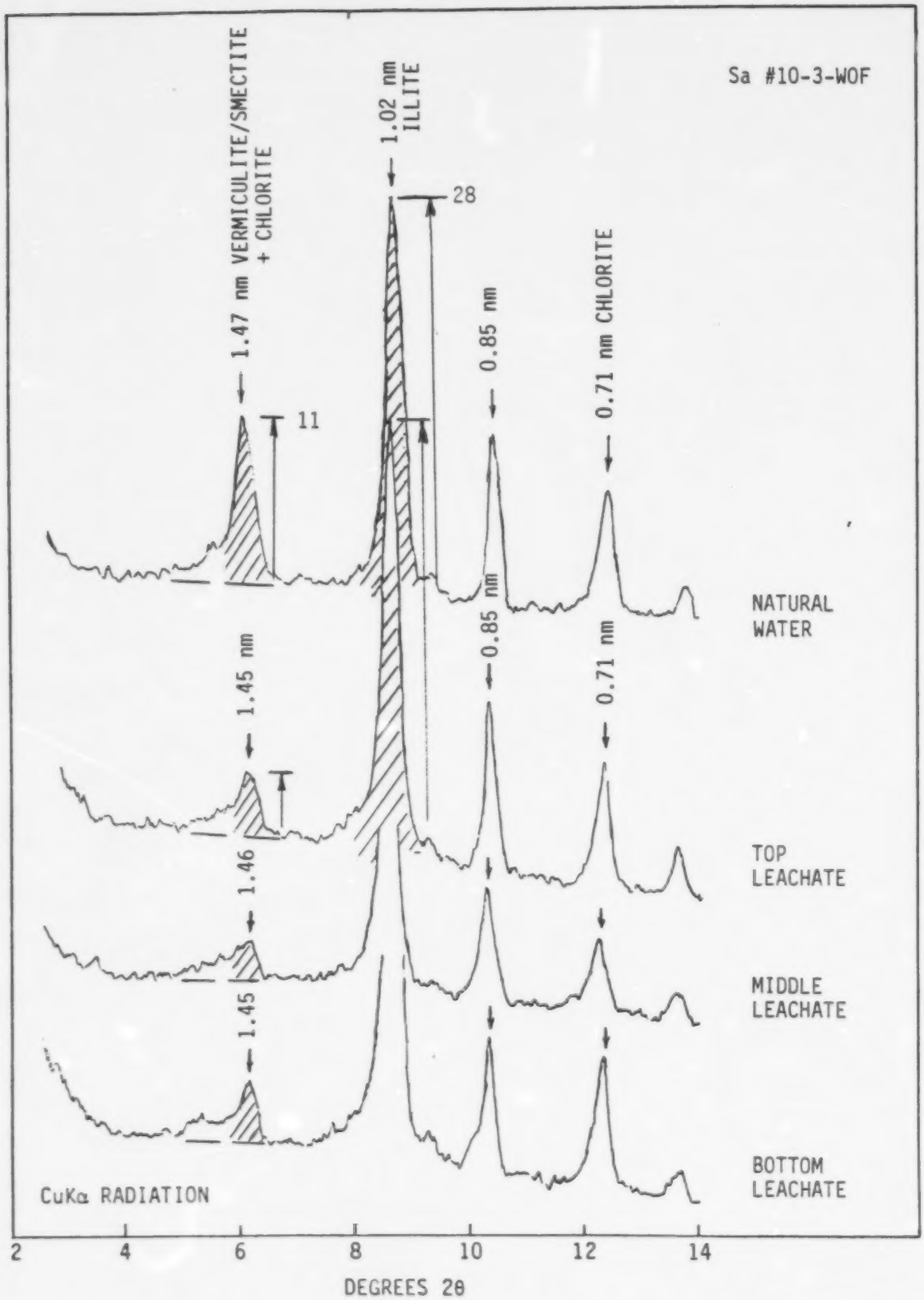

FIGURE 26. X-RAY TRACES OF PRESSURE ORIENTED, WHOLE SOIL SPECIMEN OF Sa #10-3-WOF, BEFORE AND AFTER LEACHATE PERMEATION

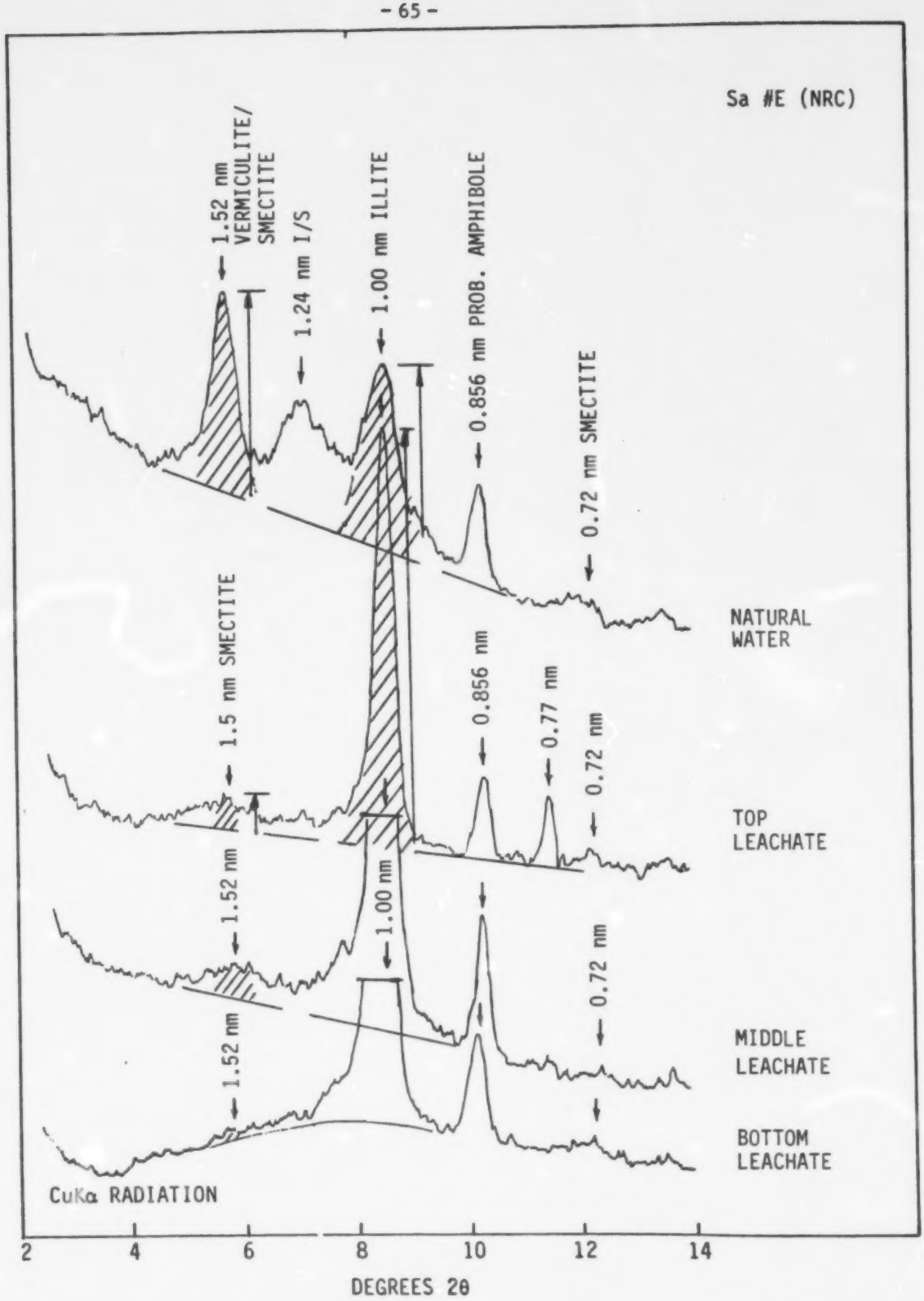

FIGURE 27. X-RAY TRACES OF PRESSURE ORIENTED, WHOLE SOIL SPECIMENS OF Sa #E (NRC)

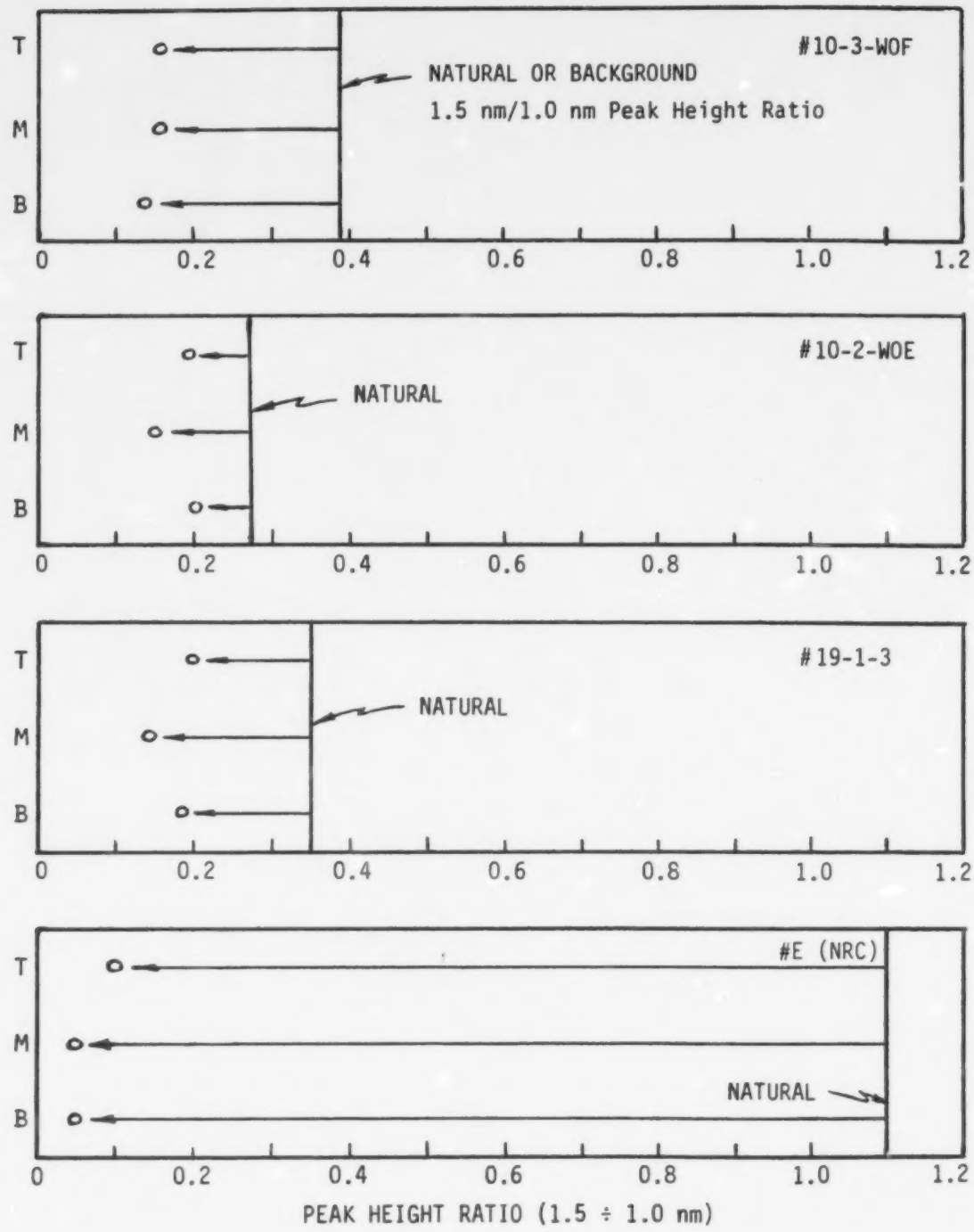

FIGURE 28. SUMMARY PLOT OF 1.5 nm/1.0 nm PEAK HEIGHT RATIOS SHOWING COLLAPSE CAUSED BY K^+ ADSORPTION AND FIXATION

[T, M, B = Top, middle and bottom of 20 mm thick test specimen]

APPENDIX I

TESTING PROGRAM TO SELECT THE FOUR TYPICAL LEDA CLAY SAMPLES

I.1 Leda Clay Sampling Locations

I.2 Laboratory Test Methods

I.3 Results

I.3.1 Site #10

I.3.2 Site #19

I.3.3 Site #E (NRC)

I.4 Discussion

I.5 Recommendations

[Most of this Appendix was submitted as Progress Report #2 on January 22, 1988. Figures 1 and 2 are modified and discussed in the main text.]

I.1 Leda Clay Sampling Locations

Following extensive discussion with MacLaren Engineers and Mr. R.A. Dunn, P.Eng., our Ministry of the Environment Liaison Officer, three sites having different types of Leda clay were selected for study.

Details concerning the boreholes, sample numbers and elevations of available samples from the three sites are presented in Table I-1. A brief summary of each group of samples is presented below:

Site #10 (Candidate Landfill Site)

Soil samples from this important site were obtained on July 31, 1987 by Mr. F. Fernandez who participated in the field investigations carried out by Geocon Inc. A total of seven 3-inch diameter Shelby tube samples (Table 1) were returned to The University of Western Ontario packed in ice for storage in a cold room at 8°C. Most of the samples consisted of soft grey Leda with high water contents of 30 to 105%. Till material underlying the clay was collected in a plastic bag and stored with the Shelby tubes.

A suite of disturbed samples obtained by Water and Earth Science Associates Ltd. during a preliminary assessment of Site #10 was received during the summer of 1987.

Site #19 (Potential Energy-from-Waste Site)

Two 3-inch diameter Shelby tube samples from this site were obtained from Geocon Inc. in October 1987. The samples were taken on September 14-15, 1987 and were surplus to the testing needs of Geocon Inc. These samples consisted of stiff to very stiff grey Leda clay at water contents of 49 to 53%.

Site #E (National Research Council)

A single 3-inch diameter Shelby tube sample, taken on October 30, 1987 was sent to Western by Dr. K.T. Law of the Geotechnical Section of the Institute for Research in Construction at NRC. The sample was a highly fissured, desiccated, very stiff grey Leda clay at a water content of 35 to 40%.

I.2 Laboratory Test Methods

I.2.1 Mineralogy

Semi-quantitative mineralogical analyses were carried out on Leda clay samples from Sites #10, #19 and #E (NRC). The investigation included the following:

(a) X-ray powder patterns on whole soil samples to identify the bulk mineralogy

(b) X-ray traces on untreated (natural), oriented < 2 μm fraction: water wet, air dried and glycolated

(c) X-ray traces on K^+ saturated, oriented < 2 μm fraction: water wet, air dried, glycolated and heat treated at 550°C for 30 minutes.

I.2.2 Soil and Porewater Chemistry

The chemical analyses included the determination of cation concentrations in solution, carbonate content, pH, salinity and chloride content.

The solution analyses were carried out on pore water squeezed from the clay samples at pressures of 10 and 17 MPa. The concentrations of Na^+, Mg^{++}, Ca^{++} and K^+ were measured by atomic absorption spectrometry.

Porewater salinity was determined by electrical conductivity measurements using NaCl reference. The chloride content was determined using a specific ion electrode, and the pH of the pore water was measured with a pH meter.

The percentage of carbonate was determined by a gasometric method using the Chittick apparatus.

I.2.3 Index Tests

Liquid limits, w_L, were determined for all clay samples using the Casagrande apparatus (ASTM 423-66). The plastic limits, w_p, were obtained according to the procedure recommended by ASTM D424-49. All moisture contents, w, were measured by oven drying the soils at a temperature of - 110°C for about twenty-four hours.

I.2.4 Consolidation Tests

A total of six consolidation tests were run on the Leda clay samples using lever type, fixed ring oedometers. The samples from Sites #E (NRC) and #19 were tested applying loads in a geometrical progression with a load increment ratio, $\Delta p/p = 1$ (25, 50, 100, 200, 400, 800 and 1600 kPa). Additional intermediate loading steps were used for the samples from Site #10 to allow for accurate determination of preconsolidation pressures (25, 37.5, 50, 75, 100, 150, 200, 300, 400, 500, 800 and 1600 kPa). In all cases the loads were maintained for a period of twenty-four hours. Preconsolidation pressures, σ_p', were obtained using a Casagrande construction. The values of k corresponding to each load increment were determined using Taylor's square root of time method.

I.3 Results

I.3.1 Site #10

Mineralogy:

X-ray powder diffraction traces of Leda clay samples from Site #10 show that the typical mineralogical components are quartz, feldspar and the clay minerals illite and chlorite. Selected powder patterns are shown on Figures I-3 to I-5. Some swelling clay mineral phases are also seen to be present based on broad peaks at 1.5 to 1.6 nm.

Diffraction traces obtained on oriented < 2 μm fines of clays from Site #10 are shown on Figures I-6 to I-8. Near surface at a depth of 2.34 m (Figure I-6) the clay components are chlorite and illite, with a significant swelling phase shown by the presence of many low angle peaks, and illite peaks with low angle side doublets. Potassium saturation produced some reduction in abundance of the swelling and interlayered phases. Heat treatment produced a strong 1.42 nm chlorite peak and a weak 0.71 nm peak, implying an iron-rich chlorite phase. A small stable peak at 0.85 nm is attributed to an interlayered clay phase.

Diffraction traces obtained on natural fines from 4.78 m and 8.38 m (Figures I-7 and I-8) are very similar to those from 2.34 m.

The carbonate content varied from 2% to 9% (Table I-2), with more calcite generally present than dolomite as shown by the x-ray traces. The total carbonate plot on Figure 9 shows that there is a general trend of decreasing carbonate content with depth.

Porewater Chemistry:

The geochemical data from boreholes at Site #10 are presented in Table I-3 and plotted on Figure I-9. The salinity measurements indicate

soluble salt concentrations of 0.8 g/L near surface, increasing to about 6.5 g/L at 12 m depth then decreasing to 2.5 g/L at 18.6 m.

The most predominant cation in solution is Na^+ followed in decreasing order by Mg^{++}, Ca^{++} and K^+. The salt is predominantly sodium chloride as indicated by chloride values as high as 3600 mg/L. Figure I-9 also shows that there is more magnesium in solution than Ca^{++}, except near the surface. The Na^+ and Cl^- profiles are similar to the salinity profile, with maximum values near 12 m depth. This is also true for K^+, Ca^{++} and Mg^{++}, although these are present in lower concentrations.

Sodium adsorption ratio (SAR) values calculated using the squeezed porewater chemical data show that Na^+ would occupy 2% of exchange sites on the near surface clays, increasing to 22% at - 12 m depth. The pH of the samples range from 8 to 8.8, which is typical of Leda clay samples.

Index Tests:

The natural water content, w_n, values of the Site #10 samples (Table I-4) are plotted on Figure I-10a. With the dashed boundaries as shown, there appears to be a trend of decreasing w_n with depth from an average value of about 72% at surface to about 62% at depth. Within any single tube sample, however, there was a tremendous variation in water content as shown by both Figures I-10a and b. This suggests significant changes in soil structure and texture at a scale not visible by eye.

The Atterberg limit tests (Figure I-11) yielded plastic limits varying from 22 to 29% with an average of about 25%. The liquid limits ranged from 60 to 67% with two low values of 51% and 47% at depths of 3.8 and 18.5 m, suggesting the presence of silty layers. The values of liquidity index are all greater than unity suggesting a very sensitive

soil.

Consolidation Tests:

Consolidation curves for four samples from Site #10 are presented on Figures I-12 to I-15. All four curves exhibit a fairly sharp break at the preconsolidation pressure and S-shaped virgin slopes indicating a sensitive soil with a bonded structure. The initial degree of saturation calculated for the consolidation test samples ranged from 98.7 to 100% at void ratios in excess of 2.1.

The preconsolidation pressure increases significantly with depth from 35 kPa at 2.31 m to 87 kPa at 8.43 m, then to 270 kPa at 18.85 m depth. These trends have already been shown on Figure 2 in the main text. If stressed above the preconsolidation pressure, the soils are extremely compressible with C_c values as high as 1.9 (max. C_c = 1.86 for Sa #10-1-WOA from 4.86 m depth).

Hydraulic conductivity values (k) calculated for each loading increment are presented in Figures I-16 to I-19. Values of k close to 10^{-7} cm/s seem characteristic of the overconsolidated region followed by large decreases in k with decreasing void ratio in the normally consolidated region.

I.3.2 Site #19

Mineralogy:

Two x-ray powder patterns are presented on Figure I-20 for the samples from Site #19. The traces indicate the presence of abundant quartz and feldspar along with a series of "erratic" peaks from 0.72 nm to 1.87 nm which indicate the presence of abundant clay minerals. Although carbonates comprise 4 to 7.5% of the samples (Table I-2), calcite and

dolomite peaks are not clearly visible on the traces.

The x-ray traces obtained on the < 2 μm fines from Sa #19-1-3 are shown on Figure I-21. The natural fines contain abundant illite (1.0 nm peaks) and abundant smectite as indicated by the strong water-wet and glycolated peaks at 1.54 and 1.66 nm respectively. The illite peak shifts from 1.0 nm to 1.03 nm depending on the hydration state indicating significant interlayering with a swelling clay. Potassium saturation causes considerable decrease in the intensity of the smectite peaks but does not collapse them completely (even on air drying) suggesting a complex mixture of vermiculite and smectite. Heat treatment of the K^+ saturated specimen to 550°C produced a high 1.0 nm illite peak and no chlorite peak confirming that for this particular Leda clay the 1.5 nm and 0.7 nm peaks are indeed smectite.

Porewater Chemistry:

The chemical analyses in Table I-3 show the soil to have a pH of - 8, indicating a slightly alkaline environment. Salinity measurements of 0.3 to 0.52 g/L indicate extensive salt removal at these sample depths. Unlike the Site #10 samples, Ca^{++} is the dominant species in solution, with lower concentrations of Na^+ and Mg^{++}. There is very little K^+ in solution.

SAR values of 0.9 and 1.1, calculated using the porewater analyses presented in Table I-3, show that Na^+ probably occupies only 1 to 2% of exchange sites on the clays.

Index Tests:

Atterberg limits were performed on two samples from Site #19, corresponding to depths of 3.3 m and 6.2 m (Table I-4). The plastic

limits showed similar values of 22% and 23% with corresponding liquid limits of 49% and 40%.

The natural moisture contents of 51% and 45% were both above the liquid limits giving values of liquidity index greater than unity for both samples.

Consolidation Tests:

The consolidation curve for the 3.25 m deep sample from Site #19 (Sa #19-1-3 on Figure I-22) shows a preconsolidation pressure of 214 kPa. The sample was initially 97% saturated, had a lower e_o value of 1.43, and was less compressible than the corresponding samples from Site #10. The C_c value is about 0.7.

Figure I-23 shows hydraulic conductivity values of about 2 x 10^{-7} cm/s in the overconsolidated region followed by a steady decrease in k to about 10^{-8} cm/s in the normally consolidated region.

I.3.3 Site #E (NRC)

Mineralogy:

The powder pattern obtained on the sample from Site #E is shown on Figure I-24. The x-ray trace indicates that the mineral components consist of quartz and feldspar plus significant amounts of smectite and illite. A trace amount (0.2%) of carbonate is also present in the sample (Table I-2).

Diffraction traces obtained on oriented fines are shown on Figure I-25. The traces for the natural clay fines show them to consist essentially of smectite and illite, the illite being extensively interlayered with swelling clay. Air drying causes the 1.52 nm peak to

contract to a broad 1.05 nm peak interpreted to consist of interlayered illite/smectite. On subsequent glycolation, a strong smectite peak developed at 1.73 nm.

X-ray traces for K^+ saturated fines are illustrated on Figure I-25b. These show significant collapse of the 1.57 nm smectite peak to form an intensified 1.04 nm illite/smectite peak in the water-wet state. Air drying seems to have further intensified the 1.03 nm illite/smectite peak and subsequent glycolation produced a broad 1.58 to 2.15 nm smectite peak but did not further modify the 1.03 nm peak. The intensification of the 1.0 nm peak by K^+ saturation in the water-wet state implies the presence of some vermiculite-like minerals in the sample. Heat treatment collapses the smectite peaks completely producing a single strong peak at 1.00 nm. The absence of a 1.4 nm peak on the 550°C trace indicates an absence of chlorite.

Porewater Chemistry:

The chemical analyses of two specimens from the Shelby tube sample from the NRC site are shown in Table I-3. The soluble salt concentration is only 0.5 g/L and the pH is neutral at 7. The dominant ions in solution are Na^+ and Ca^{++} which are present in similar amounts plus minor amounts of K^+ and Mg^{++}. High chloride values of 1328 and 1859 mg/L remain to be explained.

Calculated SAR values (in $(meq/L)^{\frac{1}{2}}$), using the squeezed water chemical data, show that Na^+ should occupy approximately 5% of the exchange sites on the clays.

Index Tests:

The plastic and liquid limit values of a 1.22 m deep sample from the

NRC Site (Table I-4) are 35% and 70% respectively. Both values are noticeably larger than the average values for Sites #10 and #19, reflecting the smectite-rich clay fraction. The desiccated nature of this soil has resulted in a moisture content of 36% and consequently a very low liquidity index of 0.03.

Consolidation Tests:

The preconsolidation pressure, σ_p', of the NRC sample is difficult to establish from the e-log p curve of the specimen from 1.26 m depth. A value between 100 and 300 kPa is suggested.

The highly desiccated soil had a void ratio of 1.7 and was only 62% saturated prior to the consolidation test. It exhibited the lowest compressibility of all the samples tested (max. C_c = 0.365). The hydraulic conductivity values show steady decreases with decreasing void ratio from 2 x 10^{-6} cm/s to 2.5 x 10^{-8} cm/s on Figure I-27.

I.4 DISCUSSION

The terms of this contract required hydraulic conductivity testing of four (4) Leda clay samples typical of the Ottawa/Carleton region. Since the contract was approved, the site selection process focused on Site #10 as the most probable candidate site. Therefore, a decision on which clays to test was biased towards Site #10.

The samples available for clay/leachate compatibility testing varied in nature as follows:

1. Very soft, low salt, near surface Leda clay from Site #10.
2. Firm, salty Leda clay at 11.7 m depth at Site #10.
3. Stiff, low salt Leda clay at either 3.1 or 6.2 m depth from Site #19.

4. Stiff to very stiff, desiccated/weathered, smectite-rich, low salt Leda clay from Site #E.

Two types of Leda clay missing from the list, are a never leached marine clay at 35 g/L salt content and a rock-flour Leda "clay". Since the very salty clays are normally at depth far below a waste contact and the rock-flour varieties are normally too sensitive to build on, it is suggested that the samples at hand are excellent for the proposed hydraulic conductivity testing.

I.5 TEST SAMPLES SELECTED

The following four samples were subjected to clay/leachate compatibility testing:

1) Sample 10-2-WOC from Site #10, 2.3 m depth

Salinity = 0.83 g/L, σ_p' ≈ 35 kPa

or

Sample 10-3-WOF from Site #10, 3.8 m depth

Salinity = 1.5 g/L, σ_p' estimated ≈ 50 kPa

2) Sample 10-2-WOE from Site #10, 11.3 m depth

Salinity = 6.5 g/L, σ_p' estimated ≈ 100 kPa

3) Sample 19-1-3 from Site #19, 3.3 m depth

Salinity = 0.3 g/L, σ_p' ≈ 214 kPa

4) Sample NRC from Site #E, - 1.2 m depth

Salinity = 2 g/L, σ_p' ≈ 100-300 kPa

Table I-1. List of Shelby Tube Samples Obtained for Study

Sample No.	Surface Elevation (m)	Sample Depth (m)	Sample Elevation (m)
Candidate Site #10			
10-1-WOA	77.47	4.58 - 5.19	72.28 - 72.89
10-1-WOB	77.47	18.30 - 18.91	58.56 - 59.17
10-1-13	77.47	26.23 - 26.54	50.93 - 51.24
10-2-WOC	76.27	2.21 - 2.52	73.75 - 74.06
10-2-WOD	76.27	6.84 - 7.14	69.13 - 69.43
10-2-WOE*	76.27	11.29 - 11.90	64.37 - 64.98
10-3-WOF*	75.87	3.66 - 3.96	71.91 - 72.21
10-3-WOG	75.87	8.24 - 8.54	67.33 - 67.63
Potential Energy from Waste Site #19			
19-1-3*	69.67	3.05 - 3.36	66.32 - 66.62
19-1-5	69.67	6.10 - 6.25	63.42 - 63.57
NRC Site #E			
E-NRC*	94.55	0.76 - 1.525	93.03 - 93.79

* Hydraulic conductivity test specimen.

Table I-2. Carbonate Contents of Test Soils[1]

Sample No.	Sample Depth (m)	Sample Elevation (m)	Carbonate %
10-2-WOC	2.35	73.92	7.3
10-3-WOF	3.69	72.18	6.1
10-1-WOA	4.78	72.69	3.8
10-2-WOD	7.02	69.25	7.8
10-3-WOG	8.39	67.48	9.2
10-2-WOE	11.72	64.55	3.0
10-1-WOB	18.89	58.58	2.2
10-1-13	26.38	51.09	12.3
19-1-3	3.20	66.47	7.5
19-1-5	6.17	63.50	4.0
E-NRC	1.31	93.24	0.2

(1) Arranged in order of increasing depth at Site #10.

Table I-3. Porewater Chemistry(1)

Sample No.	Sample Depth (m)	pH	Salinity (g/L)	Na mg/L	K mg/L	Ca mg/L	Mg mg/L	Chloride (mg/L)	S.A.R. $(meq/L)^{\frac{1}{2}}$
10-2-WOC	2.25	8.0	0.83	125	8	60	50	220	2.9
10-3-WOF	3.72	8.1	1.5	285	15	34	61	634	6.8
10-1-WOA	4.82	8.2	0.5	85	9	14	25	122	3.2
10-2-WOD	7.10	8.1	3.5	910	33	26	97	1770	18.4
10-3-WOG	8.27	8.1	3.8	100	35	30	125	1880	1.8
10-2-WOE	11.67	8.1	6.5	1530	57	43	185	3555	22.6
10-1-WOB	18.68	8.8	2.5	735	27	6	38	1224	24.4
19-1-3	3.13	8.2	0.3	32	11	45	33	14	0.9
19-1-5	6.18	8.0	0.5	53	24	75	62	23	1.1
E-NRC	0.79	7.0	1.4	335	15	350	38	1859	4.5
E-NRC	1.31	7.4	2.0	250	13	365	48	1328	3.3

(1) In order of increasing depth of samples from Site #10.

Table I-4. Physical Test Results

Sample No.	Sample Depth (m)	Sample Elevation (m)	σ_p' (Kpa)	w_n %	w_L %	w_p %
10-2-WOC	- 2.3	- 74.0	35	74	67	26
10-3-WOF	- 3.8	- 72.1	-	68	51	23
10-1-WOA	- 4.8	- 72.7	52	82	61	23
10-2-WOD	- 6.9	- 69.3	-	71	60	22
10-3-WOG	- 8.5	- 67.4	87	76	63	28
10-2-WOE	-11.3	- 65.0	-	73	65	29
10-1-WOB	-18.7	- 58.8	270	50	47	28
19-1-3	- 3.3	- 66.4	214	51	49	22
19-1-5	- 6.2	- 63.4		45	40	23
E-NRC	- 1.2	- 93.3	100-300	36	70	35

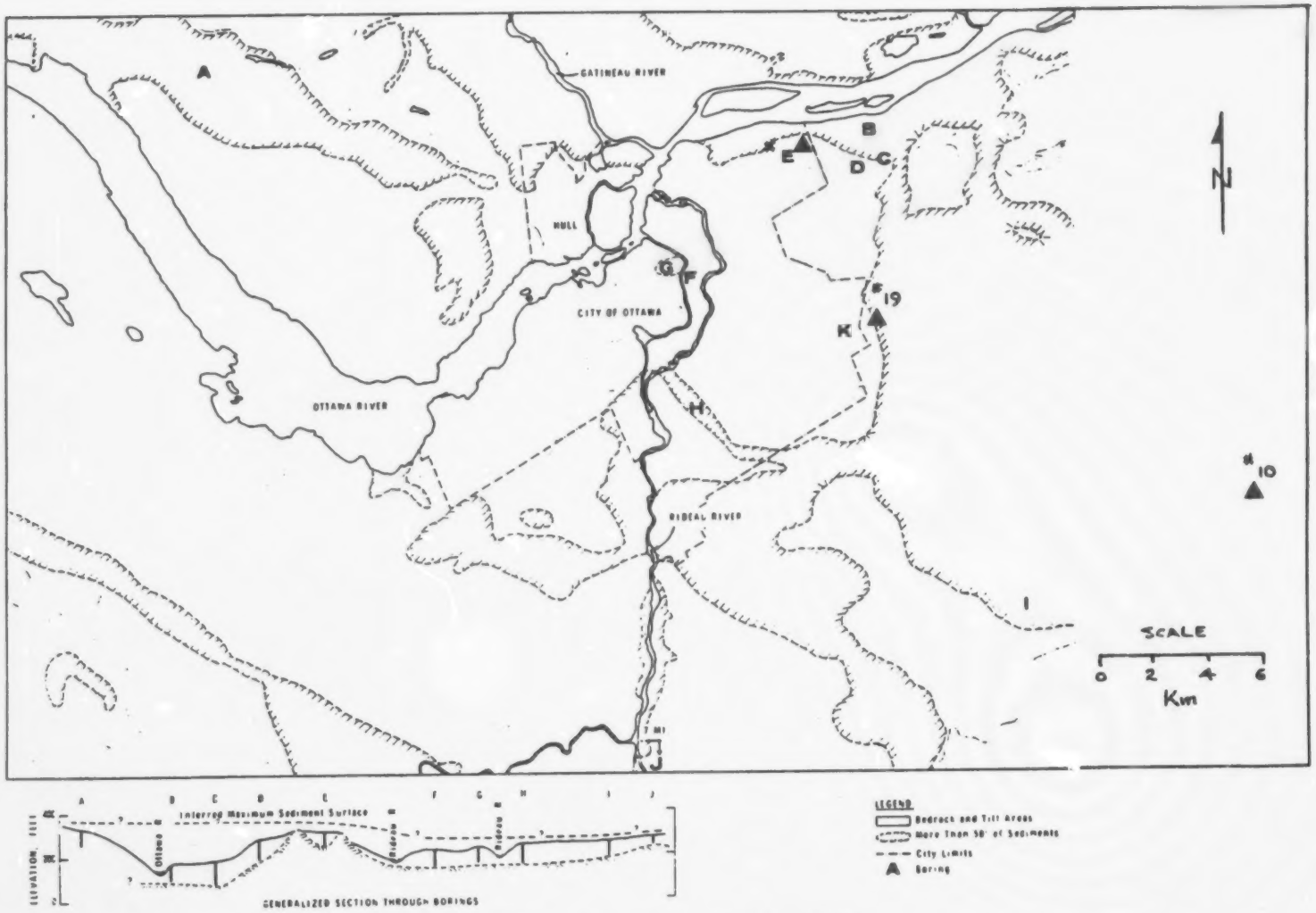

FIG. 1. Map of Ottawa region (geology after Gadd (1963) and Brandon (1961)).

FIGURE I-1. LOCATION MAP OF OTTAWA-CARLETON REGION SHOWING LOCATION OF THREE STUDY SITES (▲) (Adapted from Crawford and Eden, 1965)

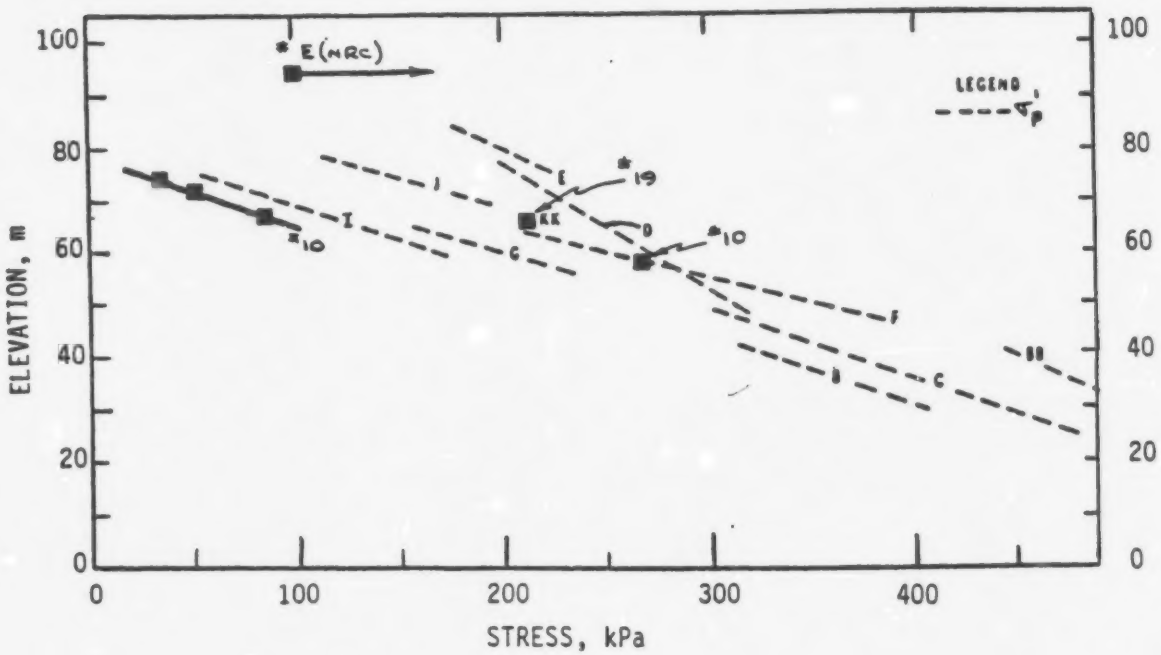

FIGURE I-2. REGIONAL RELATIONSHIPS BETWEEN ELEVATION AND PRECONSOLIDATION PRESSURE, σ_p'

(Adapted directly from Crawford and Eden, 1965)

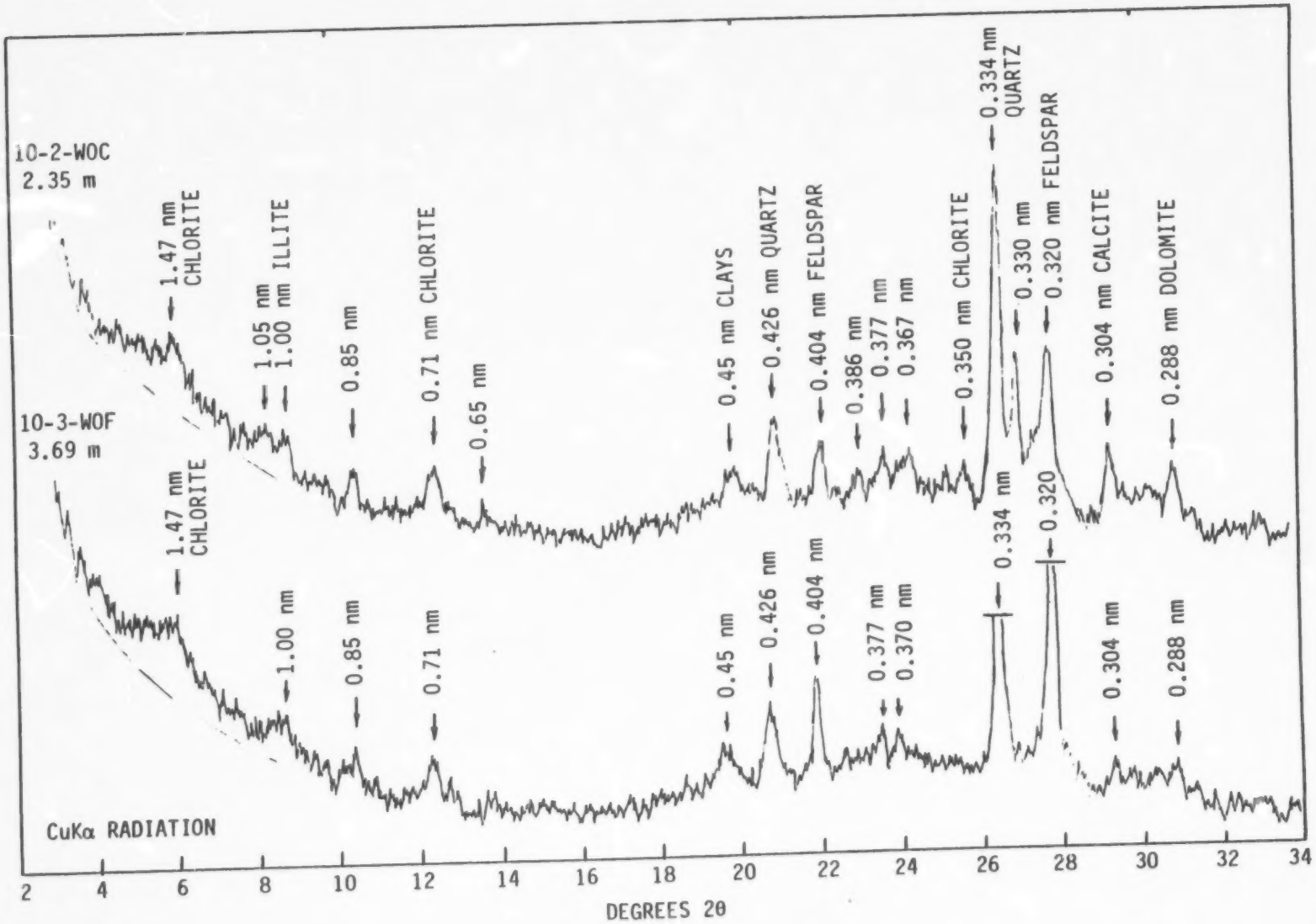

FIGURE I-3. X-RAY POWDER PATTERNS OF WHOLE SOIL SAMPLES OF LEDA CLAY FROM SITE 10, DEPTHS 2.35 AND 3.69 m

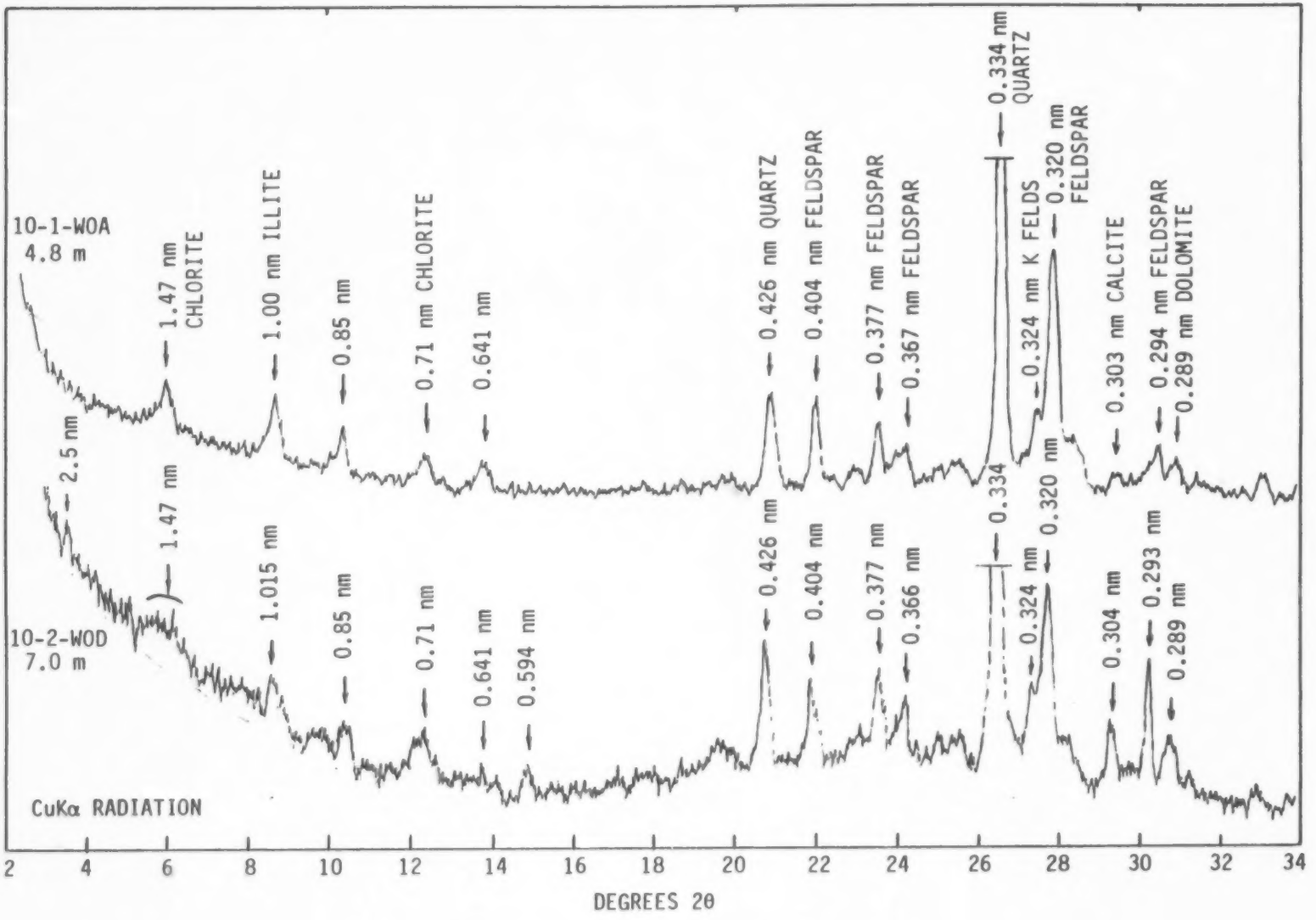

FIGURE I-4. X-RAY POWDER PATTERNS OF WHOLE SOIL SAMPLES OF LEDA CLAY FROM SITE 10, DEPTHS 4.8 AND 7.0 m

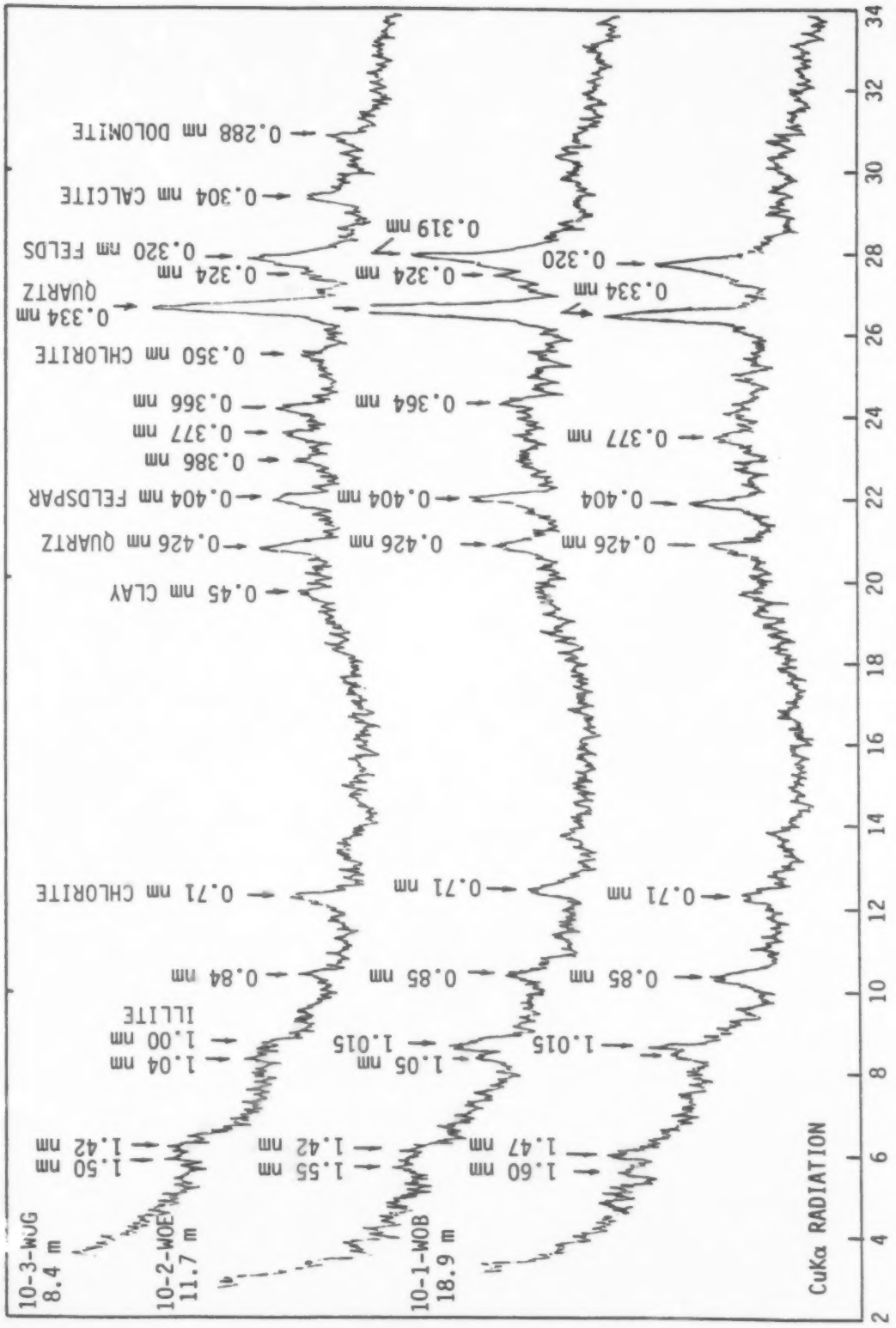

FIGURE I-5. X-RAY POWDER PATTERNS OF WHOLE SOIL SAMPLES OF LEDA CLAY FROM SITE 10, DEPTHS 8.4, 11.7 AND 18.9 m

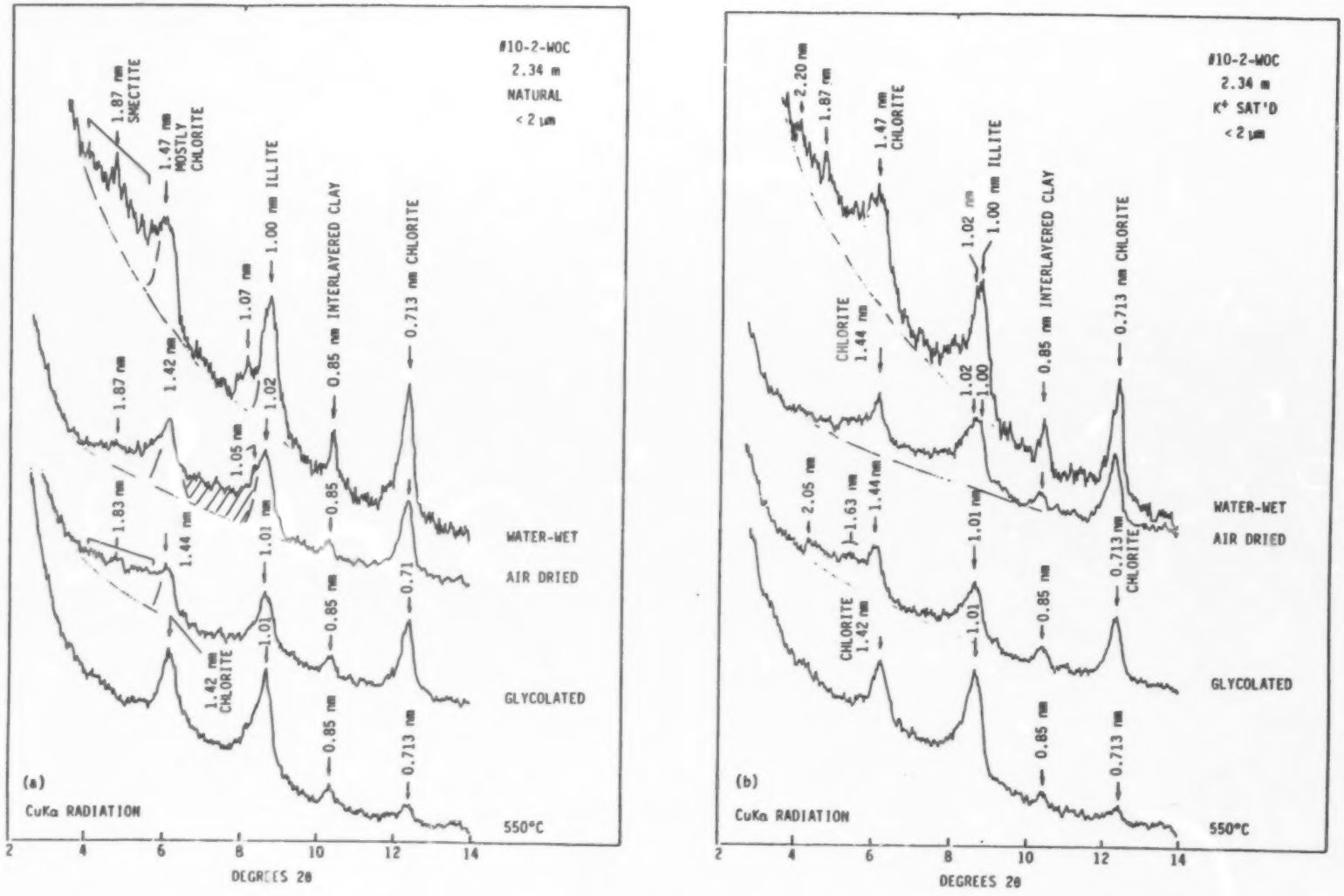

FIGURE I-6. X-RAY DIFFRACTION TRACES OF ORIENTED, < 2 µm FRACTION OF LEDA CLAY SAMPLES FROM SITE #10, DEPTH 2.34 m: (a) UNTREATED EXCEPT FOR DISTILLED WATER FRACTIONATION; (b) K^+ SATURATED

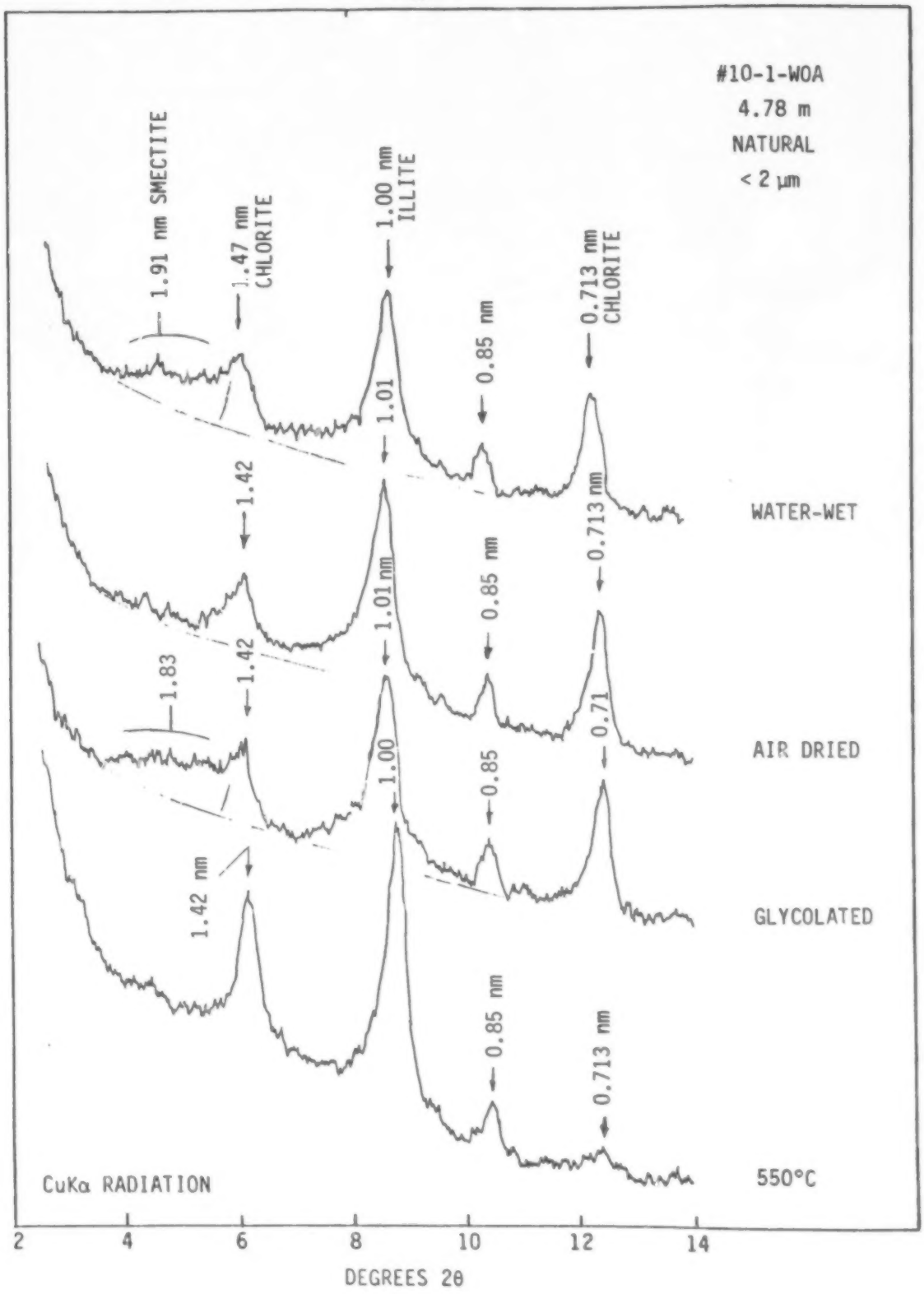

FIGURE I-7. X-RAY DIFFRACTION TRACES OF ORIENTED, < 2 µm FRACTION OF LEDA CLAY SAMPLES FROM SITE #10, DEPTH 4.78 m, UNTREATED EXCEPT FOR DISTILLED WATER FRACTIONATION

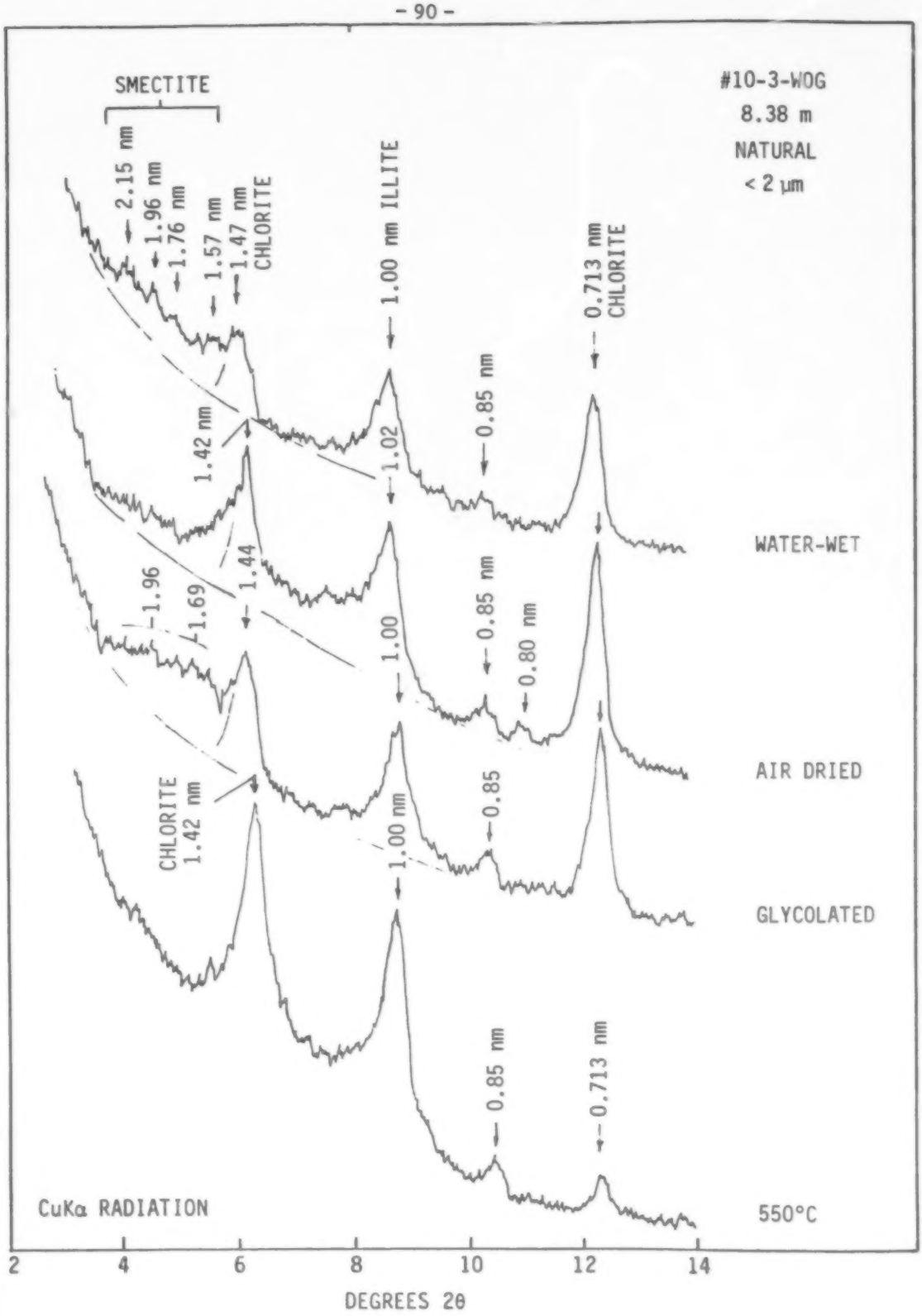

FIGURE I-8. X-RAY DIFFRACTION TRACES OF ORIENTED, < 2 µm FRACTION OF LEDA CLAY SAMPLES FROM SITE #10, DEPTH 8.38 m, UNTREATED EXCEPT FOR DISTILLED WATER DIFFRACTION

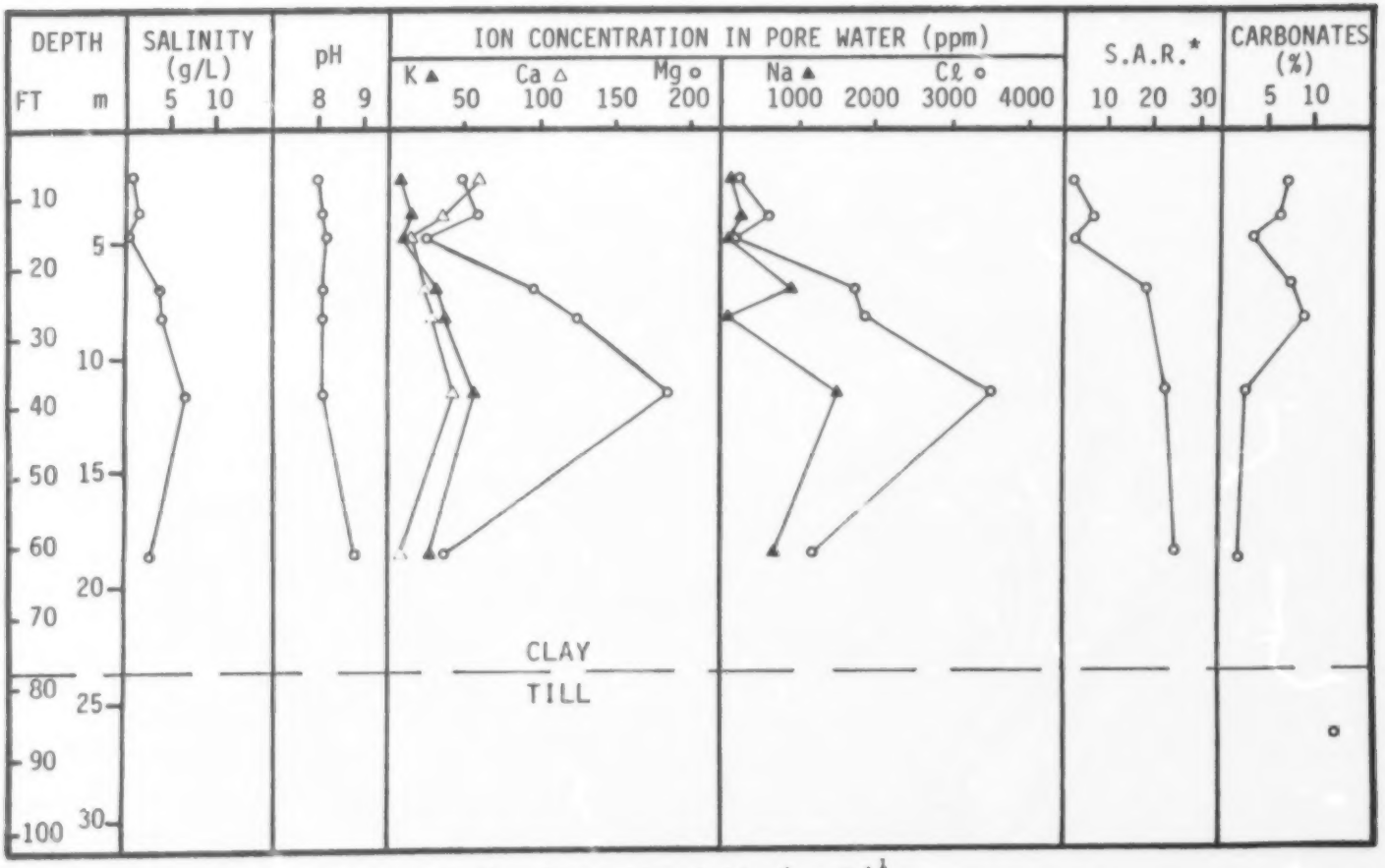

Note: * S.A.R. = Sodium Adsorption Ratio $(meq/L)^{\frac{1}{2}}$.

FIGURE I-9. COMPOSITE OF GEOCHEMICAL DATA FROM BOREHOLES 10-1, 10-2 AND 10-3

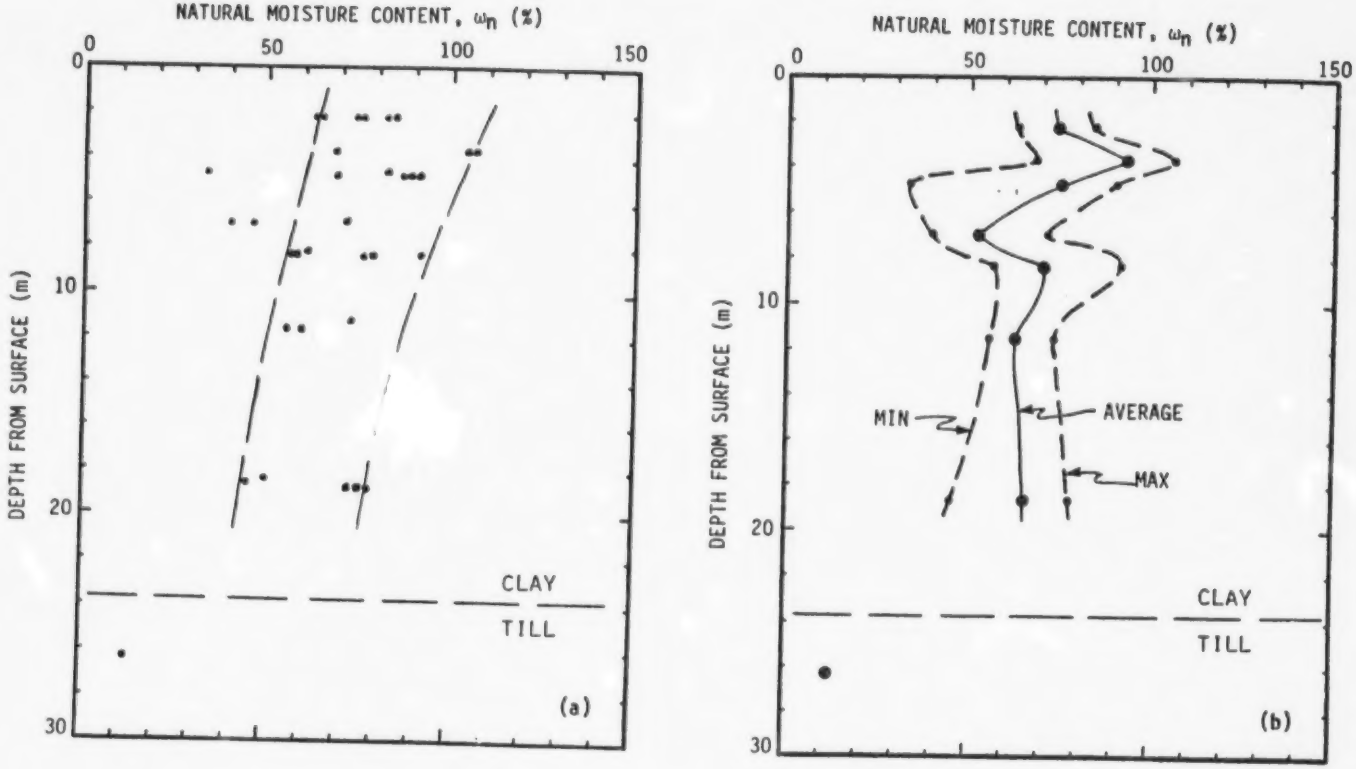

FIGURE I-10. NATURAL MOISTURE CONTENT (ω_n) VS DEPTH: (a) INDIVIDUAL DATA POINTS; (b) STATISTICAL INTERPRETATION

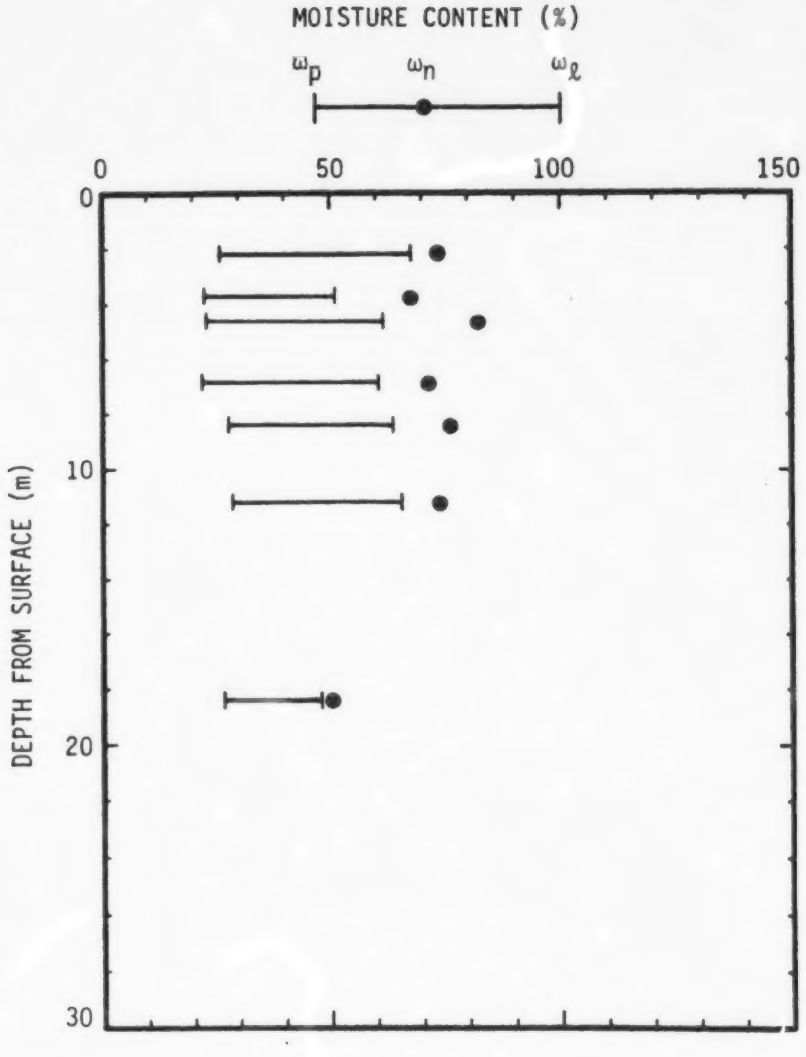

FIGURE I-11. ATTERBERG LIMITS (ω_p AND ω_ℓ) AND NATURAL MOISTURE CONTENT (ω_n) VS DEPTH

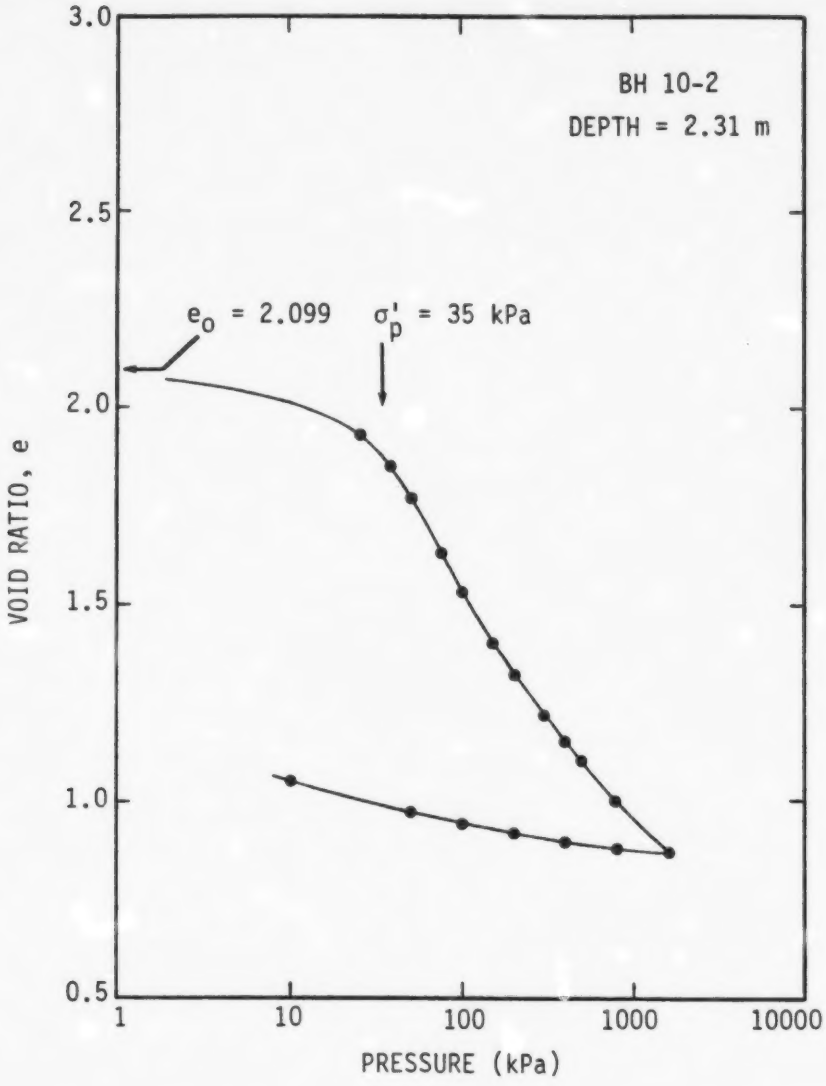

FIGURE I-12. CONSOLIDATION CURVE FOR BOREHOLE 10-2, 2.31 m DEPTH (73.96 m ELEV.)

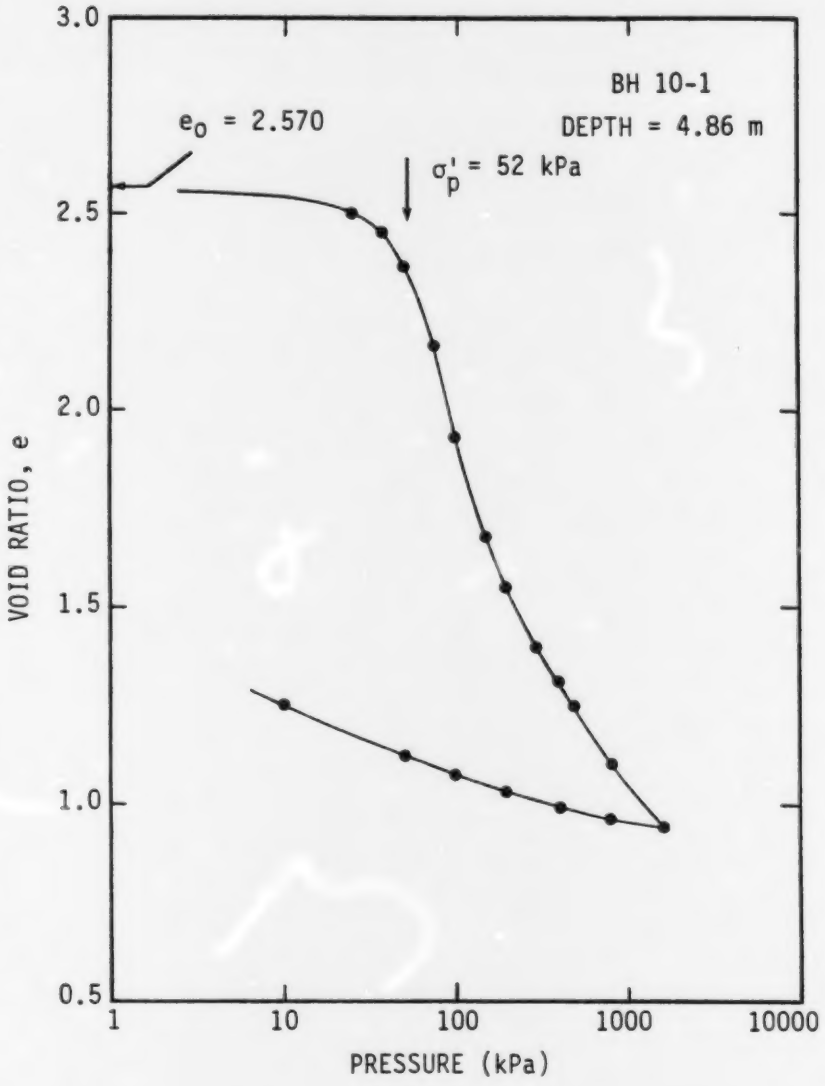

FIGURE I-13. CONSOLIDATION CURVE FOR BOREHOLE 10-1, 4.86 m DEPTH (72.61 m ELEV.)

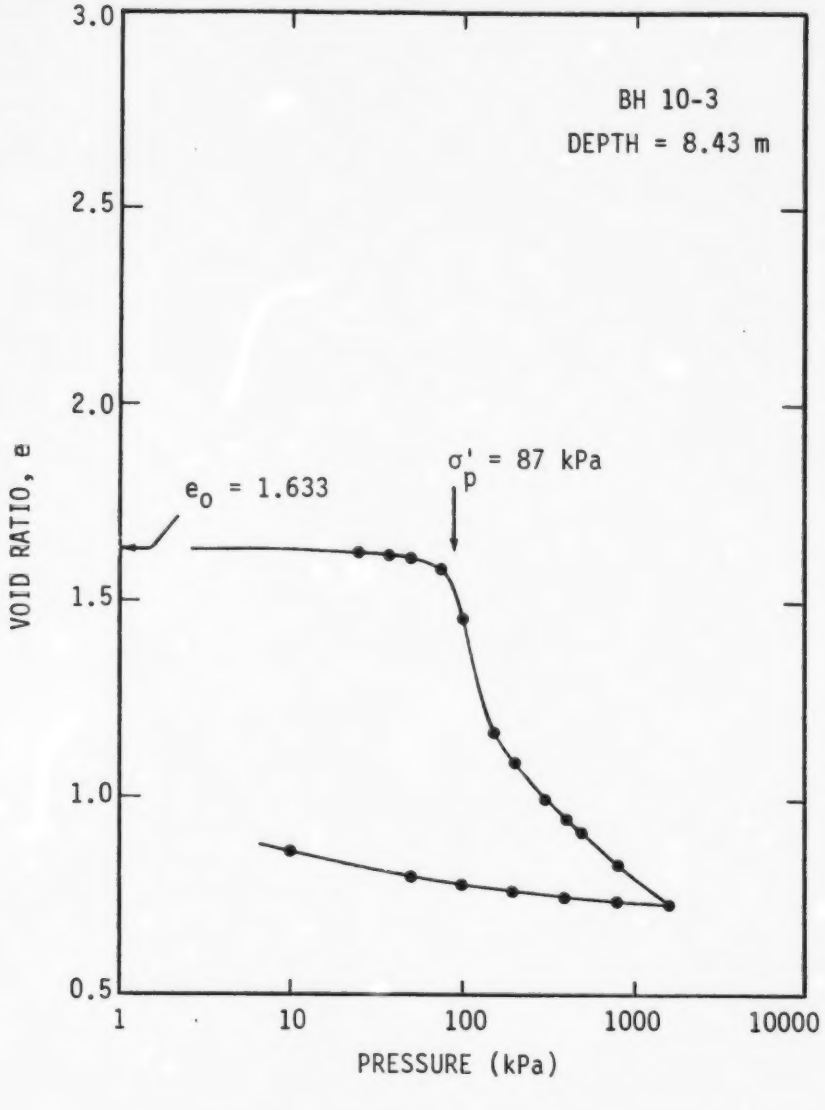

FIGURE I-14. CONSOLIDATION CURVE FOR BOREHOLE 10-3, 8.43 m DEPTH (67.44 m ELEV.)

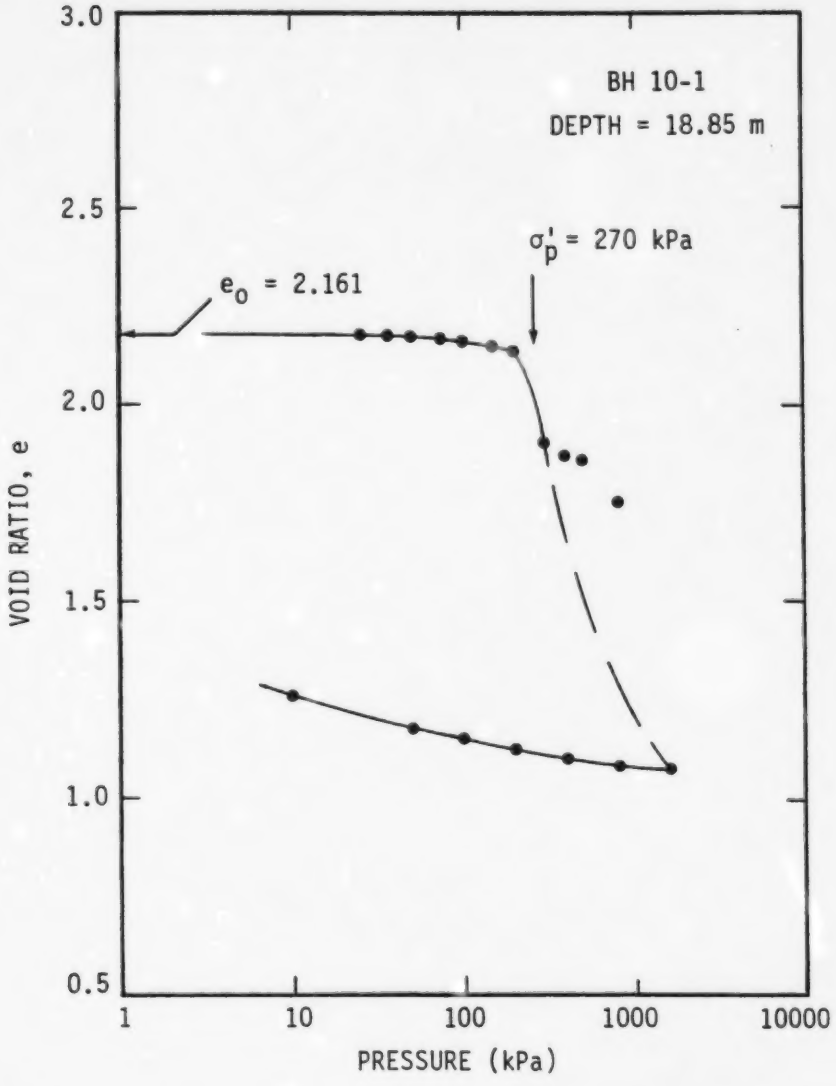

FIGURE I-15. CONSOLIDATION CURVE FOR BOREHOLE 10-1, 18.85 m DEPTH (58.62 m ELEV.)

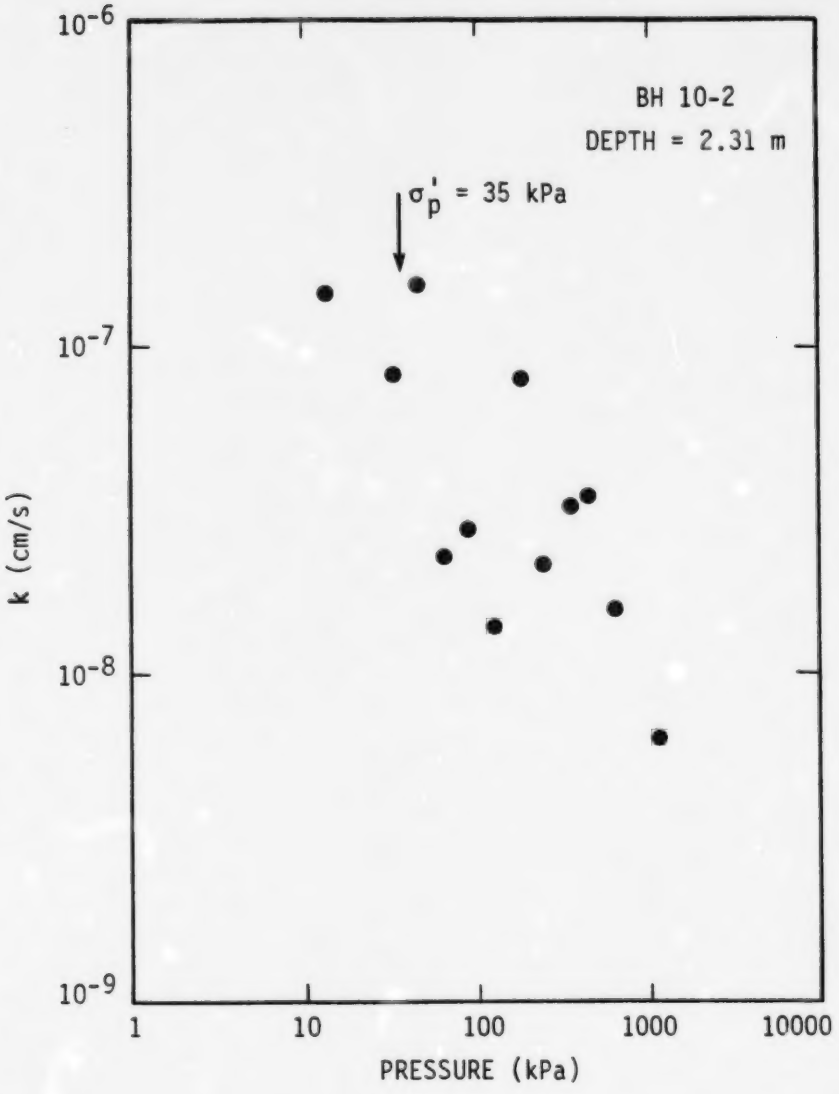

FIGURE I-16. HYDRAULIC CONDUCTIVITY, k, FROM CONSOLIDATION TEST (BOREHOLE 10-2, 2.31 m DEPTH)

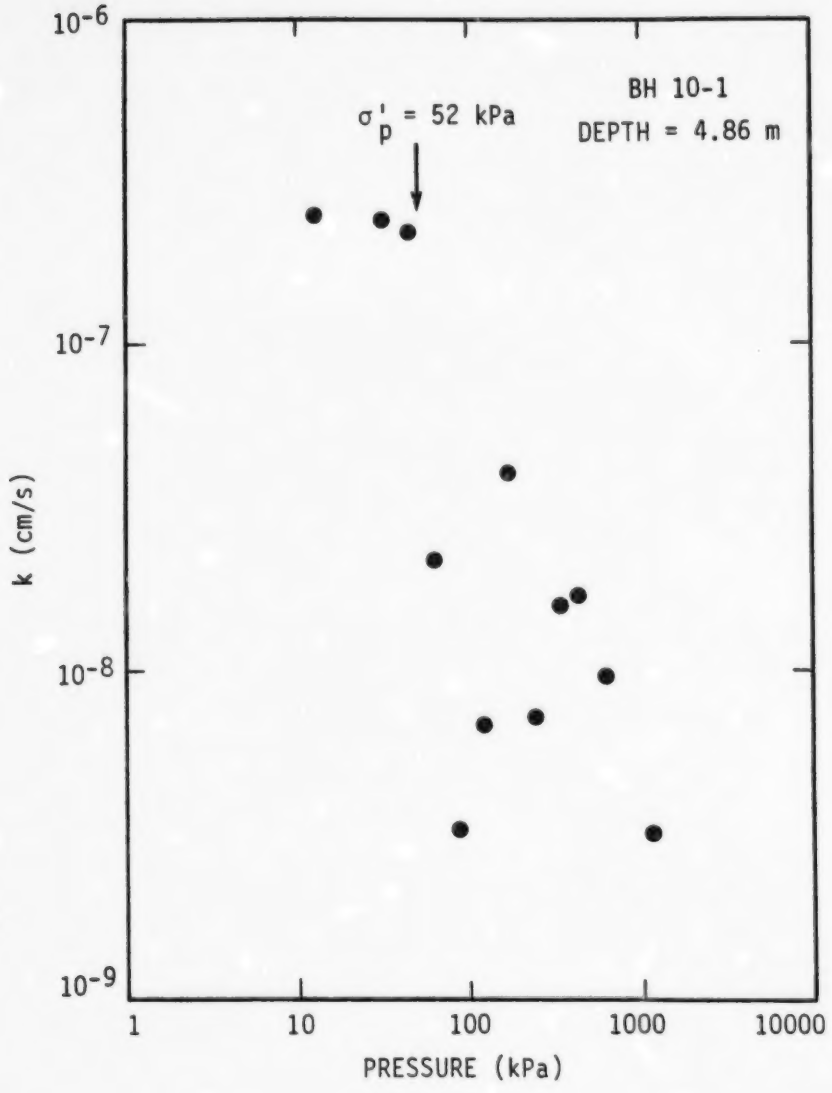

FIGURE I-17. HYDRAULIC CONDUCTIVITY, k, FROM CONSOLIDATION TEST (BOREHOLE 10-1, 4.86 m DEPTH)

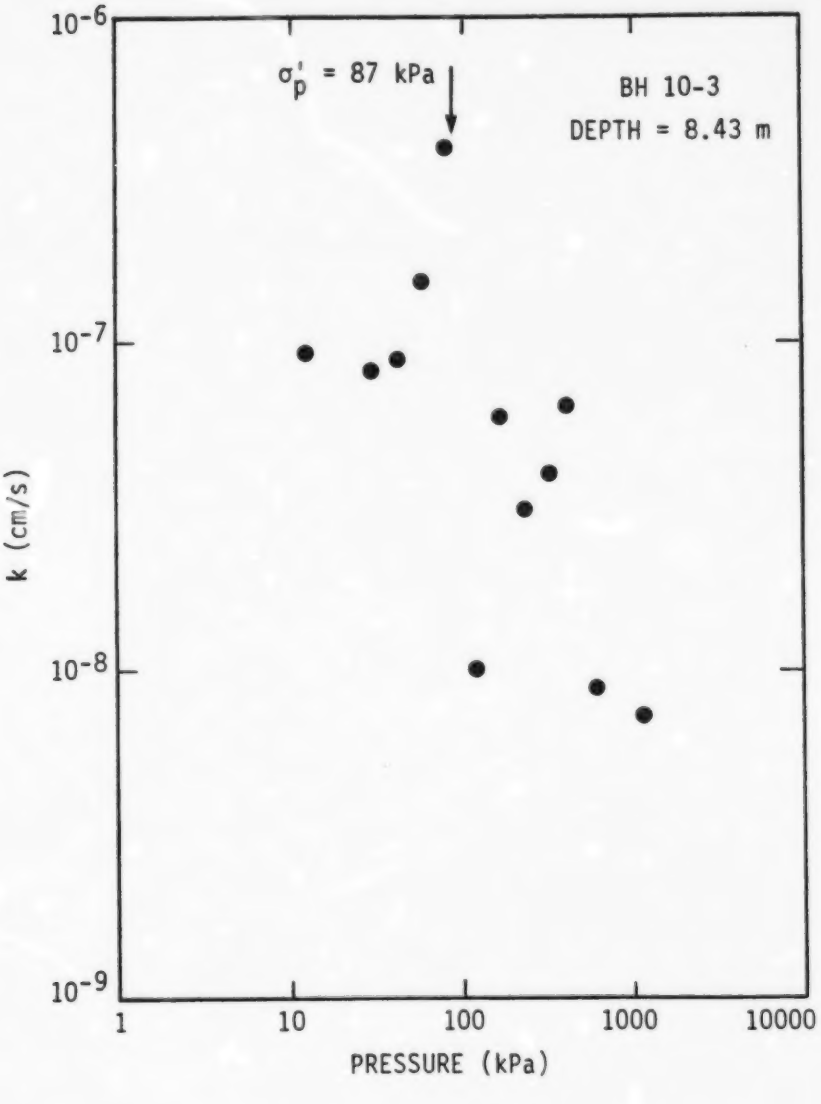

FIGURE I-18. HYDRAULIC CONDUCTIVITY, k, FROM CONSOLIDATION TEST (BOREHOLE 10-3, 8.43 m DEPTH)

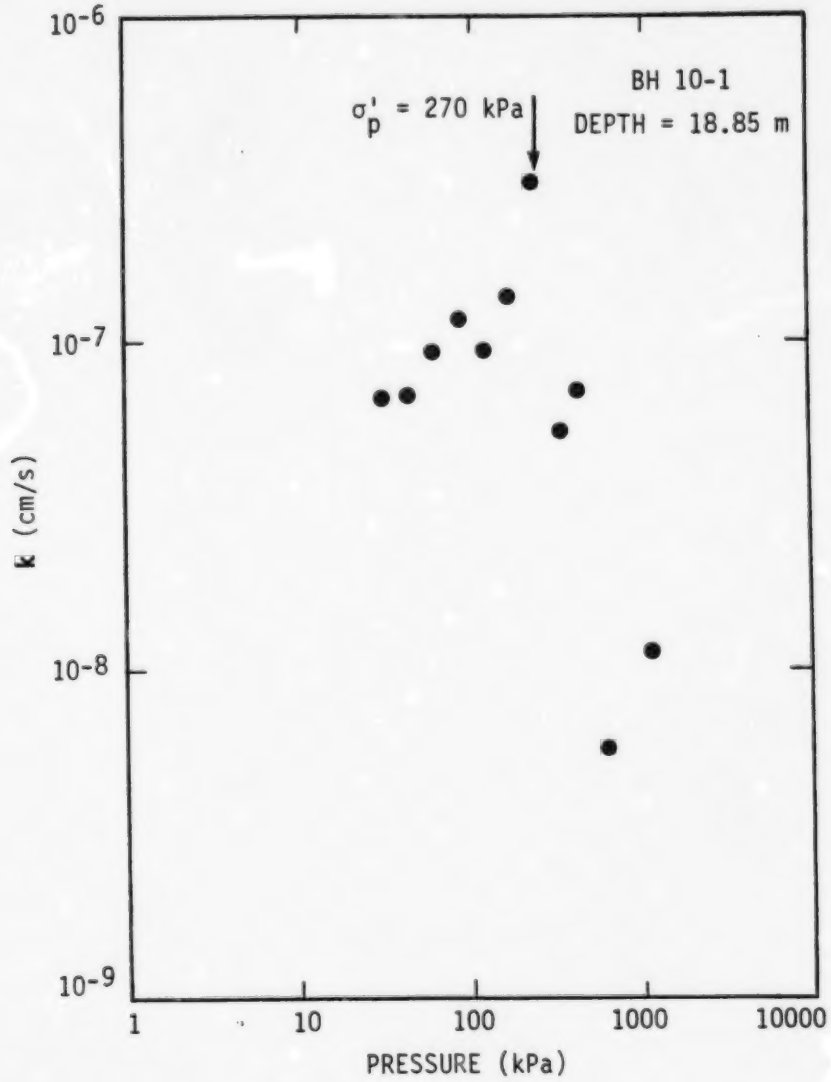

FIGURE I-19. HYDRAULIC CONDUCTIVITY, k, FROM CONSOLIDATION TEST (BOREHOLE 10-1, 18.85 m DEPTH)

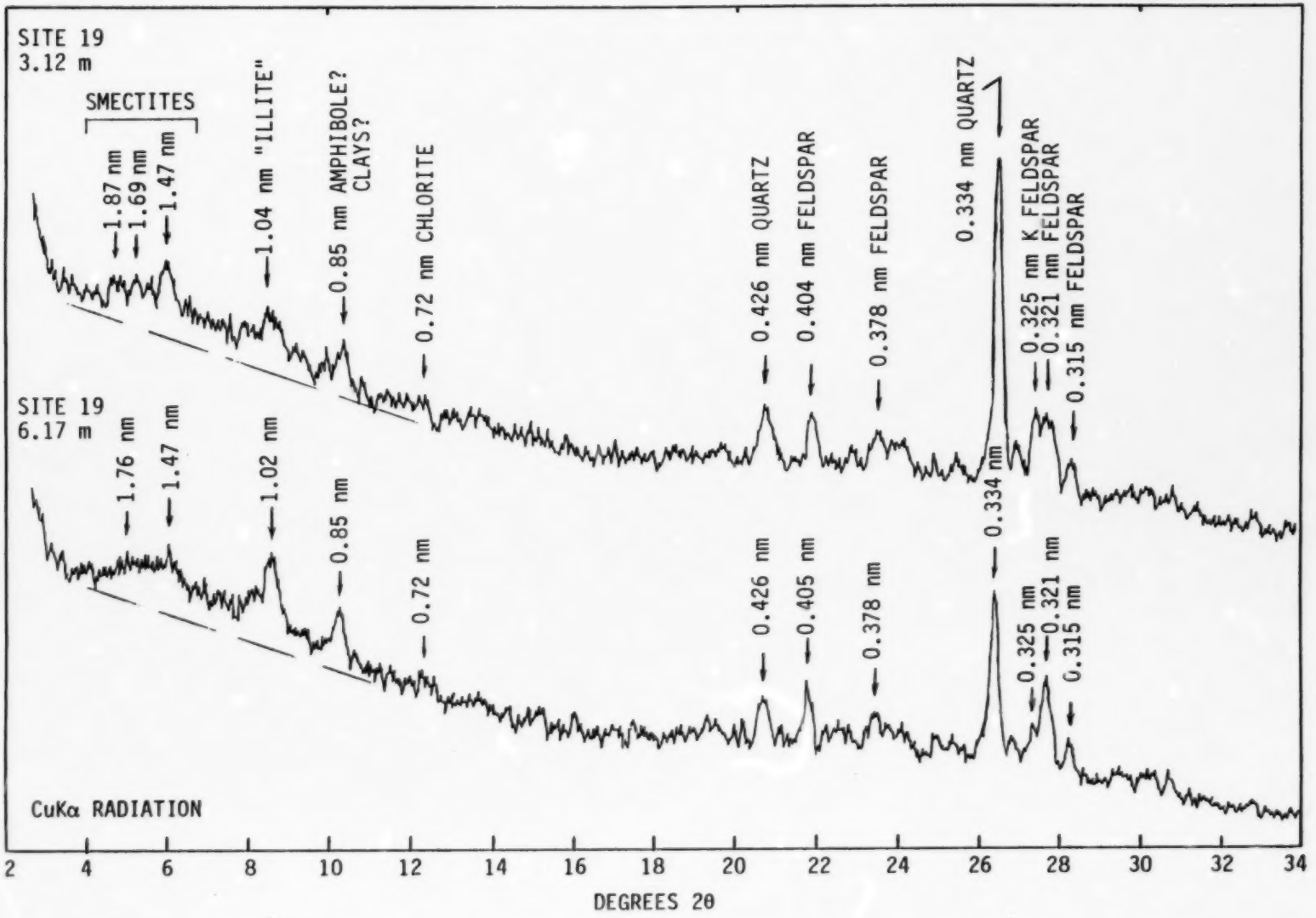

FIGURE I-20. X-RAY POWDER PATTERNS OF WHOLE SOIL SAMPLES OF LEDA CLAY FROM SITE 19, DEPTHS 3.12 AND 6.17 m

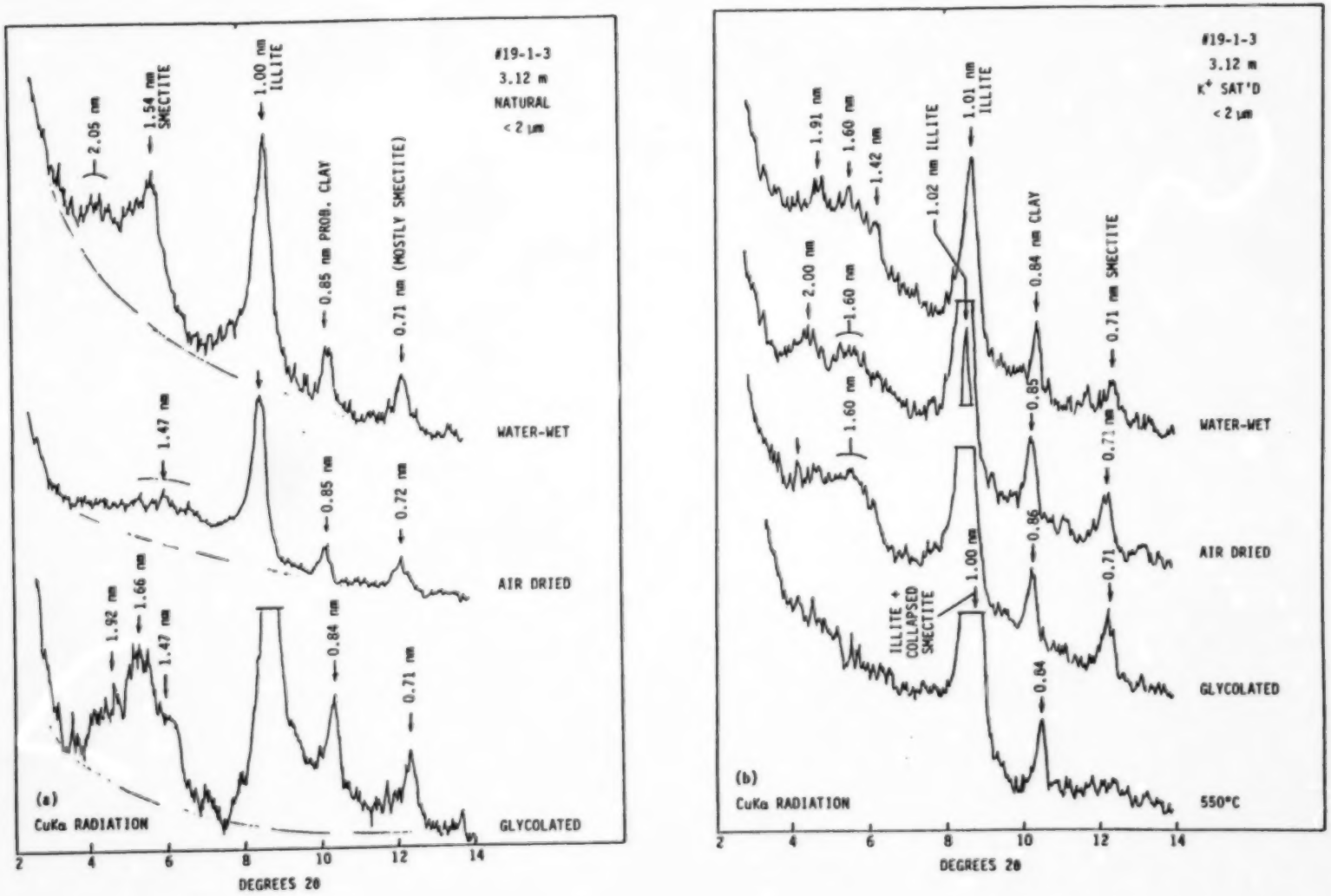

FIGURE I-21. X-RAY DIFFRACTION TRACES OF ORIENTED, < 2 µm FRACTION OF LEDA CLAY FROM SITE #19, DEPTH 3.12 m: (a) UNTREATED EXCEPT FOR DISTILLED WATER FRACTIONATION; (b) K^+ SATURATED

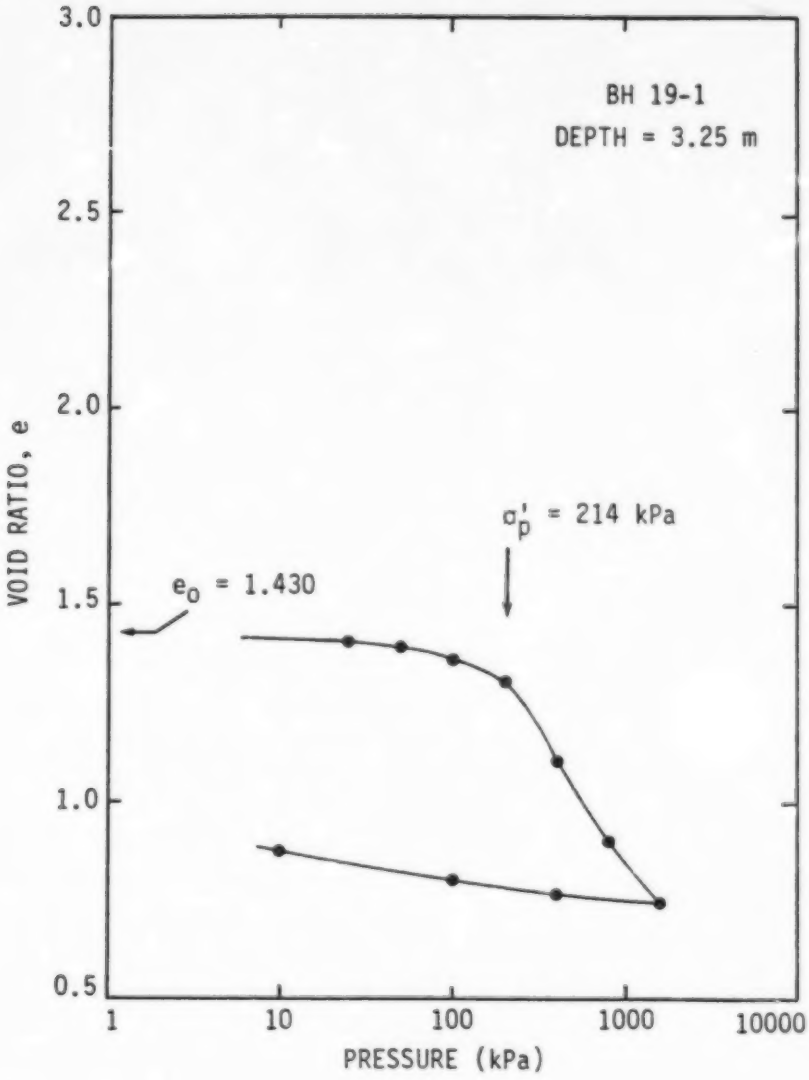

FIGURE I-22. CONSOLIDATION CURVE FOR BOREHOLE 19-1, 3.25 m DEPTH (66.42 m ELEV.)

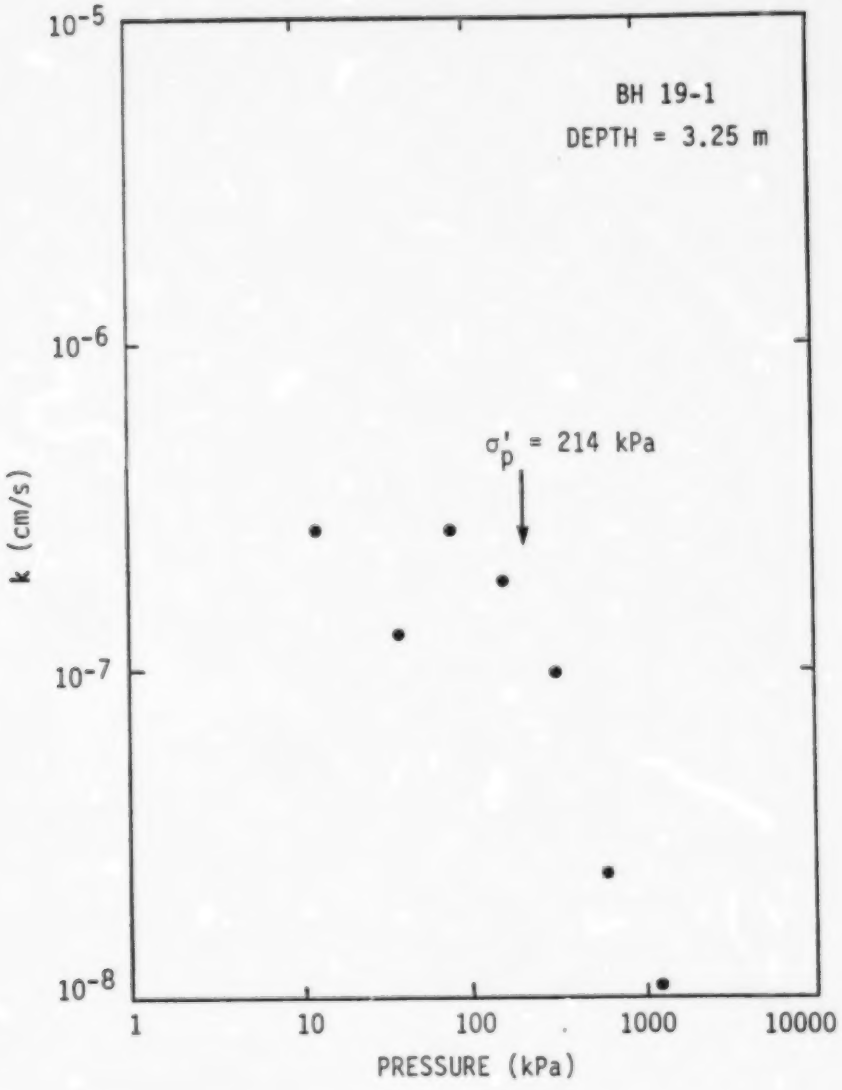

FIGURE I-23. HYDRAULIC CONDUCTIVITY, k, FROM CONSOLIDATION TEST (BOREHOLE 19-1, 3.25 m DEPTH)

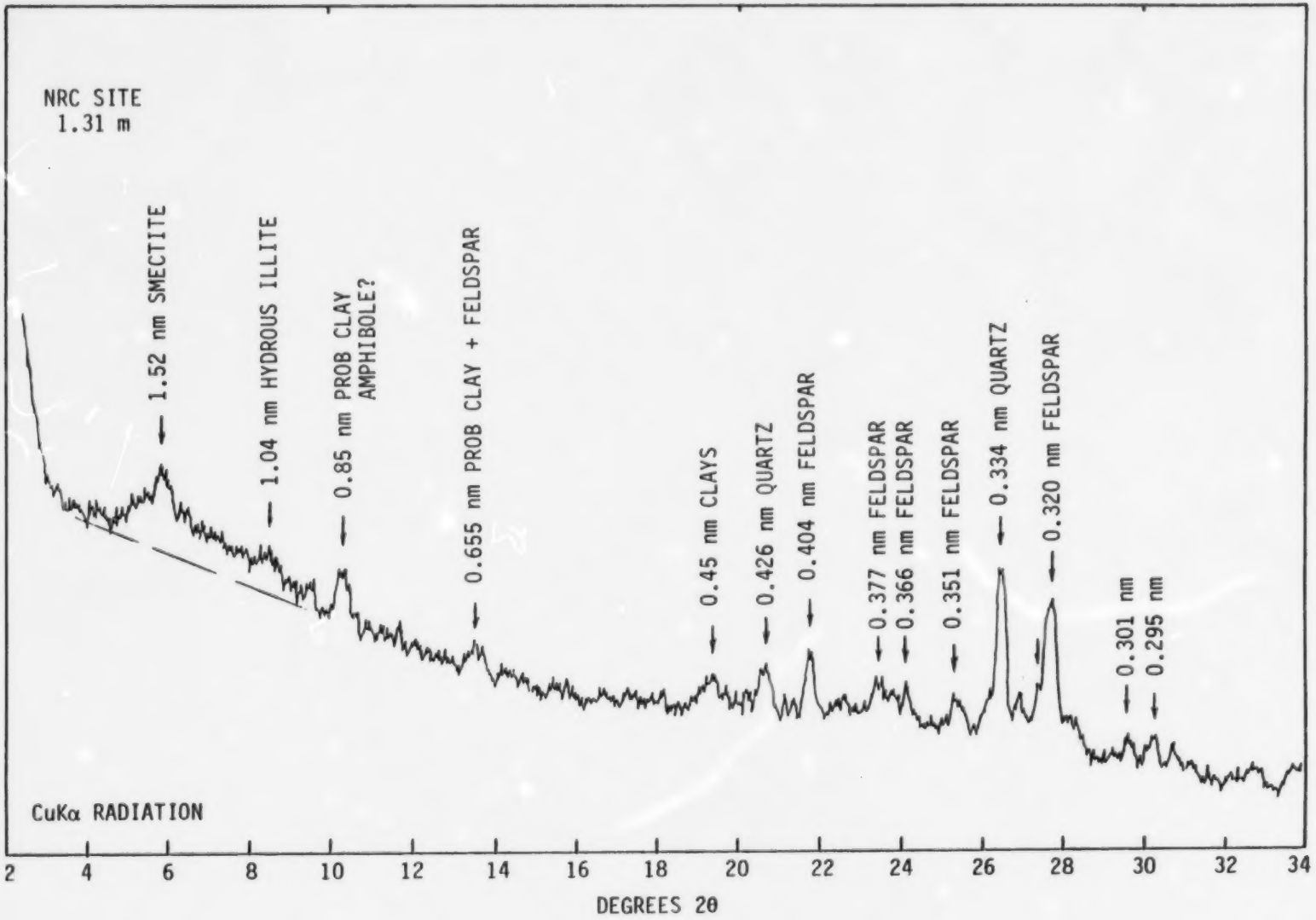

FIGURE I-24. X-RAY POWDER PATTERN OF WHOLE SOIL SAMPLE OF LEDA CLAY FROM NRC SITE, DEPTH 1.31 m

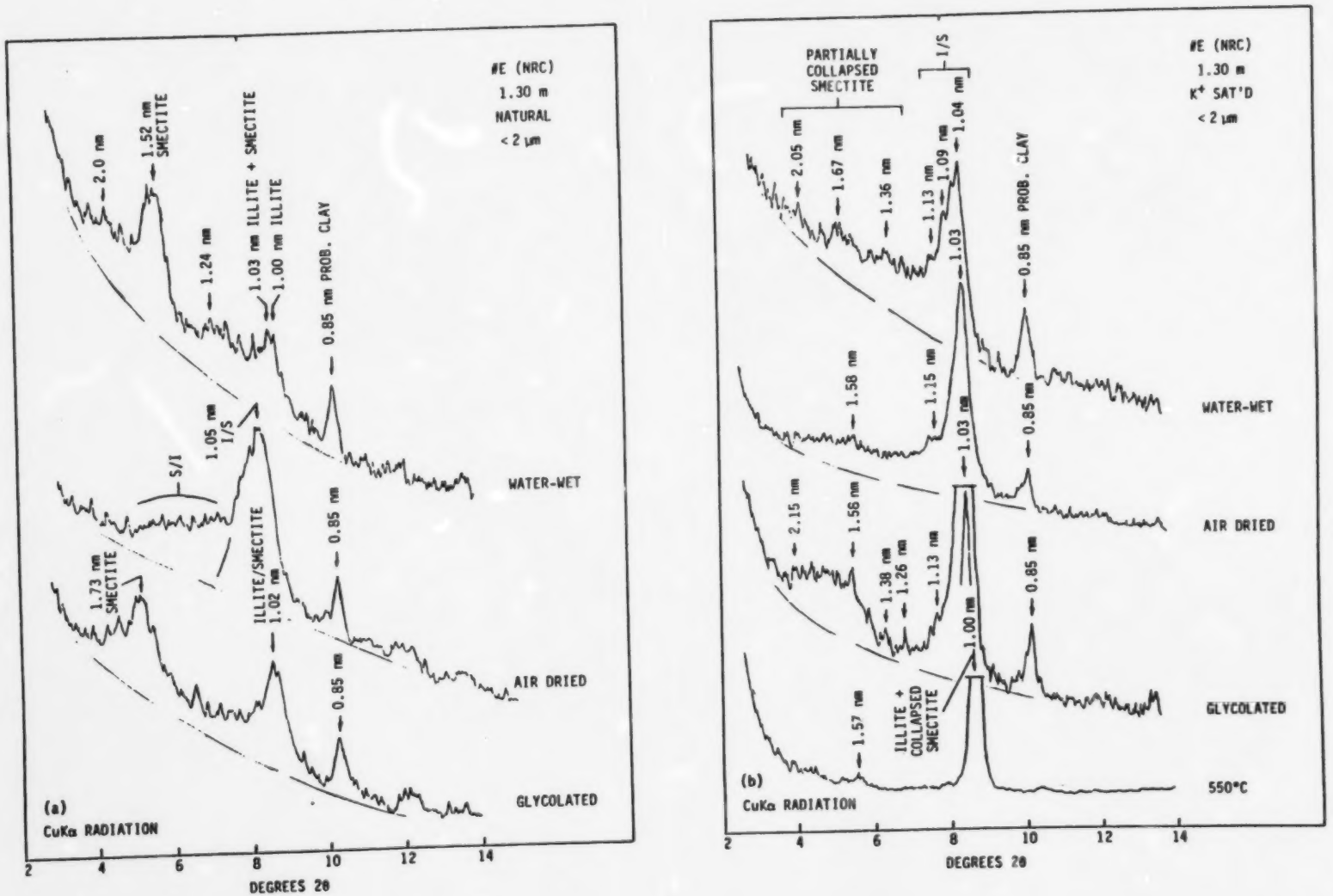

FIGURE I-25. X-RAY DIFFRACTION TRACES OF ORIENTED, < 2 µm FRACTION OF LEDA CLAY FROM NRC SITE, DEPTH 1.30 m: (a) UNTREATED EXCEPT FOR DISTILLED WATER FRACTIONATION; (b) K^+ SATURATED

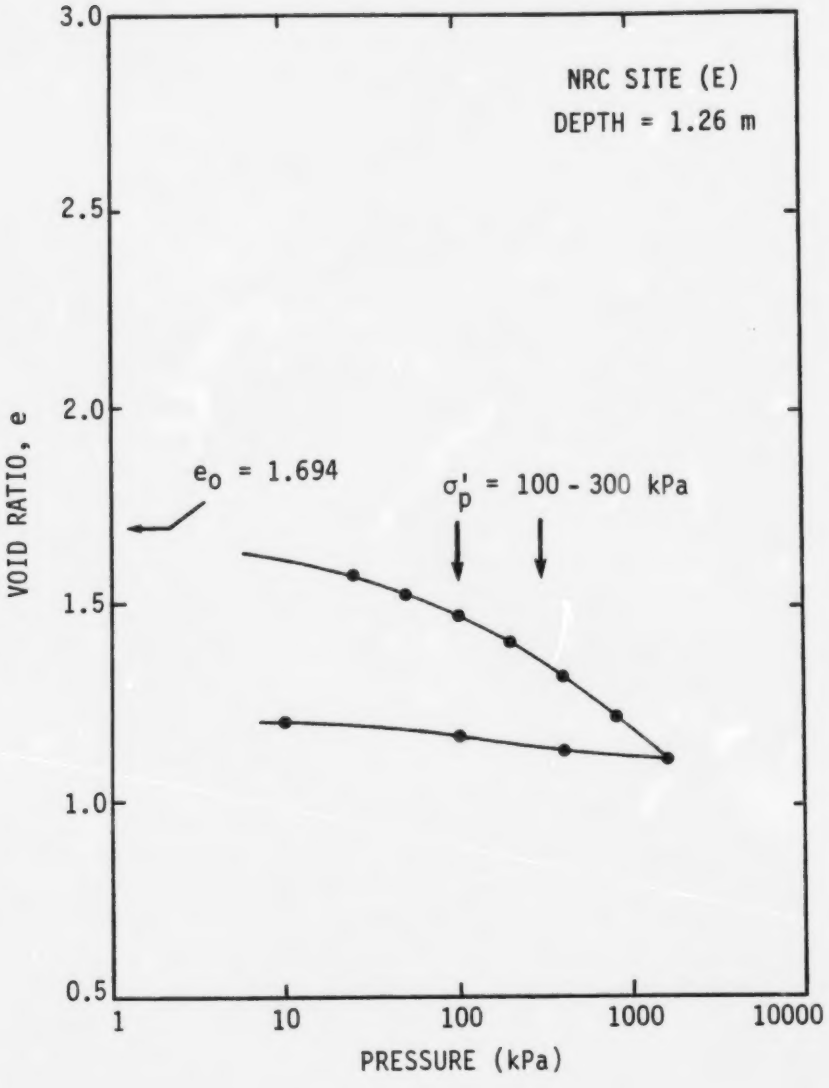

FIGURE I-26. CONSOLIDATION CURVE FOR NRC SITE (E)
1.26 m DEPTH (93.3 m ELEV.)

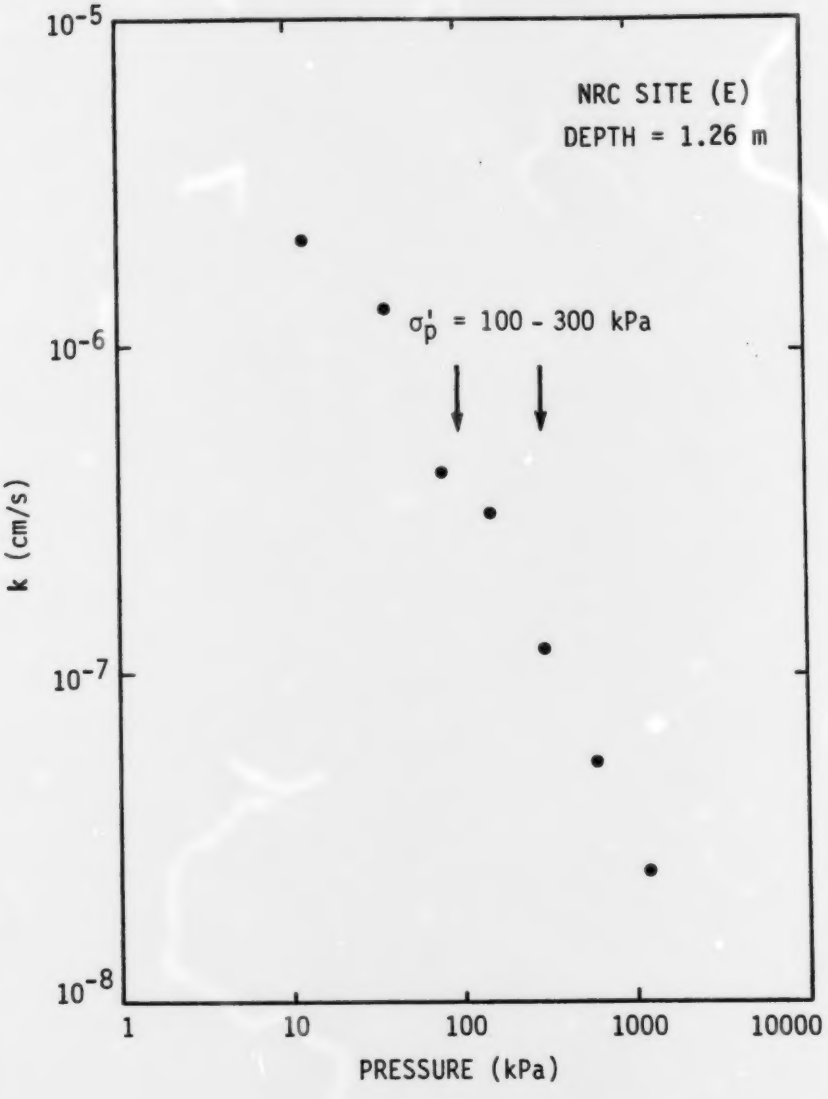

FIGURE I-27. HYDRAULIC CONDUCTIVITY, k, FROM CONSOLIDATION TEST (NRC SITE (E), 1.26 m DEPTH)

APPENDIX II

LEACHATE STABILITY

LEACHATE STABILITY

INTRODUCTION AND METHOD

The effect of storage on the chemical composition of the Westminster Landfill leachate is discussed in this Appendix. The purpose was to assess the chemical changes that occur in the leachate while stored at room temperature compared to storage at 10°C. Since the k tests are carried out at room temperature in runs lasting one to two weeks, some knowledge of the leachate stability is important.

Waste leachate from the Westminster Landfill site was collected in a 4 L polypropylene bottle and stored in 23 smaller sampling bottles (30 mL) wrapped with duct tape to prevent exposure to light. Each analysis was made on leachate from one small bottle and then discarded. The room temperature varied from 19 to 25°C whereas the constant temperature room stayed at 10°C. The samples were analyzed sequentially for pH, calcium and iron over a period of 68 days. The cation analyses were conducted on acid digested samples by atomic absorption spectrometry, while the pH was monitored using a specific electrode.

RESULTS

The results of the leachate stability study are illustrated on Figure II-1 and summarized in Tables II-1 and II-2. Table II-1 shows the results of chemical changes at room temperature (- 21°C) while Table II-2 shows results for the refrigerated sample. In comparison to leachate stored at room temperature, storage at the lower temperature (- 10°C) slows down the chemical changes that occur within the leachate.

Since the leachate stored at 10°C looks fairly stable, its values for pH, Ca^{++} and total Fe can be used as reference values for room temperature storage. The C_o values so determined for Cl^-, Na^+, K^+, Ca^{++}, Mg^{++} and total Fe are presented at the bottom of Table II-2 and also in Table 3 of the main text.

The chemical data obtained on leachate samples from the 23 bottles stored at room temperature display a huge scatter probably related to slightly different biochemical conditions in each bottle. Nevertheless the plotted data on Figure II-1 do display important trends as follows:

1. If the three anomalously high pH values are ignored a definite trend of rapidly increasing pH from 6.9 to 7.1 or 7.2 occurs during the first day or two followed by little change.

2. If the Ca^{++} is taken to start at an average bottle value of 247 mg/L, then a definite trend of decreasing Ca^{++} with time to about 85 mg/L is observed. The three low values flagged by question marks remain a mystery. The lowest values measured in the permeameter cells (reservoir values) were 105, 108, 65 and 160 mg/L.

3. The total Fe for the three 10°C leachate samples averaged 66 mg/L which was considerably below a value of 95 mg/L suggested by Figure II-1. The rapid drop in dissolved total iron reflects rapid bacterial reduction and precipitation as amorphous FeS_2.

4. Half of the Ca^{++} losses seem to occur within 7 to 15 days and half of the Fe losses occur within 12 days. If a leachate permeation run takes 7 to 14 days, then there seems to be little benefit from storing the leachate at 10°C. In fact, rapid decreases in C_o really

complicate interpretation of the effluent chemistry.

In any event, it was decided that the influent leachate would be stored at the same room temperature at which the k tests would be run.

An x-ray powder pattern of air dried, black slimy precipitate is presented on Figure II-2. The trace shows the flocs to contain abundant calcite. No visible pyrite is observed at 33.0° 2θ, the location of a strong 0.271 nm peak. Tiny peaks at 0.339 nm and 0.433 nm could represent aragonite and a form of hydrated calcite.

Table II-1. Results of Leachate Stability Assessment (Room Temperature Storage)

Elapsed Time		Cation Conc. (mg/L)		pH
Hours	Days	Ca^{++}	Total Fe	
0	0	215	90	6.9
5	0.21	-	94	-
8	0.33	415	83	7.0
25	1.04	255	100	7.1
31	1.29	243	78	7.1
49	2.04	230	93	7.2
52	2.17	-	-	-
55	2.29	215	90	7.2
73	3.04	233	95	7.2
97	4.04	235	85	7.1
145	6.04	228	75	7.1
151	6.29	205	58	7.1
175	7.29	168	50	7.0
199	8.29	238	70	7.0
217	9.04	230	38	7.0
241	10.04	280	78	7.3
265	11.04	300	60	6.9
554	23.08	50	45	8.2
724	30.17	20	10	7.7
862	35.92	38	21	8.8
1128	47.00	110	31	7.2
1392	58.00	102	7	7.1
1632	68.00	85	8	7.0

Table II-2. Chemical Composition of Refrigerated Leachate with Increasing Time (T = 10°C)

Elapsed Time (days)	Ion Concentration (mg/L)						pH
	Cl^-	Na^+	K^+	Ca^{++}	Mg^{++}	Total Fe	
0	-	740	-	190	300	70	6.9
20	1451	540	328	300	250		6.9
40(1)	1195	660	416	250	290	62	6.9
Selected C_o (Average Value)	1323	647	372	247	280	66	6.9

Notes: (1) Trace amounts of suspended black slime observed.

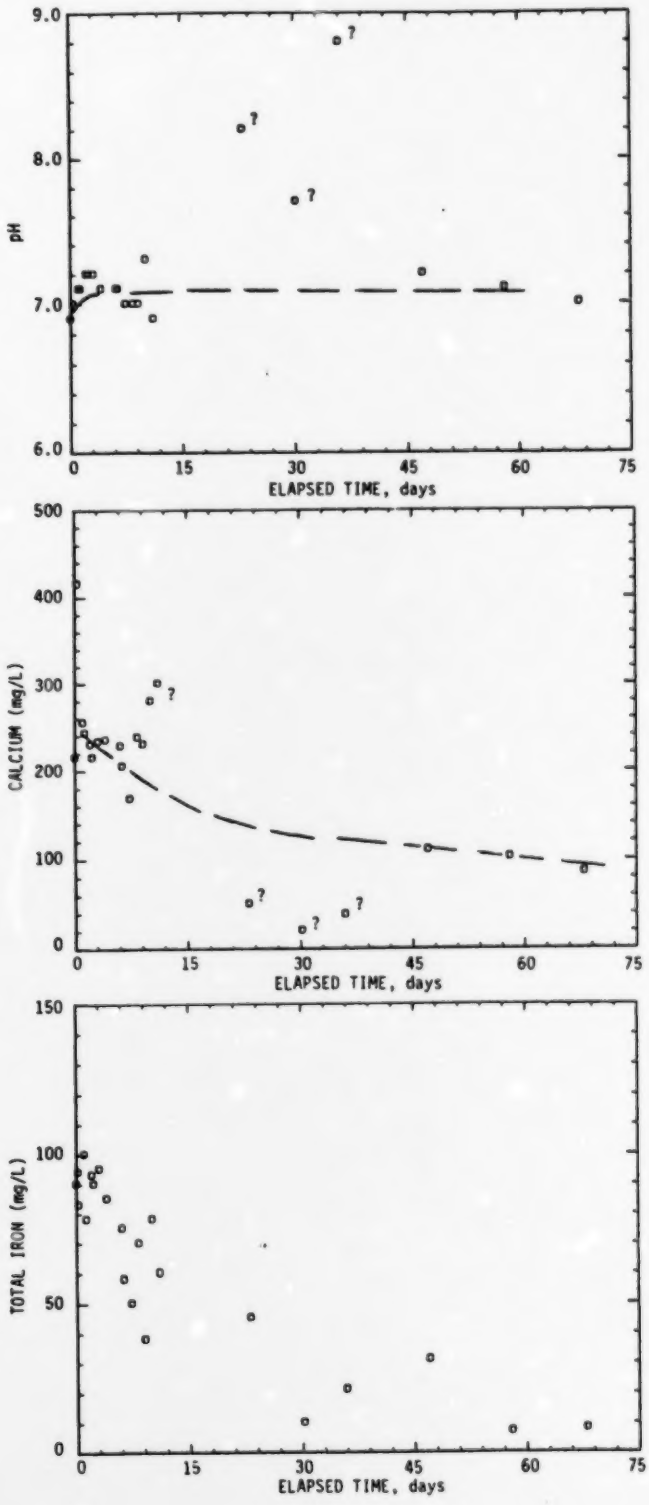

FIGURE II-1. pH, CALCIUM AND IRON VS TIME FOR DOMESTIC LEACHATE STORED AT ~ 21°C

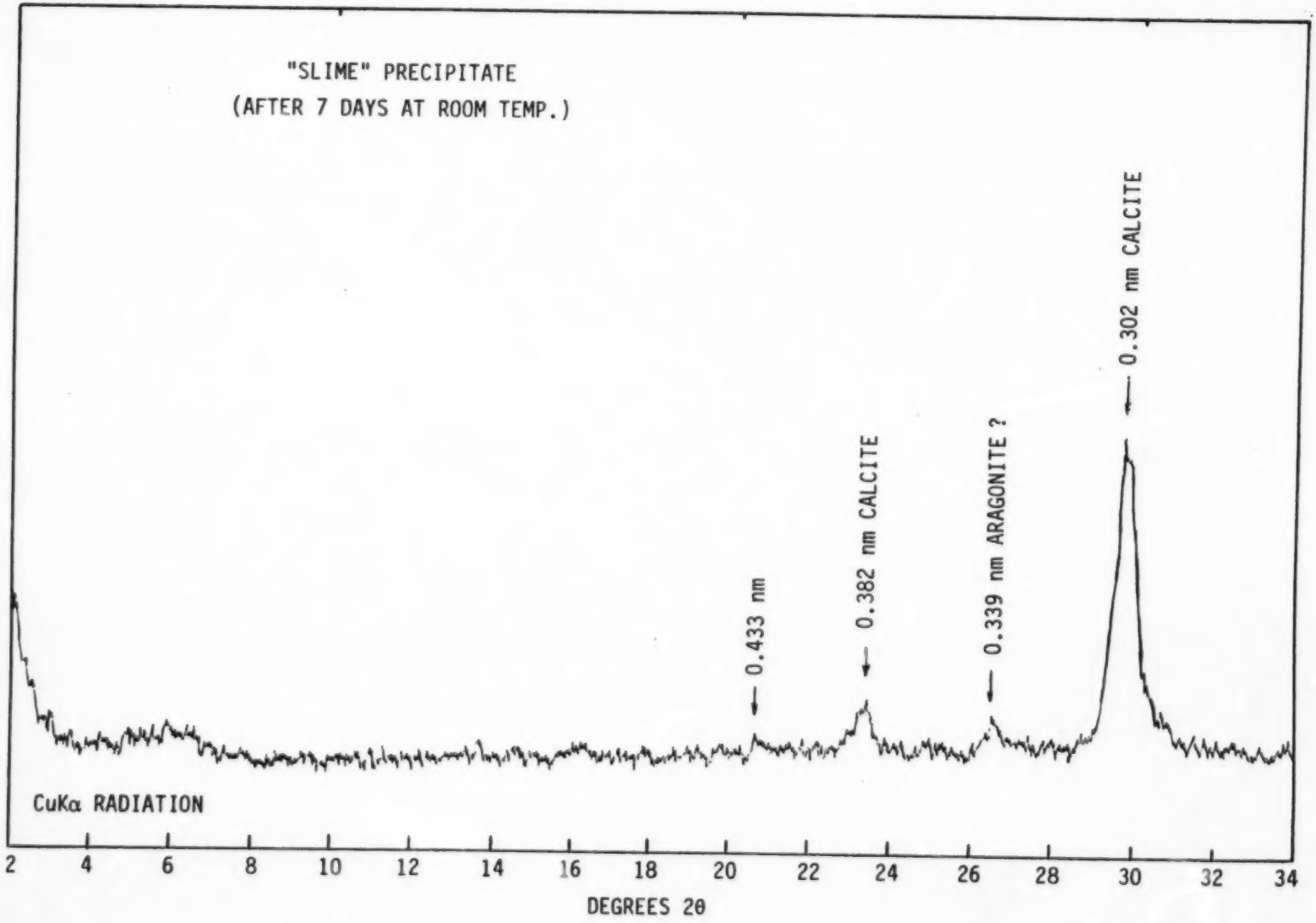

FIGURE II-2. X-RAY POWDER DIFFRACTION TRACE OF AIR DRIED, BLACK "SLIME" PRECIPITATE

APPENDIX III

PRELIMINARY CHEMICAL ASSESSMENT

OF SITE #10 SAMPLES

(Disturbed samples received from

Water and Earth Science Associates Ltd.

Carp, Ontario)

Special thanks are extended to Water and Earth Science Associates Ltd.

for their assistance during the early phases of this project.

INTRODUCTION

A large volume of disturbed samples was received from Water and Earth Science Associates Ltd. in the spring of 1987. Also received was a copy of their RMOC report for our use, courtesy Derek P. Smith, Hydrogeologist.

As a first run on sample selection, the disturbed samples from WESA were analyzed for water content and salinity.

RESULTS

The salinity and water content vs depth profiles are presented on Figure III-1. The soil was shown to consist of high water content clays (- 60 to 85%) with a preliminary profile that looked bow shaped.

The preliminary salinity profile (run on air dry soil wetted to a soil:water ratio of 1:5) showed a near surface salt content of almost zero, increasing to about 12 g/L at depth. The salinity data were particularly useful since they indicated that Site #10 could yield both low and intermediate salinity samples.

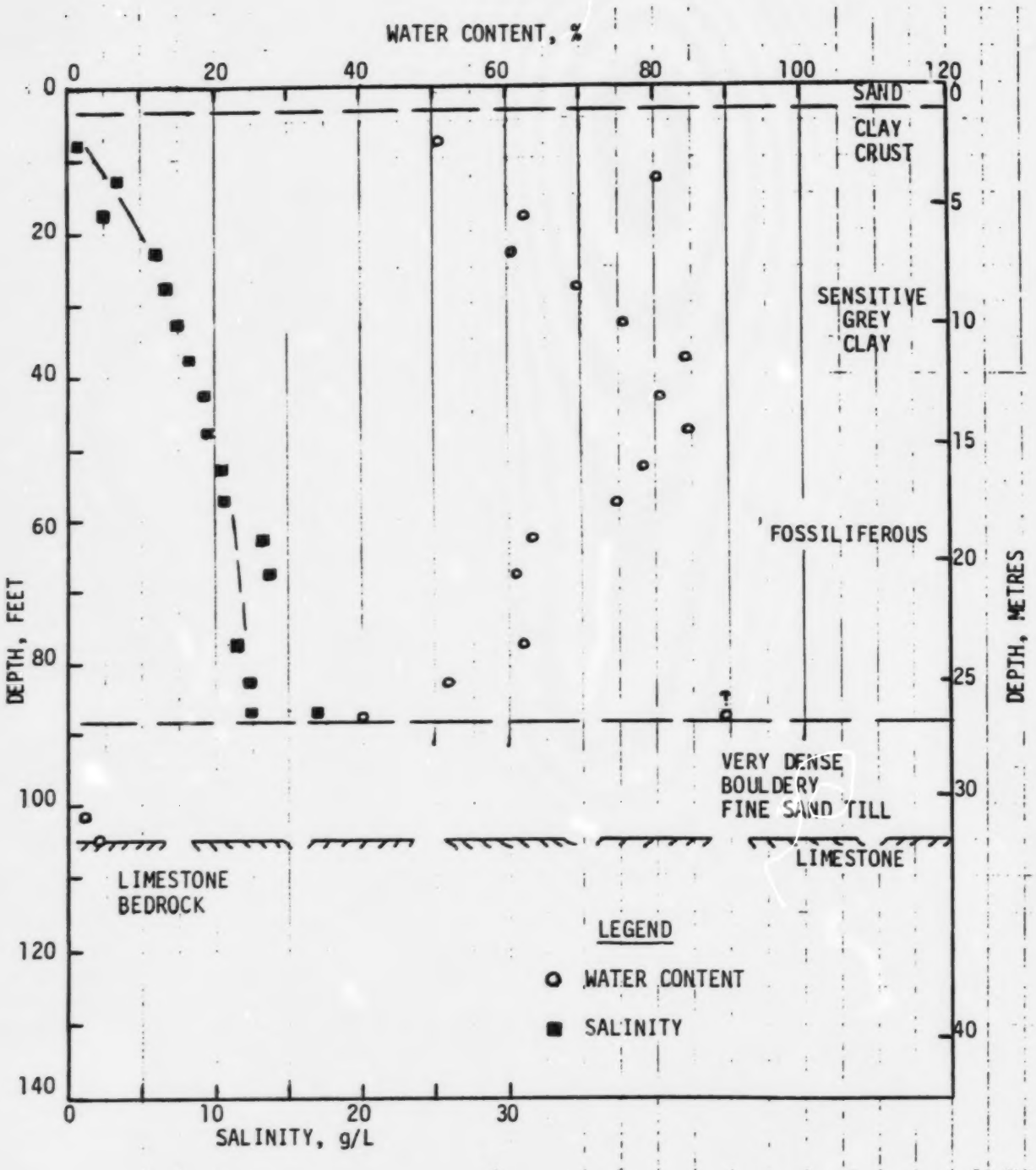

FIGURE III-1. WATER CONTENT AND SALINITY PROFILES, RMOC SITE #10, TEST HOLE 10 (Disturbed samples from Water and Earth Science Associates, Ltd.)